AD_____

GRANT NUMBER DAMD17-94-J-4389

TITLE: Optimization of Technique Factors for Conventional Mammography

PRINCIPAL INVESTIGATOR: R. Edward Hendrick, Ph.D.

CONTRACTING ORGANIZATION: University of Colorado
Health Sciences Center
Denver, Colorado 80262

REPORT DATE: September 1997

TYPE OF REPORT: Annual

PREPARED FOR: Commander
U.S. Army Medical Research and Materiel Command
Fort Detrick, Frederick, Maryland 21702-5012

REPORT DOCUMENTATION PAGE

Form Approved
OMB No. 0704-0188

1. AGENCY USE ONLY *(Leave blank)*	2. REPORT DATE	3. REPORT TYPE AND DATES COVERED
	September 1997	Annual (15 Aug 96 - 14 Aug 97)

4. TITLE AND SUBTITLE
Optimization of Technique Factors for Conventional Mammography

5. FUNDING NUMBERS
DAMD17-94-J-4389

6. AUTHOR(S)
R. Edward Hendrick, Ph.D.

7. PERFORMING ORGANIZATION NAME(S) AND ADDRESS(ES)
University of Colorado Health Sciences Center
Denver, Colorado 80262

8. PERFORMING ORGANIZATION REPORT NUMBER

9. SPONSORING/MONITORING AGENCY NAME(S) AND ADDRESS(ES)
Commander
U.S. Army Medical Research and Materiel Command
Fort Detrick, Frederick, Maryland 21702-5012

10. SPONSORING/MONITORING AGENCY REPORT NUMBER

11. SUPPLEMENTARY NOTES

12a. DISTRIBUTION / AVAILABILITY STATEMENT
Approved for public release; distribution unlimited

12b. DISTRIBUTION CODE

13. ABSTRACT *(Maximum 200*

This report summarizes progress achieved during year three of a three and one-half year postdoctoral research project to determine the optimum technique factors for conventional mammography. This year's work centered on separately analyzing the effects of mammography film, processing conditions, and technique factor selection on image contrast and low-contrast lesion detection. Methods of evaluating film, processing, and technique factor selection for screen-film mammography were applied to approximately one dozen clinical sites involved in the Colorado Mammography Advocacy Project (CMAP), improved technique factors were recommended, and the resulting improvement in image quality at CMAP sites was evaluated. Work being performed now during the one-half year extension of this project centers on completion of analysis and publication of all study results.

14. SUBJECT TERMS		15. NUMBER OF PAGES
Breast Cancer	mammography system performance mammography, image quality mammography, breast doses	79
breast imaging technology	mammography, optical densities	16. PRICE CODE

17. SECURITY CLASSIFICATION OF REPORT	18. SECURITY CLASSIFICATION OF THIS PAGE	19. SECURITY CLASSIFICATION OF ABSTRACT	20. LIMITATION OF ABSTRACT
Unclassified	Unclassified	Unclassified	Unlimited

FOREWORD

Opinions, interpretations, conclusions and recommendations are those of the author and are not necessarily endorsed by the U.S. Army.

____ Where copyrighted material is quoted, permission has been obtained to use such material.

____ Where material from documents designated for limited distribution is quoted, permission has been obtained to use the material.

__✓__ Citations of commercial organizations and trade names in this report do not constitute an official Department of Army endorsement or approval of the products or services of these organizations.

____ In conducting research using animals, the investigator(s) adhered to the "Guide for the Care and Use of Laboratory Animals," prepared by the Committee on Care and Use of Laboratory Animals of the Institute of Laboratory Resources, National Research Council (NIH Publication No. 86-23, Revised 1985).

____ For the protection of human subjects, the investigator(s) adhered to policies of applicable Federal Law 45 CFR 46.

____ In conducting research utilizing recombinant DNA technology, the investigator(s) adhered to current guidelines promulgated by the National Institutes of Health.

____ In the conduct of research utilizing recombinant DNA, the investigator(s) adhered to the NIH Guidelines for Research Involving Recombinant DNA Molecules.

____ In the conduct of research involving hazardous organisms, the investigator(s) adhered to the CDC-NIH Guide for Biosafety in Microbiological and Biomedical Laboratories.

R E Hendrick 9/12/97

PI - Signature Date

TABLE OF CONTENTS

INTRODUCTION

This report summarizes the work performed in year three of the postdoctoral fellowship grant on optimization of technical factors in screen-film mammography. This work includes analyzing the effects of mammography film, processing, and technique factor selection to optimize image contrast and low-contrast lesion detection in screen-film mammography.

The first year's work on this research project was directed at collecting data on the variations in equipment performance, image quality and dose that exist in the practice of mammography. The work in the second year of this project was directed at designing, constructing, and testing two phantoms that were used to quantitatively determine the low-contrast detection capabilities, limiting spatial resolution capabilities, and optical density variations as a function of tissue composition for film-screen mammography units.

The work in year 3 of this project was conducted in three separate, but related, areas. The first area was on the effects of film and processing on image contrast, primarily by use of gamma plots. The second area was on the effects of technique factor selection on image contrast. The third area was on analysis of CMAP site data indicating the improvement in the quality of mammography by attention to technique factor selection. Methods and results are presented in this report for each of these three areas of investigation.

Because of the unanticipated departure of the first postdoctoral fellow and the time required to hire a second postdoctoral fellow, there were approximate six months when the postdoctoral position was not filled and during which progress on this project was limited. To complete the project, we therefore asked for and received a no-cost six month extension of the postdoctoral grant. Although most of the work proposed for this grant has been completed, this extension over the next six months will allow us to complete our analysis of results and submit additional publications of our results over the next six months. Thus, rather than being a final report, this report is an annual report summarizing the last year's work on this project.

BODY OF REPORT

This report consists of two sections with three subsections each:

I. METHODS
1. Film and Processing
2. Technique Factor Selection
3. CMAP Summary Results

II. RESULTS
1. Film and Processing
2. Technique Factor Selection
3. CMAP Summary Results

I. METHODS

1. Film and Processing

A. Theory: Light sensitometry using a 21 step sensitometer yields optical density values for each of 21 steps on the processed mammography film: OD_i, i=1,2,...,21. The H&D curve plots $y_i = OD_i$ versus step number $x_i = i$ (or $x_i = \log(E_i)$, where E_i is the light exposure to the film under step i).

The gamma plot is constructed by plotting a different set of (x_i, y_i) pairs from the same data. In the gamma plot, y_i is the slope of the H&D curve from point to point:

$$y_i = \frac{OD_{i+1} - OD_i}{\log_{10}(\text{sqrt}(2))}, \qquad [1]$$

the point-to-point change in y on the H&D curve being the difference between optical densities at adjacent steps, delta $y = OD_{i+1} - OD_i$, the point-to-point change in x on the H&D curve being the difference in the logarithm of light exposure from step to step: delta $x = \log_{10}(E_{i+1}) - \log_{10}(E_i) = \log_{10}(E_{i+1}/E_i) = \log_{10}(\text{sqrt}(2))$. The x_i coordinate in the gamma plot is the average of optical densities at the two adjacent steps:

$$x_i = \frac{OD_{i+1} + OD_i}{2} \qquad [2]$$

for i=1, 2, ...,20, so that the slope of the H&D curve is attributed to an optical density point midway between the two adjacent points on the H&D curve.

Gamma plots more fully represent film and processing contrast over the full range of optical densities, but are more difficult to plot over time as an indicator of processor performance than simple sensitometric parameters such as mid-density or density difference. Therefore, a single parameter is proposed to characterize film contrast over the full range of optical densities. The film-processing contrast index, A_g, is defined as the area under the gamma plot curve:

$$A_g = \text{integral}_{OD_{min}}^{OD_{max}} \text{gamma}(OD)\, d(OD), \qquad [3]$$

where OD_{min} is the base plus fog optical density of the film and OD_{max} is the maximum optical density of the film. A_g can be determined in closed form from the 21 optical density steps read from the sensitometric strip by assuming a linear interpolation between adjacent gamma plot points (or a trapezoidal approximation for the area under the gamma plot curve), yielding:

$$A_g = (1/4) \sum_{i=1}^{19} (OD_{i+2} - OD_i)^2 \; . \qquad [4]$$

The sum in Eq. [4] combines the areas of the 19 trapezoids formed from the 20 gamma plot points. Interpolation between gamma plot points can be other than linear, including cubic spline interpolation using the information from a set of 4 adjacent gamma plot points and least square fits to the entire set of 20 gamma plot points. The effect of different methods of interpolating between gamma plot points on A_g was investigated.

B. Experiment: Five types of mammography film were exposed using the same 21 step light sensitometry. Films were processed using the same processing conditions with 90 second processing time, as specified by each film manufacturer. Gamma plots were compared for each of the five film types to assess contrast over the full range of optical densities from each film. The gamma plot contrast index A_g also was calculated for each film type using linear interpolation between gamma plot points. Conventional sensitometric parameters also were calculated: the mid-density (MD) or speed step for each film (which is defined by the ACR QC Manuals as the step closest to 1.20), the density difference (DD) which is defined by the ACR QC Manuals as the difference between the step closest to 2.2 and the step closest to, but not less than, 0.45), and the base plus fog (B+F), the optical density of an unexposed portion of the film. To permit intercomparison between films where the MD or DD steps shifted from one film to another (because of the ACR definition), the optical density from a single step (step 11, which is the speed step in most cases) and the density difference between two fixed steps (step 13- step 10) are also listed for each film.

Sources of normal variations in gamma plots using the same film and processing conditions were determined. Sample variation of gamma plots was determined by sensitometric exposure of ten consecutive films from the same film emulsion batch. The ten films were processed under identical processing conditions by processing films in the same processor, temperature, and chemistry within a few minutes of each other. Normal temporal variations of gamma plots were determined by taking one gamma plot each week for ten weeks from a processor determined to be "in control" by standard processor sensitometry. In each case, mean gamma plot curves were constructed by averaging the vertical heights of the ten individual gamma plot curves at each OD value;

both linear interpolation and cubic spline interpolation between gamma plot points was assumed for each individual gamma plot curve. Gamma plot curves representing one standard deviation above and below each mean gamma plot curve were determined by establishing the symmetric vertical range of contrast that would included 68.3% of the individual gamma plot points at each OD value.

The dependence of gamma plots on the specific sensitometer used was established by exposing films from the same film batch using 8 different 21-step sensitometers, processing each strip in the same manner in the same processor within a few minutes of each other. The dependence of gamma plots on the specific densitometer used was established by measuring ODs of the 21 steps of a single sensitometer strip using 9 different densitometers. In each case, gamma plots were superimposed on the same graph for comparison to the sample variations and temporal variations determined above.

The effect of latent image fade on gamma plots was studied using two different types of mammography film (Kodak MRH-1 and Min R-2000). Films from the same emulsion batch and box were exposed 1, 2, 3, 4, and 7 days prior to processing; gamma plots, A_g, MD, DD, and B+F values were compared to those of a film exposed immediately prior to processing.

The effect of film fog on gamma plots was studied using a single type of mammography film (Kodak Min R-2000). Films from the same emulsion batch and box were exposed by a sensitometer and then placed on a darkroom counter directly beneath and approximately 4 feet from a ceiling-mounted darkroom safelight for 1, 2, 4, 8, and 16 minutes. The resulting gamma plots, A_g, and conventional sensitometric parameters were compared to a film exposed by sensitometry and processed immediately without exposure to the darkroom safelight.

The effects of different developer chemistry conditions on gamma plots were studied by producing sensitometric strips with old chemistry, fresh chemistry without starter, fresh chemistry with starter, and the same chemistry plus starter after 1, 2, and 5 days of "seasoning", which consisted of running a normal mammography schedule of approximately 20 patients (80-100 films) per day. All films were taken from the same emulsion batch.

The effect on gamma plots and A_g values of different emulsion batches of the same film type (Kodak Min R-2000) were studied by producing gamma plots using the same sensitometer and by processing films from three different emulsion batches one after another in the same processor.

The effects of processor developer temperature on gamma plots, A_g values, and conventional sensitometric parameters were studied by exposing films from the same box by a sensitometer and processing films at the recommended developer temperature and at $1^{o}C$ steps from $25^{o}C$ to $40^{o}C$.

2. Technique Factor Selection

A contrast-detail (CD) phantom of our own design was used to quantitatively evaluate image quality over the full range of compressed breast thicknesses (2-6 cm) and compositions (100% fatty to 70% glandular/30% fatty). The CD phantom consists of a 9 by 9 array of low-contrast circular test objects milled into a D-shaped 1 cm thick section of breast equivalent material, to which additional 1 cm thick sections of D-shaped breast materials of different compositions were added to give the total thicknesses and compositions listed above. Each row of the CD pattern contains 9 objects at a fixed level of contrast (ranging from 0.29% to 3.95%), with object diameters ranging from 0.25 mm to 4 mm.

The CD phantom was scored by medical physicists trained in scoring the phantom under standardized viewing conditions that included masking of phantom images and fixed low ambient room light. Reviewers were instructed to read the phantom starting with the row of objects with highest contrast, and reading from largest to smallest detectable in that row. Once an object was too faint to "detect", counting was stopped and the number of consecutively visible objects for that row was totaled. Reviewers were instructed not to skip over an undetected object in a given row. They were also instructed to compare marginally detected objects to the background of the phantom and to not count objects that were no more visible that artifacts. Since the locations of the objects in the phantom were known in advance, this guarded against overscoring the phantom and provided greater consistency in scoring. The CD score for each reviewer under each imaging condition was determined by summing the area of detected objects in contrast-detail space. Thus, the more low-contrast objects of a given size and level of contrast detected, the higher the CD score. If all 81 objects in the CD phantom were detected, a maximum score of 16.0 would be obtained. If no objects in the CD phantom were detected, a minimum score of zero would occur.

Three independent sources of error contribute to the uncertainty in CD area scores: between-observer (or inter-reader) variations, within-observer (or intra-reader) variations and sample variations in the area of the detected contrast-detail region. In a CD phantom experiment where N_s identical sample films are acquired under each different exposure condition, and each film is read N_i times by N_r independent reviewers, the expected standard deviation of CD area measurements is:

$$\sigma_{total} = \{\sigma_s^2/N_s + \sigma_b^2/N_r + \sigma_w^2/(N_s N_r N_i)\}^{1/2},$$

where σ_s is the standard deviation in CD area due to sample variation, σ_b is the standard deviation in CD area due to between-observer variation, and σ_w is the standard deviation in CD area due to within-observer variation.

To permit theoretical estimation the total standard deviation in measured CD area in any experiment (potentially involving

multiple samples, multiple readers, and multiple readings of each image), an experiment was conducted to determine separately each source of standard deviation. This was done by taking five different samples under each imaging condition using a GE DMR mammography unit and Kodak Min R-2000 cassette and film, all film taken from the same batch and box. Each image was read three times, each pair of readings separated by at least two weeks time, by four different medical physicist reviewers. To avoid recall bias, the five actual test images acquired under identical conditions were randomly interspersed with fifteen other images with a range of image quality and CD scores.

Calculation of root mean squared (rms) deviation across multiple readings of the same film and averaged over all films allowed determination of σ_w independently for each reviewer and collectively for all reviewers. Calculation of rms deviation across multiple samples determined:

$$S_{samples} = \{\sigma_s^2+\sigma_w^2\}^{1/2}$$

for each reader or collectively for all readers, from which σ_s was determined by subtracting out σ_w in quadrature. Calculation of rms deviation across different readers scoring each film determined:

$$S_{between} = \{\sigma_b^2+\sigma_w^2\}^{1/2}$$

from which σ_b was determined by subtracting out σ_w in quadrature.

The results of this initial experiment were used to determine the optimum number of multiple images generated under each imaging conditions, the number of readers, and the number of independent readings of each image for subsequent experiments.

All subsequent experiments involved acquisition of two identical images under each exposure condition, and reading of each acquired image independently by two experienced reviewers. Reviewers were blinded to exposure conditions and images were mixed so that a reviewer would encounter a variety of images under different exposure conditions at each reading session.

All image acquisition was done on a GE-DMR mammography unit using Kodak Min R-2000 cassettes and film. Either a single cassette or a set of three cassettes matched for optical densities were used. Images were processed on a Kodak M6B processor with Kodak chemistry and autoloading.

The first experiment on technique factor selection repeated a previously performed experiment (in which a different screen-film combination was used) to study the effect of optical densities on low-contrast detection. kVp was fixed (at 26), phantom thickness was fixed (at 6 cm) and simulated breast tissue composition was fixed (at 50% glandular/50% fat); three different target-filtration combinations were used (Mo/Mo, Mo/Rh, and Rh/Rh), acquiring images at different mAs values to span the range of optical densities used in mammography.

The second series of experiments, based on the results of the first, employed fixed film optical densities of 1.65-1.75 to maximize contrast and lesion detection as a function of OD and to eliminate the effects of ODs on technique factor optimization. These experiments varied breast thickness (2, 4, and 6 cm), composition (100% fat, 30% glandular/70% fat, 50% glandular/50% fat, and 70% glandular/30% fat), target-filtration (Mo/Mo, Mo/Rh, and Rh/Rh), and kVp values (over the range from 24-32 for Mo/Mo and Mo/Rh and from 26-32 for Rh/Rh), with commensurate adjustment of mAs values to keep film optical densities constant. Again, two CD phantom images were acquired under each imaging condition and CD phantom images were scored independently by two reviewers. mAs values were recorded to determine exposure time and breast doses for each exposure were calculated based on previously measured half-value layer (HVL) and exposure outputs (in milliRoentgen/mAs) using the GE-DMR.

In separate measurements, a latitude phantom of our own design was used to determine the range of optical densities occurring in uniformly thick compressed breasts due to breast tissue heterogeneities. Breast thicknesses ranging from 2-7 cm and breast compositions ranging from 100% fatty to 100% glandular were used with the three different target-filter combinations and with the AEC detector set over an area of 100% fat, 50% fat/50% glandular tissue, or 100% glandular tissue, to measure the range of optical densities occurring in the resultant image. These tests were performed using both the Min R-2000 screen-film system and the Min-R/MRH-1 screen-film system.

3. CMAP Summary Results

Results from medical physics testing at CMAP sites between 1990 and 1996 were analyzed to determine trends in the quality of mammography over that time period. Data from approximately 100 site surveys were analyzed to determine whether trends toward improved mammography existed in the data. Data analyzed included phantom scores, film-processing A_g values (based on data acquired using the site's film and processing, but a single sensitometer and densitometer for all sites), film optical densities and exposure times for 2, 4, and 6 cm breasts using standardized 50% fatty/50% glandular breast tissue-equivalent BR-12 material.

II. RESULTS

The H&D curves for six different mammography films processed under the same processing conditions are shown in **Figure 1**. The corresponding six gamma plot curves for these films under the same processing conditions are shown in **Figure 2**. Several results are apparent from these gamma plot curves. First, differences in the heights of these gamma plot curves indicate that there are substantial differences in the levels of contrast produced by different mammography films, even under the same processing conditions. Second, the different widths of different curves show that some films have broad optical density ranges

over which maximum contrast is preserved, while other films have relatively narrow ranges of maximum contrast. A narrow range of maximum contrast reflects a limited linear portion of the H&D curve. Third, different films have peak contrast occurring at different optical densities. For example, Fuji film has maximum contrast between 1.0 and 1.5, MRH-1 and MR-2000 film have maximum contrast near 2.0, while 3M and Dupont Microvision have contrast peaking at optical densities above 2.0.

Fourth, and perhaps most importantly, **Figure 2** demonstrates that all mammography films operate at reduced contrast for optical densities below 1.2, with substantial reductions in contrast for optical densities below 1.0. The shape of the gamma plots for lower optical densities is the same regardless of the particular film used. **Table 1** lists the integrated area under the entire gamma plot curve, A_g, for each of the mammography films included in **Figure 2**. Note the sizable differences between A_g values, with greater contrast over the full range of optical differences producing greater A_g. Table 1 also lists the mid-density (MD) or speed step for each film (the step closest to 1.20), and the optical density from a single step (step 11, which is the speed step in most cases) to permit intercomparison of speed between films. The density difference (DD) as defined in the ACR QC Manuals (the difference between the step closest to 2.2 and the step closest to, but not less than, 0.45), and the density difference between two fixed steps (step 13- step 10) are also listed, to permit intercomparison between films. The base plus fog (B+F) of each film is also listed.

Figure 3A illustrates the sample variation of gamma plots by displaying ten gamma plot curves acquired under identical processing conditions with one type of mammography film (Kodak MRH-1). **Figure 3B** illustrates the mean gamma plot curve and the $\pm$ one standard deviation gamma plot curves reflecting sample variation for film from the same emulsion batch processed under identical processing conditions. **Figure 4A and 4B** illustrate normal temporal variations of gamma plots acquired over a ten week period from a processor that was "in control" according to normal processor QC measures. Note that the $\pm$ one standard deviation limits are somewhat wider in **Figure 4B** than in **Figure 3B**, reflecting the increased variation of processing conditions over time, even though the same film emulsion batch was used. **Table 2** lists the A_g, MD, DD, and B+F for the normal sample variation and temporal variation illustrated in **Figures 3 and 4**. For the ten films processed at the same time, the range of A_g values was 9.5 to 10.1 and the mean and standard deviation of A_g values were 9.78 ± 0.17. For the ten films processed one week apart each, the range of A_g values was 9.8 to 11.1 and the mean and standard deviation of A_g values were 10.55 ± 0.45.

The effect on gamma plot curves of using different sensitometers is illustrated in **Figure 5**. Each of the eight curves in **Figure 5** was produced using a different 21-step sensitometer, while using the same film batch and processing conditions. The variation among the eight curves in **Figure 5** is greater than the sample variation illustrated in **Figure 3**, but

not as great as the temporal variation shown in **Figure 4**.

Figure 6 shows eight gamma plot curves determined from the same sensitometry film using five different densitometers. The variations among six of the eight are insignificant, being comparable to the sample variation of gamma plot curves illustrated in **Figure 3**; two densitometers, however, gave significantly different gamma plot results, due to densitometer inaccuracies. These two densitometers (D1 and D7) were found to yield inaccurate results for optical densities above 2.0 and were recommended for repair.

These results suggest that gamma plot curves are relatively invariant to the particular 21-step sensitometer used, but may be affected by inadequate sensitometer or densitometer performance. **Table 3** lists the A_g, MD, DD, and B+F values for the eight different sensitometers and nine different densitometers whose performance is illustrated in **Figures 5 and 6**.

The effect of a delay between film exposure and processing on gamma plots is shown in **Figures 7 and 8**. These results show that "latent image fade" had insignificant effects on film contrast for Min R-2000 film and had only a minor effect on film contrast for MRH-1 film. Interestingly, a delay between film exposure and processing actually increased film contrast slightly for MRH-1. **Table 4** lists the A_g, MD, DD, and B+F values for the latent image fade illustrated in **Figures 5 and 6**. These results indicate that a delay between film exposure and processing does not have a significant effect on image contrast for the two films tested.

The effects of darkroom fog on gamma plots, A_g, MD, DD, and B+F values are illustrated in **Figure 9** and **Table 5**. Substantial film fog does reduce film contrast and A_g values somewhat, but has far less of an effect that film type, film emulsion differences, and processing conditions in most cases (see below).

The effect of different developer chemistry conditions on gamma plots is illustrated in **Figure 10** and **Table 6**. Old chemistry and fresh chemistry plus starter after 5 days "seasoning" yielded nearly identical gamma plots. Fresh chemistry without starter yielded reduced contrast for lower optical densities and slightly increased contrast for higher optical densities, while adding starter increased contrast for lower optical densities and lowered contrast for higher optical densities. Seasoning increased contrast across the entire mid-range of optical densities. Comparison of A_g values and density difference values for these different processing conditions demonstrates that A_g gives a more complete description of film contrast that DD.

Gamma plots for three different batches of the same type of mammography film (Kodak Min R-2000) are shown in **Figure 11**. These gamma plots show significant variations from batch to batch. The corresponding A_g, MD, DD, and B+F values for the three batches are given in **Table 7**. The differences in gamma

plots between emulsion 1 and the other two emulsions demonstrate that film contrast can differ significantly from batch to batch of the same type of mammography film. Those differences are apparent as differences in the height of gamma plot curves across the mid-range of optical densities. Those differences also are apparent as differences in A_g values in **Table 7**, but are less apparent as differences among conventional film sensitometry values of MD, DD, and B+F.

The effect of developer temperature on gamma plots and summary parameters are illustrated in **Figures 12-14** and **Table 8**. As developer temperature increases from 25°C to 33°C, gamma plot curves and A_g values increase (**Figures 12 and 13**). Gamma plot curves and A_g values remain high and approximately constant for developer temperatures between 33°C and 37°C, and then decrease as developer temperature continues to increase. These results show optimization of film contrast at developer temperatures between 33°C and 37°C (**Figure 13**). Note the decrease in contrast at optical densities at and around 1.0 for these high developer temperatures (**Figure 12**). In contradistinction, fixed step ODs and fixed step OD differences continue to increase monotonically as developer temperature is increased from 25°C to 40°C (**Figure 14**). Conventionally defined MD and DD values cannot be used to analyze the effect of temperature because of the need to shift steps to keep the reference step for MD the step closest to 1.20 OD and the two reference steps for DD those closest to 2.20 and closest to, but not less than, 0.45. These results indicate the utility of gamma plots and the A_g value as a summary indicator of film and processing contrast.

These results suggest at least two possible methods for a site to use gamma plots to determine if their processing is "optimized" without the use of a standardized sensitometer and densitometer. The first method is based on the fact that gamma plots are reasonably insensitive to the particular 21-step sensitometer used. In this method, the gamma plot determined for optimized processing of a particular film type, determined using the film manufacturer's 21-step sensitometer and densitometer, can be used as a standard for film processing performance by a mammography site. The mammography site's gamma plot results, using their own sensitometer and densitometer, can be compared to the film manufacturer's gamma plot results to determine if the site is processing their mammography film appropriately. This method of comparison may result in gamma plot differences that suggest differences in processing, but are actually due to differences in the film emulsion batches, sensitometers, or densitometers used at the two sites.

The second method is based on the minimal effect of latent image fade on gamma plots for some types of mammography film (see **Figures 7 and 8**). If a mammography site uses a film for which latent image fade is not significant, such as Kodak Min R-2000, the site can use one or more sheets of their own film, flash the film using their own sensitometer, place the exposed, undeveloped film into a light-tight envelope, and mail the exposed film overnight to the film manufacturer for immediate processing under

conditions optimized for that film type. The processed film can then be mailed back to the site and optical densities measured using the site's own densitometer. The gamma plot results from the film manufacturer's optimized processing can be compared to a gamma plot constructed using the site's processing, the same film batch and box, the same sensitometer, and the same densitometer. If latent image changes are significant, this method might still be used by intentionally using the same time delay between exposure and processing at the site as for the manufacturer's processing.

2. Technique Factor Selection

Reader performance studies of the contrast-detail (CD) phantom determined that intra-reader variations are the greatest source of uncertainty, with sample variations the next most significant and inter-reader variations the least significant. For screen-film mammography with good image quality, a mean contrast-detail score of 12.3 was measured. For multiple images read by multiple readers multiple times, intra-reader standard deviations were determined to be 0.49, sample variation standard deviations were determined to be 0.24, and inter-reader standard deviations were determined to be 0.05. These results were used in the theoretical expression for propagation of error in the case of N_s identically acquired samples, each of which is read by N_r readers N_i times:

$$\sigma_{total} = \{\sigma_s^2/N_s + \sigma_b^2/N_r + \sigma_w^2/(N_s N_r N_i)\}^{1/2},$$

where σ_s is the standard deviation in CD area due to sample variation, σ_b is the standard deviation in CD area due to between-observer or inter-reader variation, and σ_w is the standard deviation in CD area due to within-observer or intra-reader variation. Use of this equation and the measured values of each source of standard deviation indicated that an efficient method of reducing variations in phantom scoring (by an estimated 36%) was to acquire two samples under each imaging condition and have each image read in a blinded fashion by two experienced observers. Other methods to reduce scoring variations, such as multiple readings of the same image, or a large number of readers of a single image, are less efficient in reducing scoring uncertainties. Consequently, all CD scoring results presented subsequently employed two identically acquired samples of each image score independently and blindly by two experienced CD phantom readers.

Using this scoring methodology, we first repeated the CD phantom testing that studied the effect of optical densities on low-contrast lesion detection for different target-filtration combinations (Mo/Mo, Mo/Rh, and Rh/Rh); the results are shown in **Figure 15A-D**. **Figure 15A** intercompares the three target-filter combinations without displaying error bars, showing the strong dependence of low-contrast lesion detection on optical densities and the lack of major differences between results at the same optical density for different target-filter combinations. Note the sharp rise in CD scores as OD increases for low optical

densities, a broad maximum in CD score for ODs between approximately 1.2 and 2.5, and a rapid decrease in CD scores for ODs above 2.5. These low-contrast detection results generally conform to the shape of the gamma plot curve for Kodak Min R-2000 film in **Figure 2**, indicating that the loss of detection at low and high ODs is a result of the reduced contrast in mammography film at low and high ODs.

Figures 15B-D show CD results for each target-filter combination, with the uncertainties on each data point displayed. The uncertainties displayed were the standard deviations based on acquisition of two images under each test condition and independent scoring of each image by two reviewers. Bonferroni t-tests were used to test for the significance of differences among the three target-filter combinations, indicating no statistically significant differences at the $p \leq 0.05$ level between images acquired with different target-filter combinations. Due to the phantom thickness and mAs limit on Mo/Mo exposures, ODs greater than 3.0 could not be produced for the Mo/Mo target-filter combination.

Based on these test results and the Min R-2000 film gamma plot, all subsequent testing with different breast thicknesses and compositions was done at a fixed OD of 1.65-1.75, so that the strong dependence of low-contrast lesion detection on OD could be removed from technique optimization experiments. The results of these experiments, which varied breast thickness (2, 4, and 6 cm), composition (100% fat, 30% glandular/70% fat, 50% glandular/50% fat, and 70% glandular/30% fat), target-filtration (Mo/Mo, Mo/Rh, and Rh/Rh), and kVp (while altering mAs to maintain constant ODs of 1.65-1.75) are shown in **Figures 16A-D. Figure 16A** illustrates the effect of increasing kVp from 24 to 32 for Mo/Mo target-filtration and 100% fatty breasts. The effect of increasing kVp while keeping ODs fixed is a slight, but in most cases a statistically significant, decrease in low-contrast detection for each breast thickness (p values for statistical significance of the decrease in contrast are listed in **Table 9**). The same general trend applies to other breast compositions (**Figure 16B-D**) and other target-filter combinations (the case of Mo/Rh for a 50%/50% breast shown in **Figure 16E**). Note the distinction between CD scores for 2, 4, and 6 cm breast thicknesses in each graph, but especially for breasts with greater glandular content. Note that the CD scores were similar for different breast compositions at the same kVp for 2 cm thick breasts, but CD scores dropped significantly with increasing tissue glandularity for 4 and 6 cm thick breasts. Mo/Rh and Rh/Rh target-filter combinations showed more gradual and less significant decreases in low-contrast lesion detection than Mo/Mo, especially for thin to intermediate breast thicknesses.

Given that kVp has a slight, but usually significant, effect on image contrast and CD scores, it would appear that the use of lower kVp is preferable for a given breast thickness and composition. kVp has a major effect, however, on mAs or exposure times, as illustrated in **Figures 17A-D** (the GE-DMR is a 100 mA unit with the large molybdenum target, 80 mA for the large

rhodium target). Thus, the prescription of using the lowest kVp possible must be modified by the requirement that exposure times be kept reasonably short (under 2 seconds) to minimize patient motion and to prevent underexposure due to automatic exposure shutoff (due to exceeding the backup time on automatic exposure control systems).

The average glandular doses to maintain the same 1.65-1.75 optical density for a 50%/50% breast of 2 to 6 cm thickness for each target-filter combination are shown in **Figures 18A-C**. Of interest are that average glandular breast doses for Mo/Rh target-filter are approximately 70% of those for Mo/Mo, and doses for Rh/Rh are approximately 60% of those for Mo/Mo. We did not include doses for a 2 cm breast using Mo/Rh or Rh/Rh, since the Roentgen to mrad conversion factors were not determined for those target-filter combinations for a 2 cm thick breast.

The film optical densities resulting from uniformly thick heterogeneous breasts of thickness ranging from 2-7 cm and compositions ranging from 100% fatty to 100% glandular tissue for different target-filter combinations and different AEC detector placements are shown in **Figures 19A-L**. Separate curves for MRH-1 film and Min R-2000 film are shown. Of particular note is that the higher contrast Min R-2000 film has a greater range of optical densities and greater loss of contrast at the lower and upper ends of the OD range, especially for thicker breasts and where the AEC detector responds to 100% fat or 100% glandular tissue. This indicates that AEC detector positioning is even more critical with Min R-2000 film than with previously used films and that some loss of contrast may occur in using this film with thicker, highly heterogeneous breasts.

3. CMAP Summary Results

Summary gamma plots demonstrating the mean and standard deviation of film-processing contrast each year from 1990 through 1995 are shown in **Figures 20A-F**. The measured A_g values from different sites are plotted against time in a scattergram (**Figure 20G**) and are summarized year by year in **Figure 20H**. While the spread of A_g values in each year is great, there is a statistically significant trend of increased A_g over time ($p < 0.05$), demonstrating a general improvement in film and processing contrast at mammography sites between 1990 and 1996.

Figure 21 shows the slight trend toward improvement in phantom image quality scores over the time period 1990-1995, as well. Perhaps more encouraging, and more reflective of the effect of site intervention of providing revised technique charts to maintain adequate optical densities and keep exposure times under 2 seconds (starting in 1993), was the narrowing of optical densities for 2, 4, and 6 cm thick phantoms and the increase in ODs for thicker breasts (**Figure 22**). Also encouraging was the decrease in exposure times for 6 cm thick breasts between 1994 and 1995 (**Figure 23**). These results suggest that the interventions made by the medical physicist at CMAP sites between 1993 and 1995, especially in recommending technique factors based

on the image optimization ideas described above, led to measurable improvements in image quality over that time period.

CONCLUSIONS

We have made a number of findings in year 3 of this project. With regard to gamma plots as a quality control tool in mammography, they are that gamma plots are useful because they:

1) graphically depict the contrast produced by film and processing as a function of optical density. The height of the gamma plot curve represents the "local contrast": the amount of contrast at each optical density. This permits intercomparison of contrast from different film types, different film batches, and under different processing conditions over the entire range of film optical densities;

2) provide a useful quality control tool for determining that processing is optimized for a given type of mammography film;

3) graphically describe the range of optical densities over which maximum (or near maximum) contrast is achieved for the specific film and processing used. This can help guide automatic exposure control set-up and clinical technique factor selection;

4) provide a useful quality control tool for assessing the consistency of film contrast, including effects of both film emulsion and processing, over time;

5) provide a useful way to intercompare one batch of film to another, for both control film and clinical film;

6) make use of data already acquired daily through processor sensitometry at every mammography facility in the U.S.;

With regard to technique factor optimization, once film and processing have been optimized:

7) that both image contrast and the ability to detect low-contrast lesions in screen-film mammography are strongly dependent on film optical densities

8) that both image contrast and the ability to detect low-contrast lesions depend weakly on kVp, assuming that optical densities are matched, with increased kVp leading to decreased image contrast.

9) that different target/filter combinations proposed for mammography have a sizable effect on average glandular breast doses, but little effect on resultant image quality in terms of low-contrast detection and little effect on the range of optical densities due to different tissue compositions within the breast.

10) that the basis for appropriate technique selection is to maximize the match between film contrast properties and ODs

occurring in the normal range of clinical mammograms, while keeping exposure times adequately short to minimize motion.

11) that positioning of the AEC detector has a dramatic effect on the range of optical densities that result due to different tissue compositions, and that the effects of AEC placement are greater with thicker breasts.

12) that the dynamic range of exposures found in thin to intermediate thickness breasts due to different tissue compositions is sufficiently narrow to permit a match between film ODs and the OD range of maximum film contrast; in thicker breasts, however, the dynamic range of exposures is too broad to permit a complete match between film ODs and the OD range of maximum film contrast, regardless of target/filter combination for the three target/filter options used in this work.

These findings provide a simple, site-specific method to optimize technique factors at any screen-film mammography site. This method has been applied to site surveys conducted through CMAP since 1993 by providing revised technique charts that were more effective at maintaining optical densities and keeping exposure times under 2 seconds for all breast thicknesses. Preliminary results of the analysis of CMAP sites demonstrate a general improvement in film-processing contrast, more consistent film optical densities, and reduced exposure times for thicker breasts. Further analysis is being conducted to establish the changes that were a direct consequence of medical physicist intervention at CMAP sites.

REFERENCES

1. Fletcher SW, Black W, Harris R, Rimer BK, Shapiro S. Report of the International Workshop on Screening for Breast Cancer. **JNCI** 1993; 85: 1644-56.

2. Elwood JM, Cox B, Richardson AK . The effectiveness of breast cancer screening by mammography in younger women. **Online Journal Curr. Clin. Trials** 1993; 1: 32-227.

3. Bird RE, Wallace TW, Yankaskas BC. Analysis of cancers missed at screening mammography. **Radiology** 1992; 184: 613-617.

4. Jackson VP, Hendrick RE, Feig SA, Kopans DB. Imaging of the radiographically dense breast. **Radiology** 1993; 188: 297-301.

5. Haus AG. Technologic improvements in screen-film mammography. **Radiology** 1990; 174: 628-637.

6. Bassett LW, Gold RH, Kimme-Smith C. History of the technical development of mammography, in **Syllabus: A Categorical Course in Physics: Technical Aspects of Breast Imaging**, 3rd Edition, Eds. AG Haus and MJ Yaffe, 1994: 9-20.

7. Haus AG. Screen-film image receptors and film processing, in **Syllabus: A Categorical Course in Physics: Technical Aspects of Breast Imaging**, 3rd Edition, Eds. AG Haus and MJ Yaffe, 1994: 85-101.

8. Johns PC, Yaffe MJ. X-ray characterization of normal and neoplastic breast tissues. **Phys. Med. Biol.** 1987; 32: 675-695.

9. Young KC, Wallis MG, Ramsdale ML. Mammographic film density and detection of small breast cancers. **Clinical Radiology** 1994; 49: 461-465.

10. Alter AJ, Kargas GA, Kargas SA, et.al. The influence of ambient and viewbox light upon visual detection of low-contrast targets in a radiograph. **Invest. Radiol.** 1982 17: 402-406.

11. **Medical Imaging -- The Assessment of Image Quality**. ICRU Report #54. Bethesda, MD: International Commission on Radiation Units and Measurements, 1996.

12. Cohen G, McDaniel DL, Wagner LK. Analysis of variations in contrast-detail experiments. **Medical Physics** 1984; 11: 469-473.

13. Robson KJ, Kotre CJ, Faulkner K. The use of a contrast-detail test object in the optimization of optical density in mammography. **The British Journal of Radiology** 1995; 68: 277-282.

14. Law J. Improved image quality for dense breasts in mammography. **The British Journal of Radiology** 1992; 65: 50-55.

15. Stanton L, Day JL, et.al. Screen-film mammographic technique for breast cancer screening. **Radiology** 1987; 163: 471-479.

16. Hendrick RE, Bassett LW, Butler PA, et. al., **Mammography Quality Control: Radiologist's Manual, Radiologic Technologist's Manual, Medical Physicist's Manual**, American College of Radiology, Revised Edition, 1994.

Table 1

Number	Film Co.	Ag	MD	K-2000 step 11	DD	K-2000 13-10	B+F
1	K-2000	11.8	0.99	0.99	1.76	1.76	0.21
2	K-MRH	9.89	1.07	1.59	1.47	1.61	0.19
3	Dupont	12.72	1.2	1.2	1..92	1.66	0.24
4	Fuji	7.54	1.44	0.61	1.76	1.02	0.21
5	Konica	7.24	1.03	1.4	1.69	1.16	0.25
6	3M	13.25	1.23	1.23	1.96	1.7	0.24

Table 2

Film #	10 Films @same time Ag	MD	step 10	DD	Steps 12-9	B+F	10 Films - 1 Per Week Ag	MD	step 10	DD	Steps 12-8	B+F
1	9.71	1.07	Same	1.46	Same	0.2	11.11	1.21	Same	1.93		0.2
2	9.63	1.08		1.45		0.19	10.97	1.23		1.91		0.19
3	9.54	1.07		1.48		0.19	10.69	1.22		1.89		0.2
4	9.85	1.07		1.44		0.19	10.9	1.23		1.94		0.2
5	9.89	1.07		1.47		0.19	10.77	1.13		1.84		0.2
6	10	1.05		1.45		0.19	10.8	1.09		1.53	1.79	0.2
7	10.05	1.06		1.46		0.19	10.19	1.12		1.78		0.2
8	9.78	1.07		1.46		0.19	10.14	1.17		1.77		0.2
9	9.65	1.06		1.49		0.19	10.16	1.15		1.79		0.2
10	9.7	1.07		1.43		0.19	9.78	1.16		1.78		0.19
Mean	9.78						10.551					
Stdev	0.16553						0.44543					

Table 3

Site	Sensitometer Ag	MD	Step 11	DD	Steps 13-9	B+F	Densitometer Ag	MD	Step 11	DD	Steps 13-9	B+F
1	12.25	1.09		2.02		0.22	9.09	1.04	Same	1.93		0.2
2	12.16	1.07		1.7	1.94	0.21	12.49	1.11		2.06		0.21
3	12.54	0.98	1.51	1.64	2.44	0.21	12.16	1.09		2.02		0.21
4	12.12	1.07		1.77	2.02	0.22	12.35	1.1		2.07		0.2
5	12.48	1.18		1.36	2.18	0.22	12.23	1.09		2.03		0.22
6	12.87	1.06	1.69	1.86	2.55	0.21	12.13	1.1		2.02		0.21
7	12.1	1.14	1.68	1.79	2.48	0.22	11.17	1.04		1.74	1.97	0.19
8							12.03	1.1		2.01		0.22
9	12.21	1.02		1.53	1.75	0.21	12.35	1.09		2.03		0.21

Table 4

Day	Latent-2000 Ag	MD	Step 12	DD	Steps 13-10	B+F	Latent MRH Ag	MD	Step 11	DD	Steps 13-10	B+F
0	14.67	1.01	1.58	1.81	Same	0.21	9.34	1.12	1.63	1.73	1.56	0.2
1	15.63	1.44		1.72		0.21	9.83	1.42		1.48		0.2
2	15.42	1.46		1.75		0.21	9.83	1.37		1.48		0.2
3	14.93	1.45		1.73		0.21	9.81	1.29		2.01		0.2
4	15.22	0.94	1.51	1.77		0.21	9.9	1.26		1.99		0.2
7	15.28	0.92	1.48	1.78		0.21	10.37	1.23		1.73	2.01	0.2

Table 5	Fog		Step		Steps	
Fog Film	Ag	MD	11	DD	13-10	B+F
No Fog	15.49	1.48	0.9	1.76	Same	0.2
1 Min	15.03	0.95		1.78		0.21
2 Min.	14.72	0.99		1.82		0.21
4 Min.	14.53	1.04		1.86		0.21
8 Min.	14.71	1.17		1.3	1.93	0.21
16 Min.	14.2	1.35		1.45	2.05	0.23

Table 6

	Old Chem		Old Chem			
	Fog		Step		Steps	
	Ag	MD	11	DD	13-10	B+F
Old Chem	14.06	1.03	Same	1.94		0.21
Fresh Chem. W/o Starter	1.41	1.26		1.39	1.95	0.21
Fresh Chem. W/ Starter	12.18	0.97		1.88		0.21
1 Day	13.22	0.99		1.93.		0.2
2 Day	13.59	1.02		1.93		0.2
5 Day	13.87	1.01		1.92		0.2

Table 7

		Ag	MD	Step 11	DD	Steps 13-10	B+F
control	Film A	12.69	0.92	Same	1.84	Same	0.21
Chuck's	Film B	11.34	0.97		1.71		0.21
clinical	Film C	11.67	0.98		1.76		0.21

Table 8

Film #	Temp	Ag	MD	Step id-Densit	DD	Steps sity Differ	ase + Fog
1	25	8.91	0.98	0.64	1.51	0.66	0.21
2	26	9.6	1.05	0.69	1.85	0.72	0.21
3	27	9.75	1.2	0.76	2.01	0.85	0.2
4	28	10.18	1.27	0.82	1.42	0.9	0.2
5	29	10.65	1.37	0.88	1.48	0.97	0.2
6	30	10.67	1.42	0.9	1.5	1.01	0.2
7	31	11.06	0.9	0.95	1.8	1.07	0.21
8	32	10.92	1.09	1.09	1.96	1.18	0.21
9	33	11.39	1.16	1.16	2.05	1.24	0.21
10	34	11.22	1.25	1.25	1.32	1.32	0.21
11	35	11.03	1.3	1.3	1.36	1.36	0.21
12	36	11.1	1.36	1.36	1.57	1.38	0.22
13	37	11	0.99	1.44	1.63	1.42	0.22
14	38	10.08	1.03	1.51	1.72	1.5	0.22
15	39	10.26	1.14	1.65	1.82	1.57	0.24
16	40	9.43	1.21	1.75	1.84	1.6	0.25
17	41	9.93	1.31	1.83	1.34	1.63	0.25

Table 9 P-Values

Mo/Mo		2 cm	4 cm	6 cm
	100% Fat	0.049609	0.046603	0.001642
	30% G / 70% F	0.307017	0.003516	0.00028
	50% G / 50% F	0.185262	0.001735	0.000000771
	70% G / 30% F	0.508897	0.59764	0.063892
Mo/ Rh	50 % G/ 50% F	0.182527	0.58817	0.03597

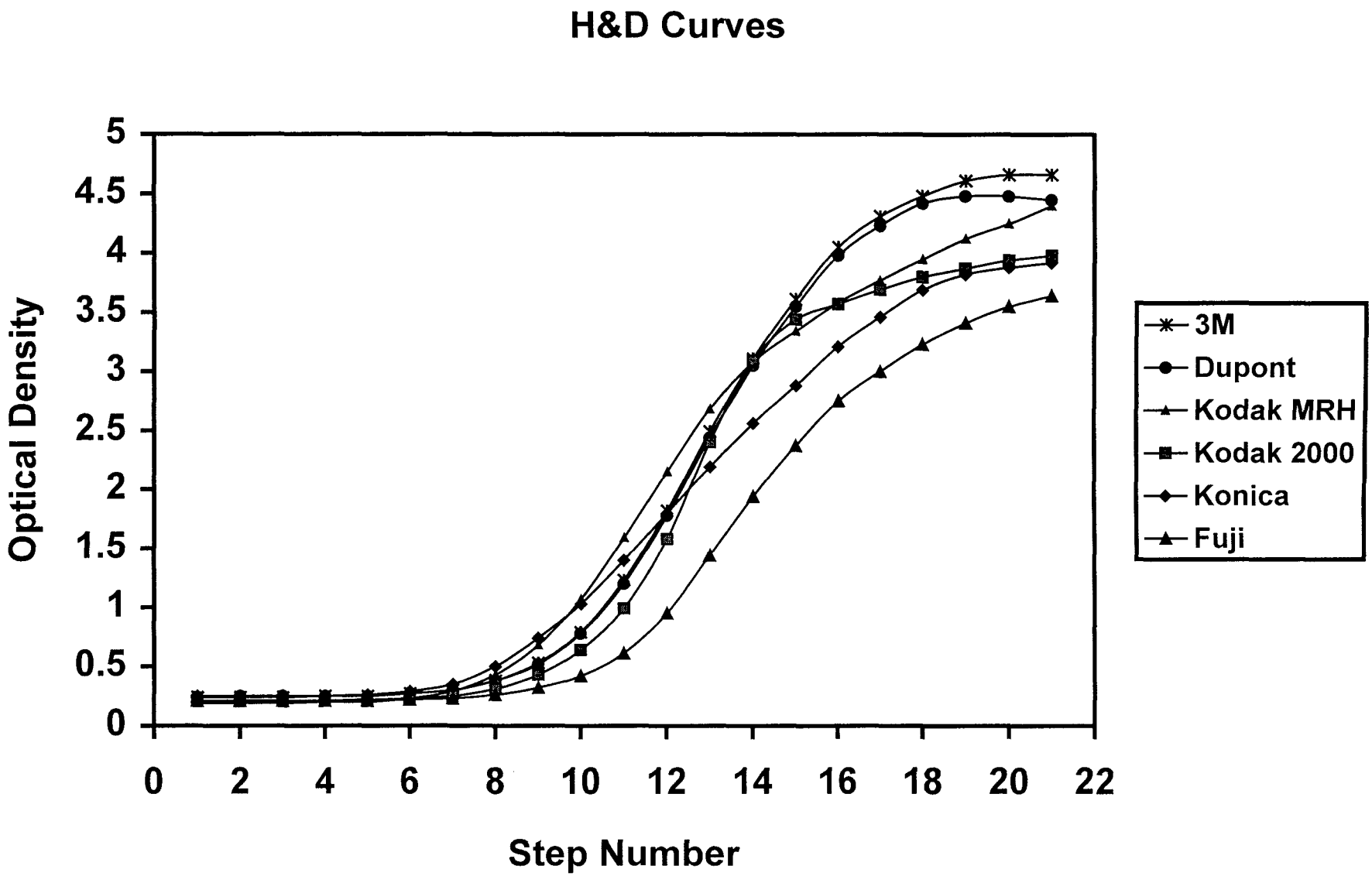
H&D Curves
Optical Density
5
4.5
4
3.5
3
2.5
2
1.5
1
0.5
0
0
2
4
6
8
10
12
14
16
18
20
22
Step Number
3M
Dupont
Kodak MRH
Kodak 2000
Konica
Fuji

Figure 1

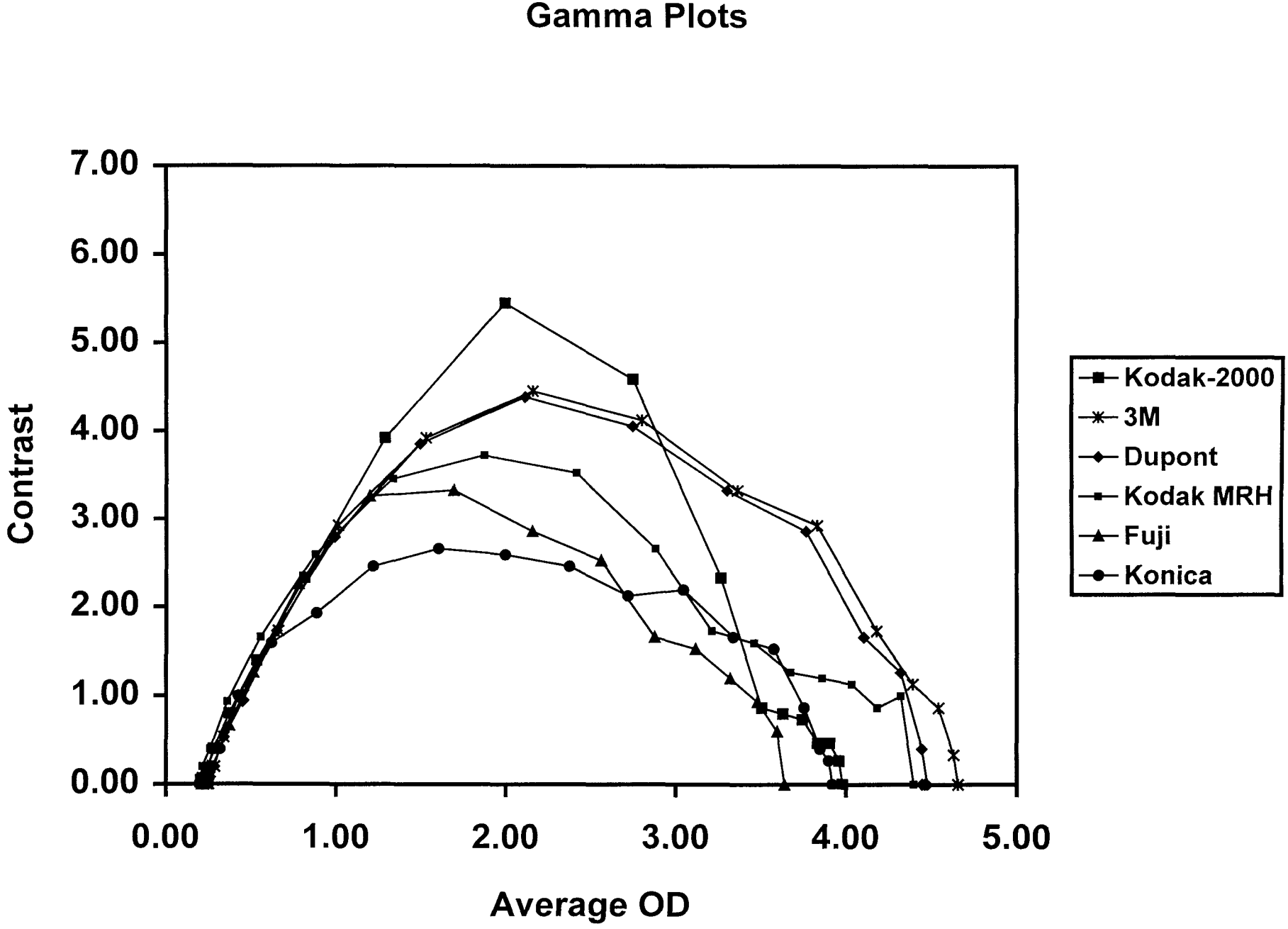
Gamma Plots
7.00
6.00
5.00
4.00
3.00
2.00
1.00
0.00
Contrast
0.00
1.00
2.00
3.00
4.00
5.00
Average OD
Kodak-2000
3M
Dupont
Kodak MRH
Fuji
Konica

Figure 2

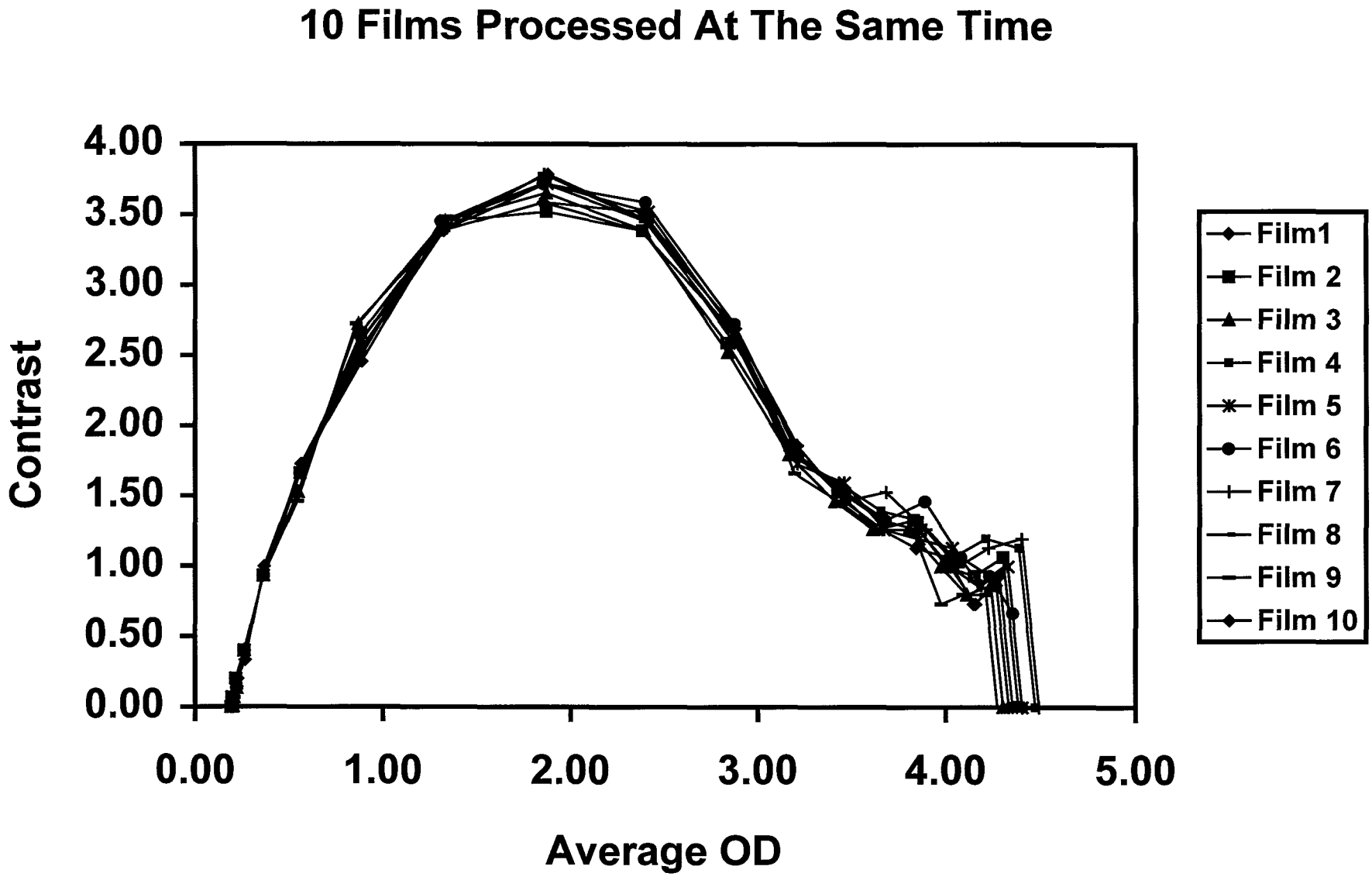
10 Films Processed At The Same Time
Contrast
4.00
3.50
3.00
2.50
2.00
1.50
1.00
0.50
0.00
0.00
1.00
2.00
3.00
4.00
5.00
Average OD
Film1
Film 2
Film 3
Film 4
Film 5
Film 6
Film 7
Film 8
Film 9
Film 10

Figure 3A

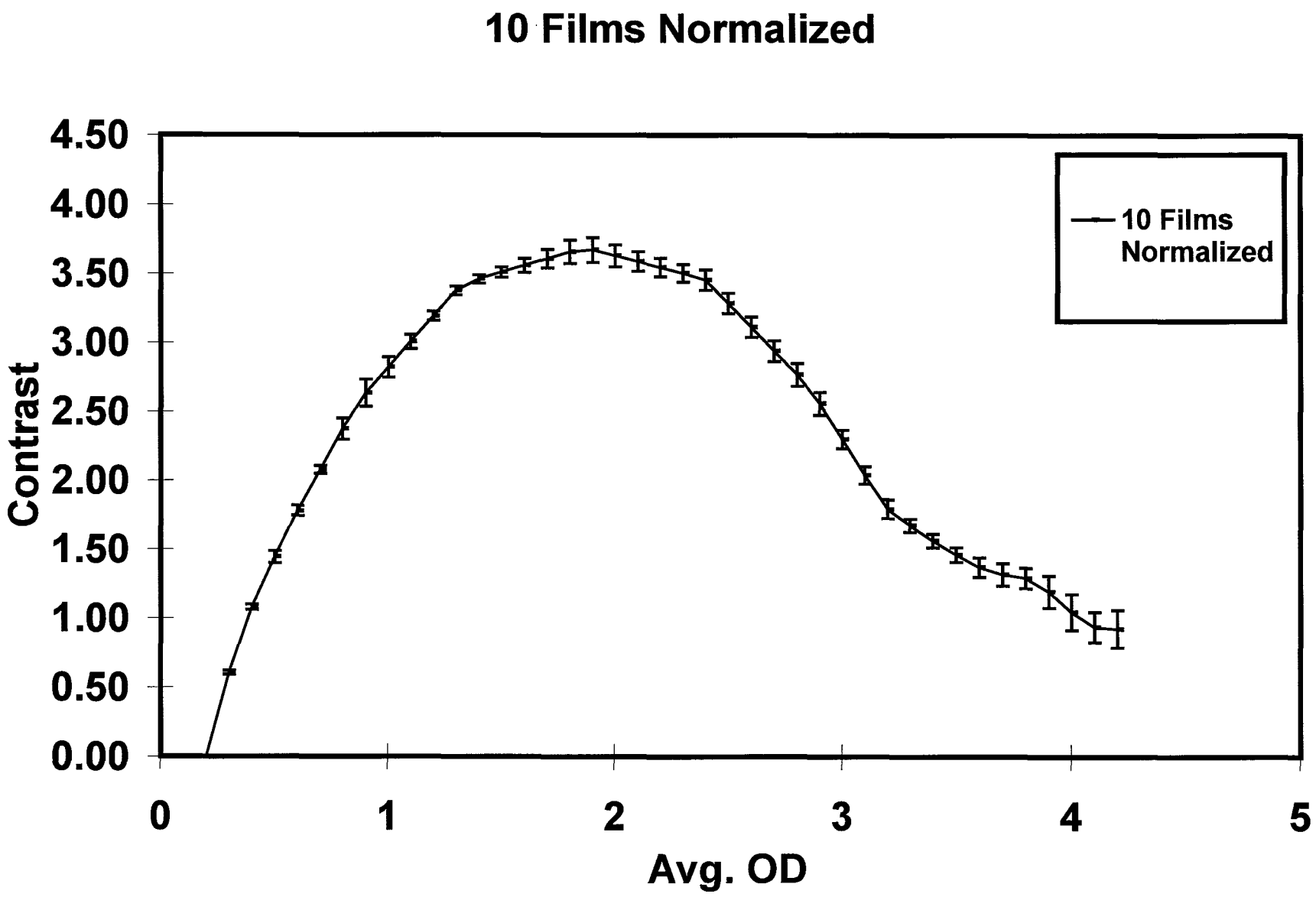
10 Films Normalized
4.50
4.00
3.50
3.00
2.50
2.00
1.50
1.00
0.50
0.00
Contrast
0
1
2
3
4
5
Avg. OD
10 Films Normalized

Figure 3B

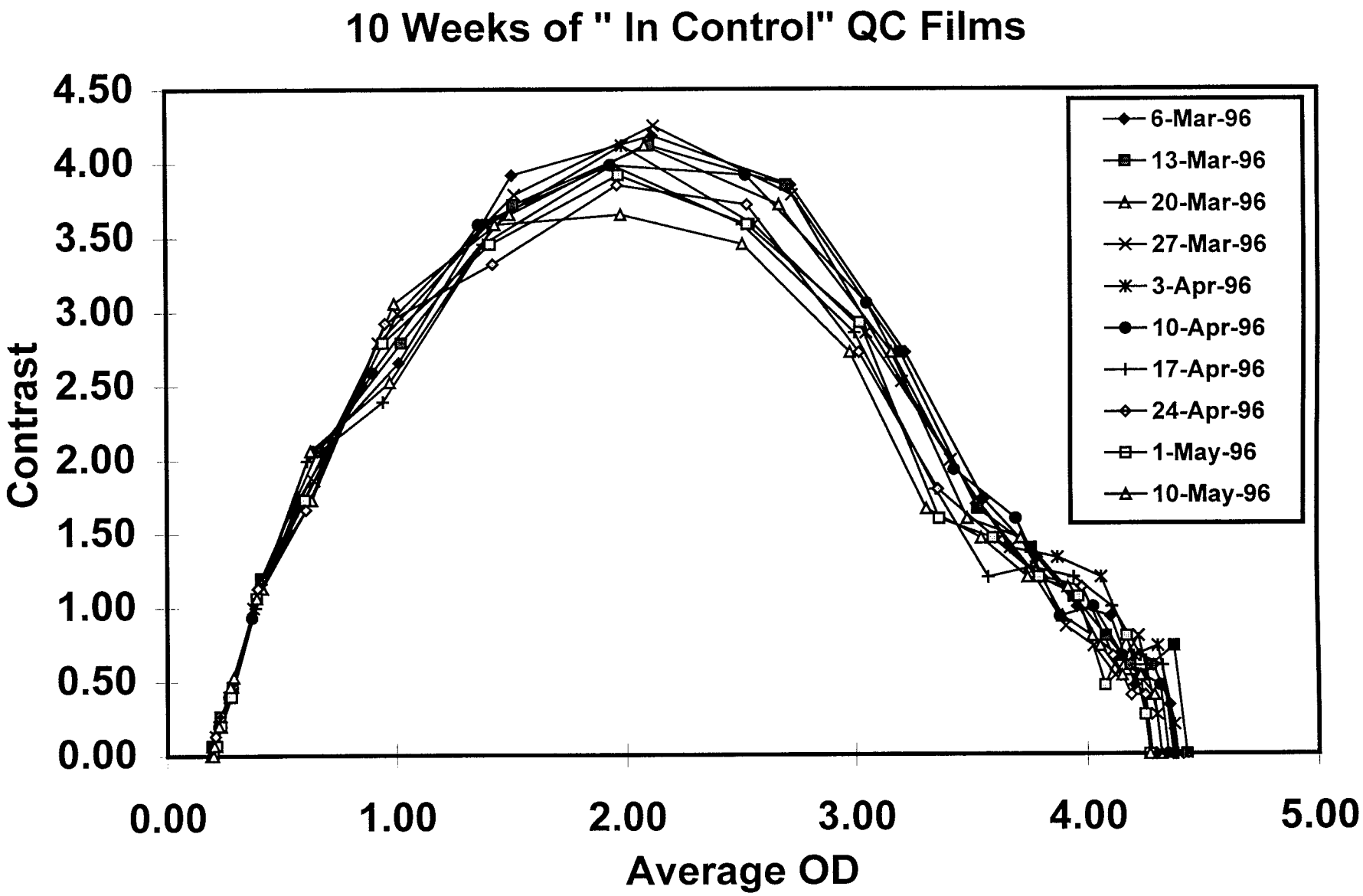
10 Weeks of " In Control" QC Films
Contrast
4.50
4.00
3.50
3.00
2.50
2.00
1.50
1.00
0.50
0.00
0.00
1.00
2.00
3.00
4.00
5.00
Average OD
6-Mar-96
13-Mar-96
20-Mar-96
27-Mar-96
3-Apr-96
10-Apr-96
17-Apr-96
24-Apr-96
1-May-96
10-May-96

Figure 4A

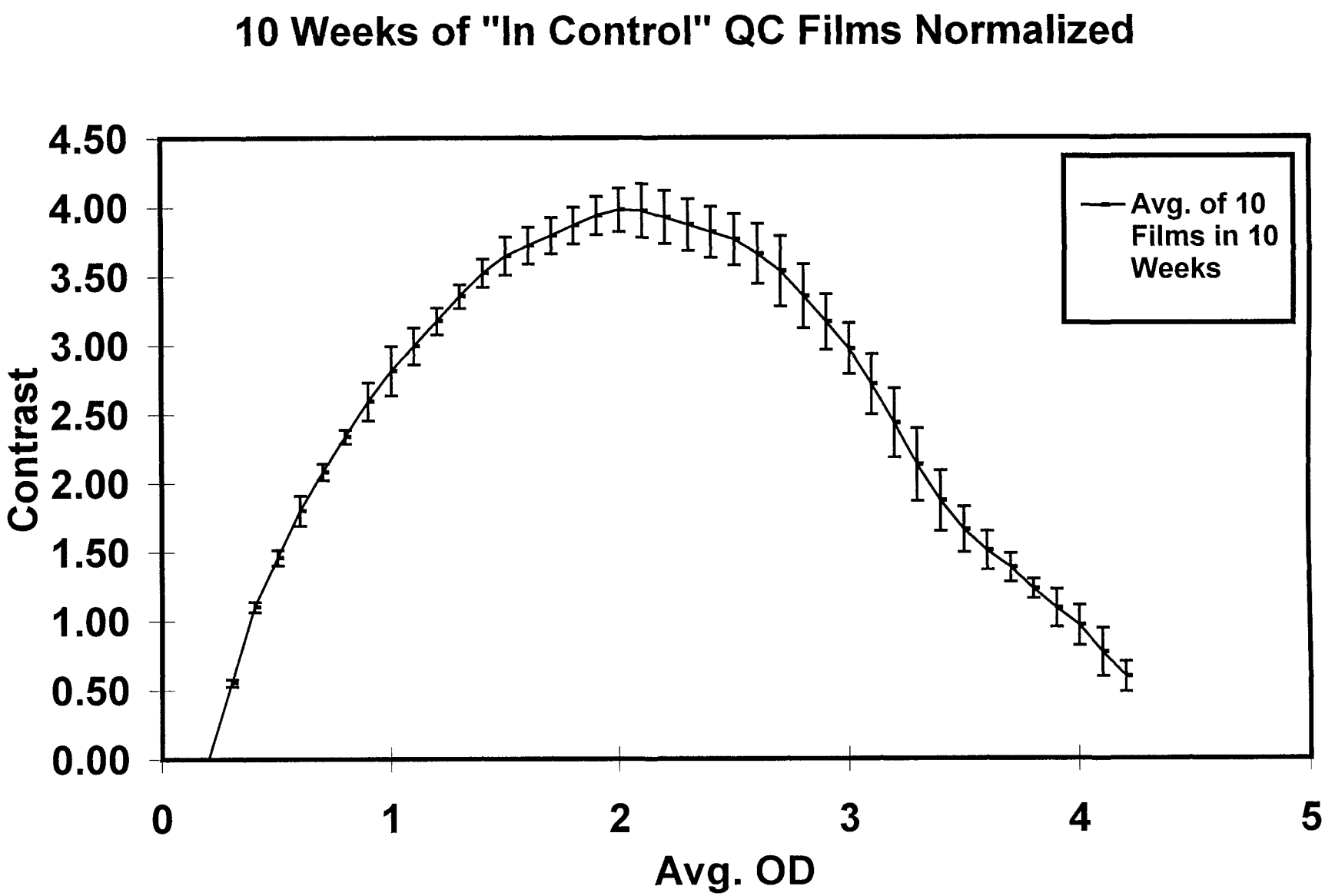
10 Weeks of "In Control" QC Films Normalized
Contrast
4.50
4.00
3.50
3.00
2.50
2.00
1.50
1.00
0.50
0.00
0
1
2
3
4
5
Avg. OD
Avg. of 10 Films in 10 Weeks

Figure 4B

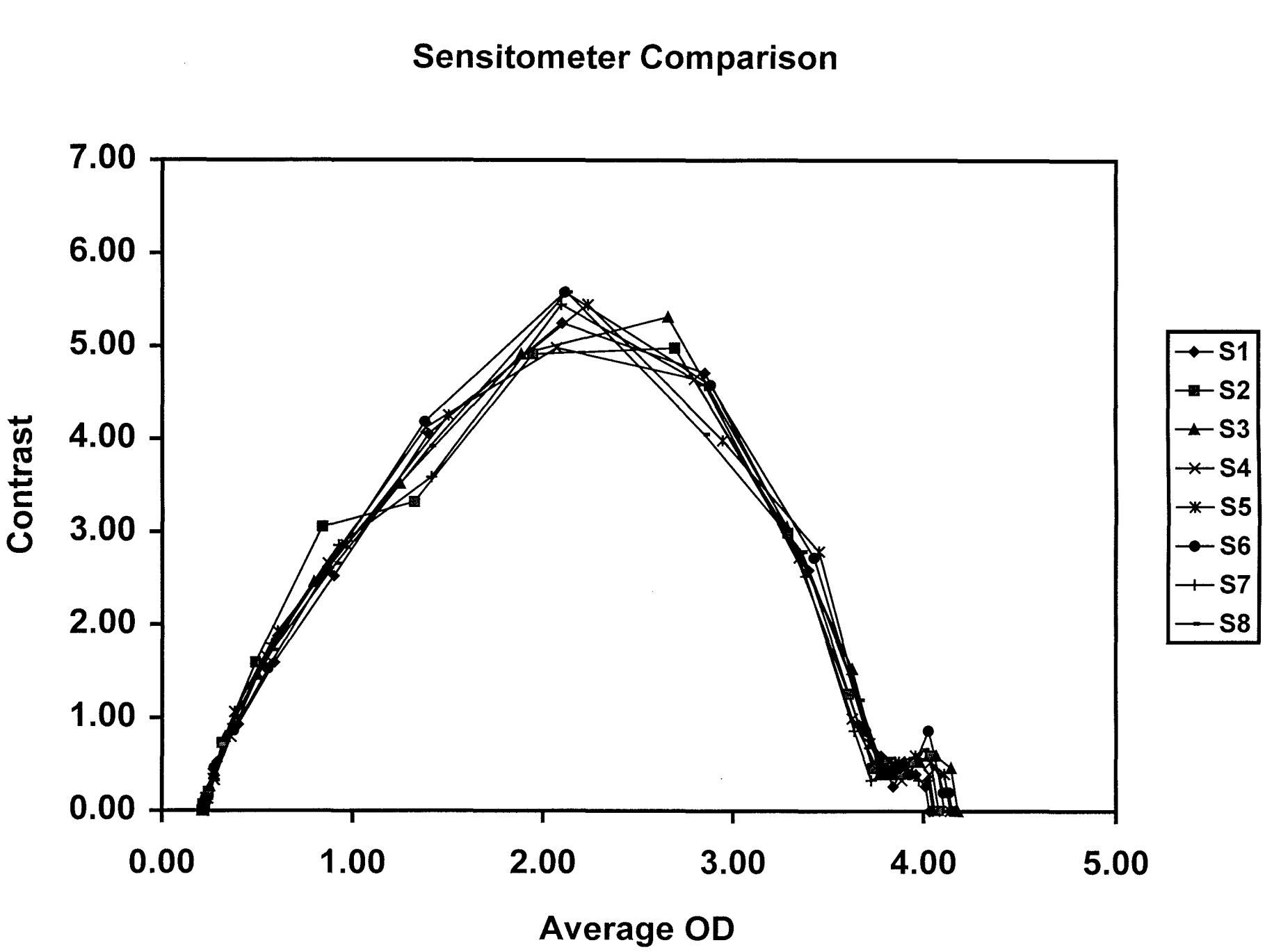
Sensitometer Comparison
7.00
6.00
5.00
4.00
3.00
2.00
1.00
0.00
Contrast
0.00
1.00
2.00
3.00
4.00
5.00
Average OD
S1
S2
S3
S4
S5
S6
S7
S8

Figure 5

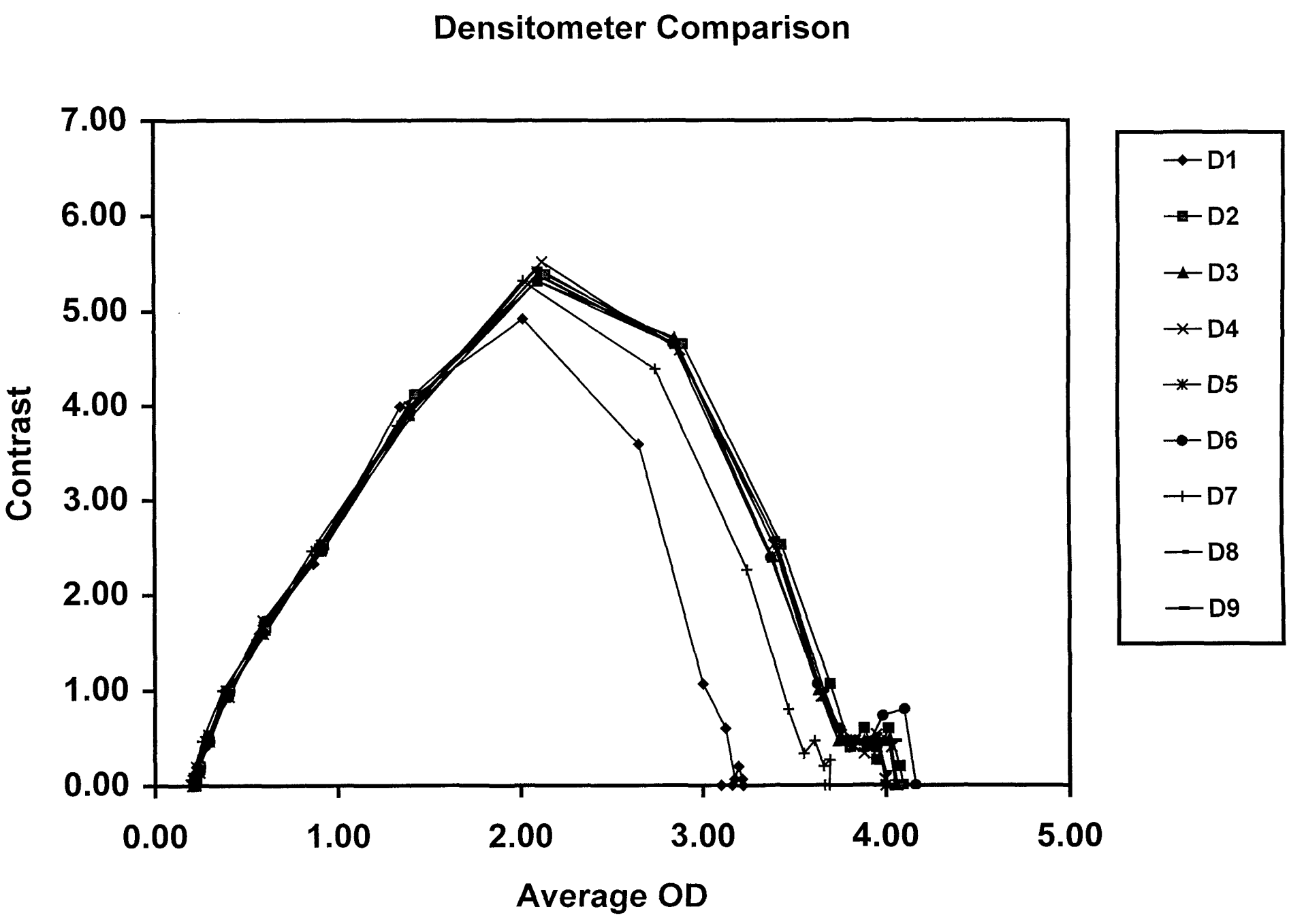
Densitometer Comparison
Contrast
7.00
6.00
5.00
4.00
3.00
2.00
1.00
0.00
0.00
1.00
2.00
3.00
4.00
5.00
Average OD
D1
D2
D3
D4
D5
D6
D7
D8
D9

Figure 6

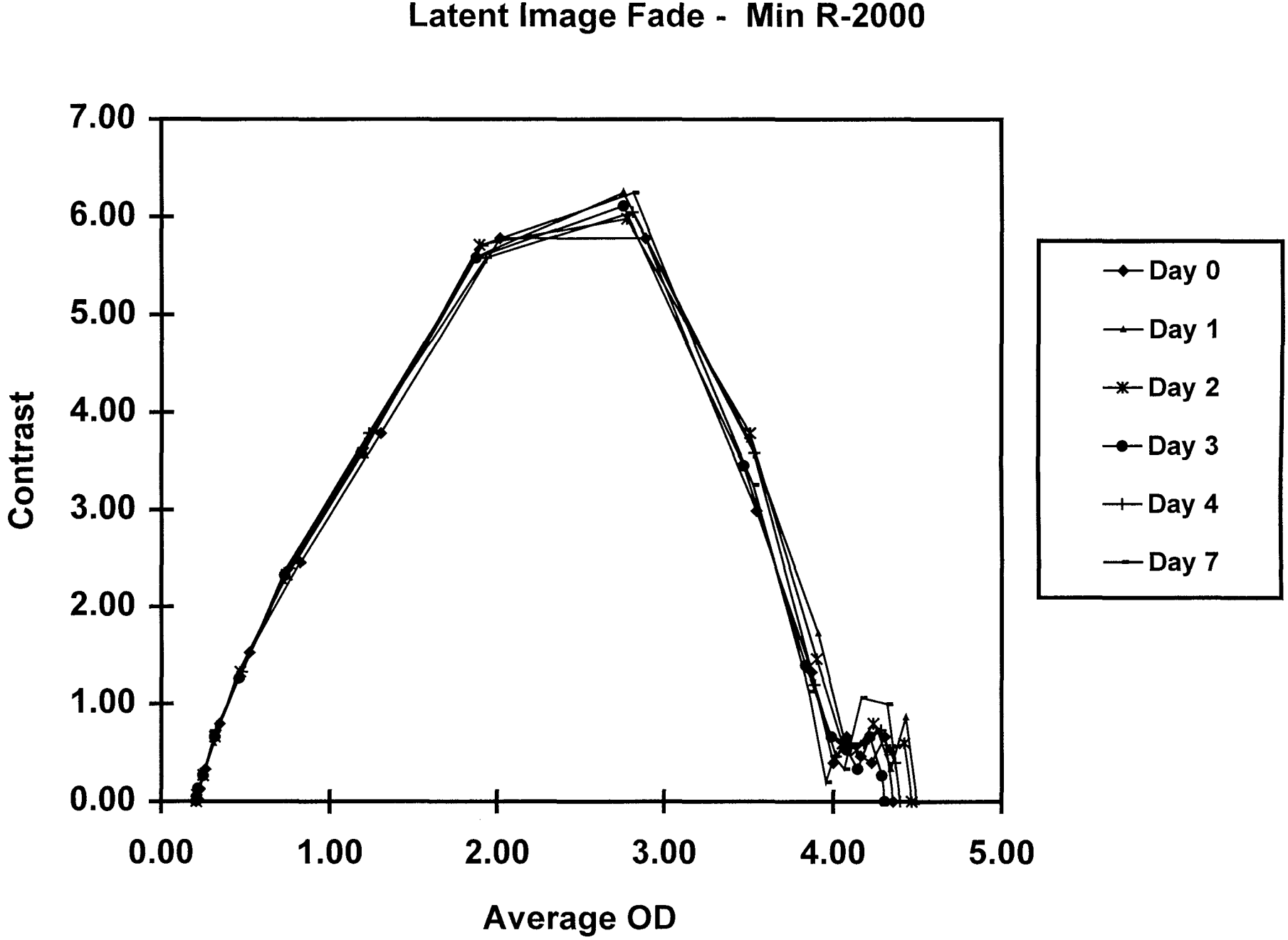
Latent Image Fade - Min R-2000
Contrast
7.00
6.00
5.00
4.00
3.00
2.00
1.00
0.00
0.00
1.00
2.00
3.00
4.00
5.00
Average OD
Day 0
Day 1
Day 2
Day 3
Day 4
Day 7

Figure 7

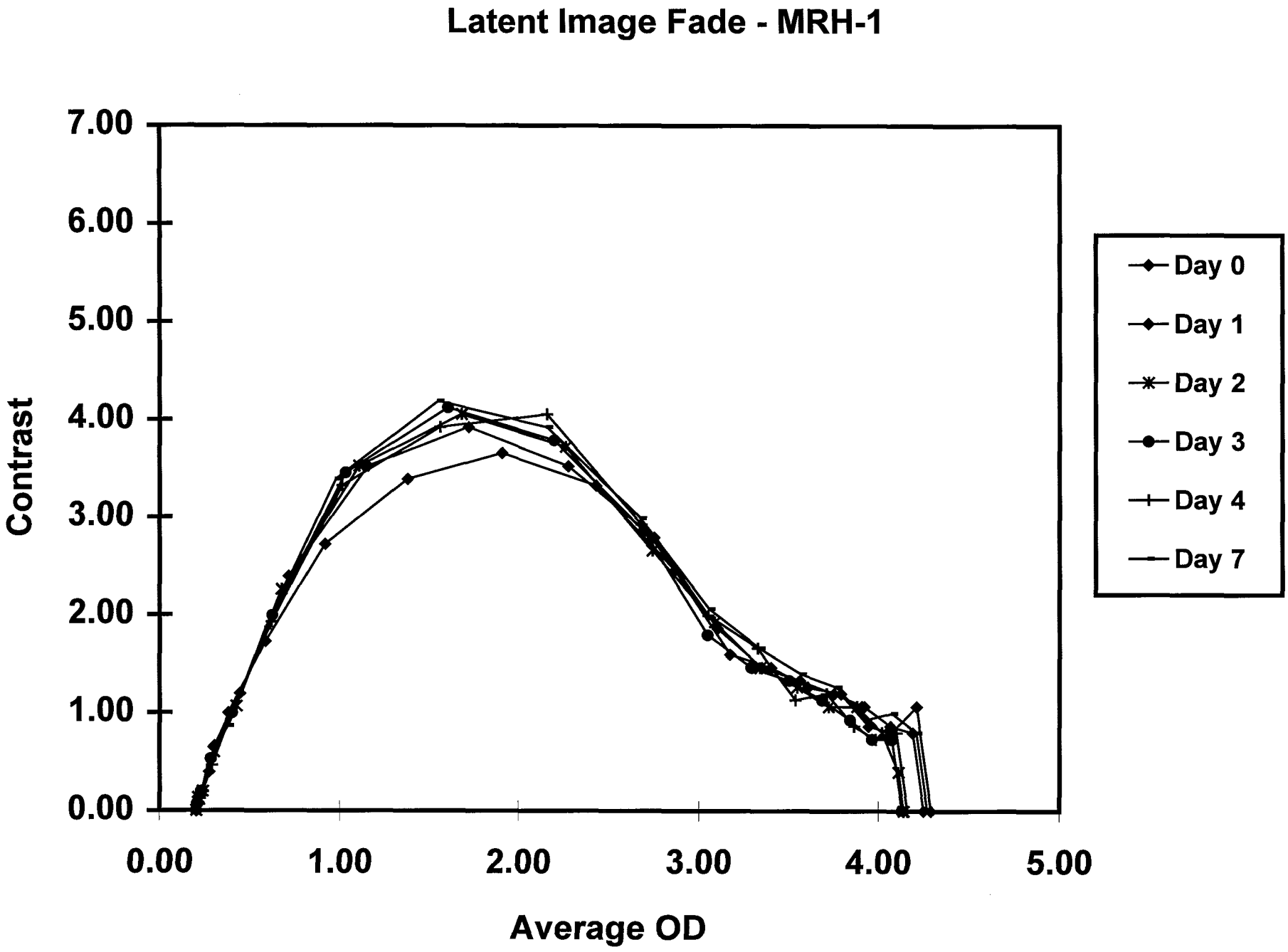
Latent Image Fade - MRH-1
Contrast
7.00
6.00
5.00
4.00
3.00
2.00
1.00
0.00
0.00
1.00
2.00
3.00
4.00
5.00
Average OD
Day 0
Day 1
Day 2
Day 3
Day 4
Day 7

Figure 8

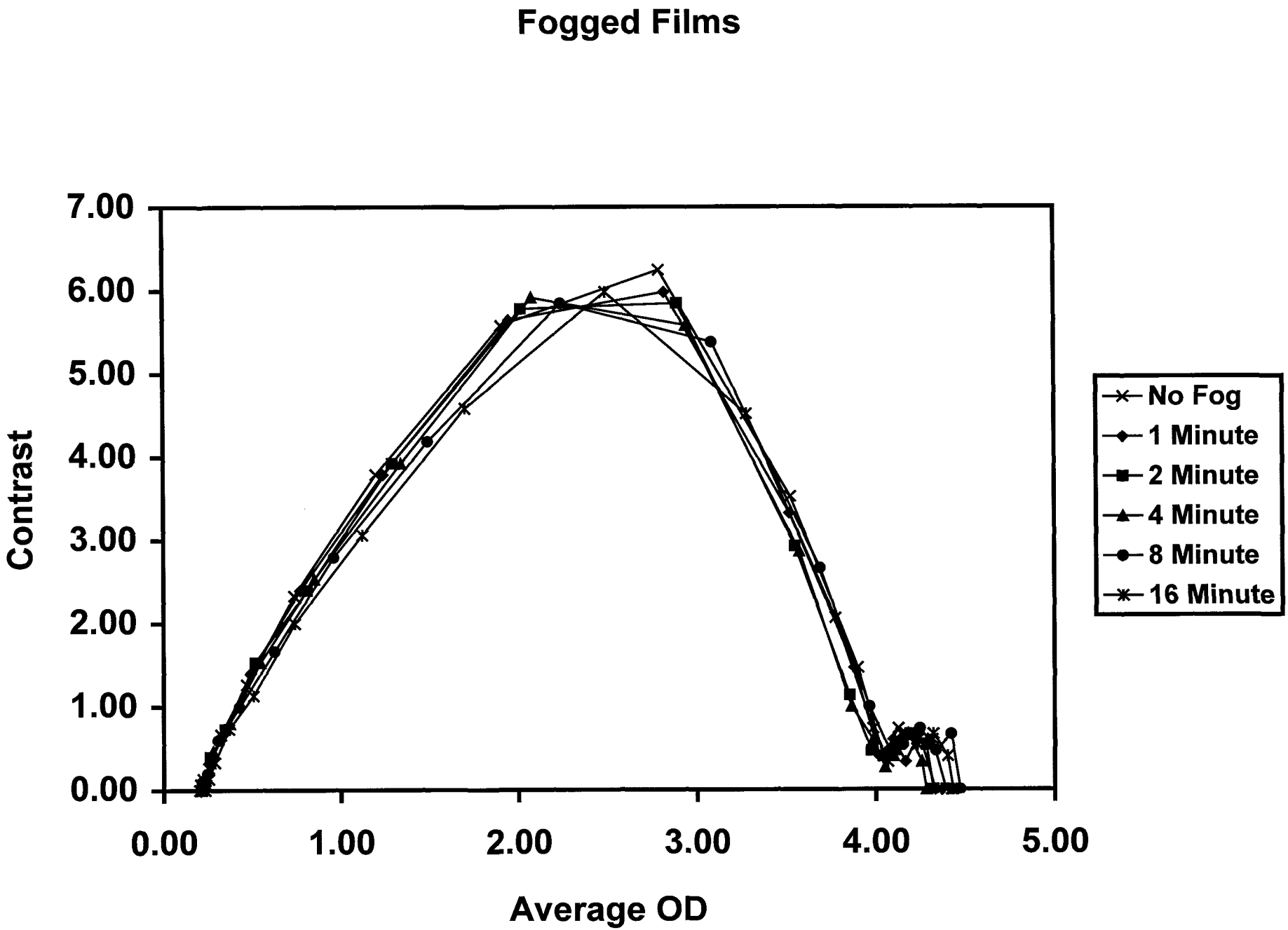
Fogged Films
Contrast
7.00
6.00
5.00
4.00
3.00
2.00
1.00
0.00
0.00
1.00
2.00
3.00
4.00
5.00
Average OD
No Fog
1 Minute
2 Minute
4 Minute
8 Minute
16 Minute

Figure 9

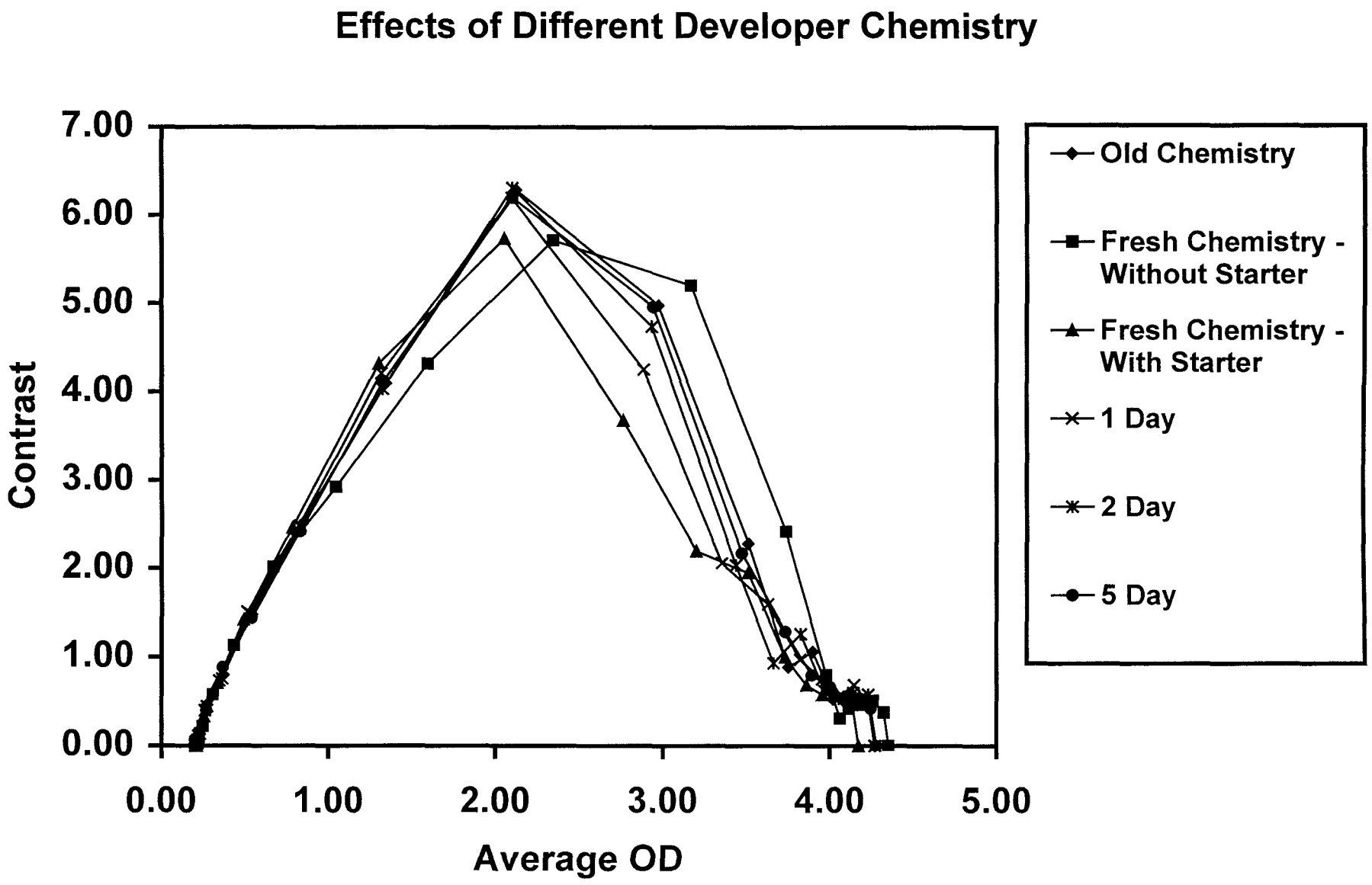
Effects of Different Developer Chemistry
Contrast
7.00
6.00
5.00
4.00
3.00
2.00
1.00
0.00
0.00
1.00
2.00
3.00
4.00
5.00
Average OD
Old Chemistry
Fresh Chemistry - Without Starter
Fresh Chemistry - With Starter
1 Day
2 Day
5 Day

figure 10

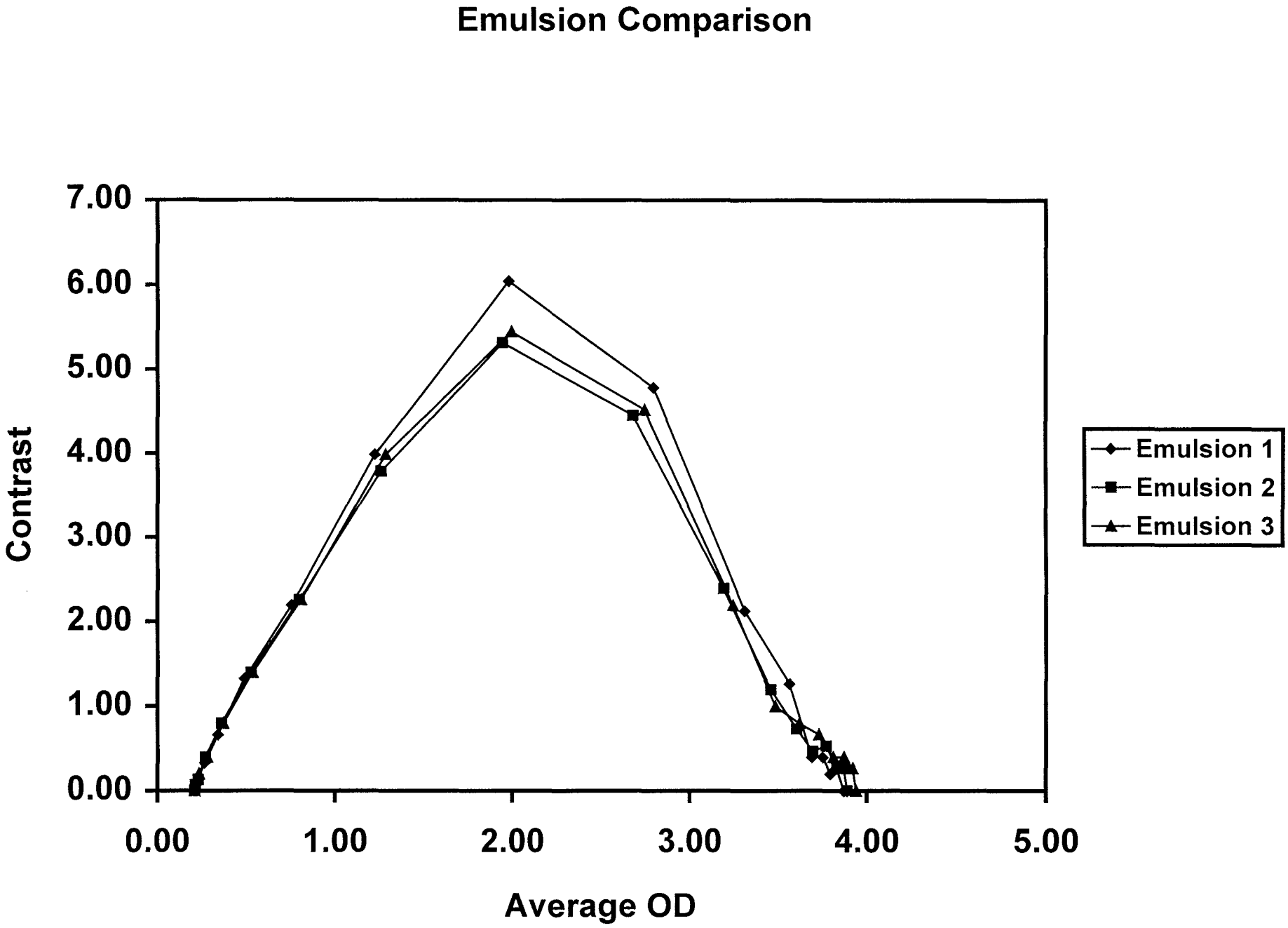
Emulsion Comparison
Contrast
7.00
6.00
5.00
4.00
3.00
2.00
1.00
0.00
0.00
1.00
2.00
3.00
4.00
5.00
Average OD
Emulsion 1
Emulsion 2
Emulsion 3

Figure 11

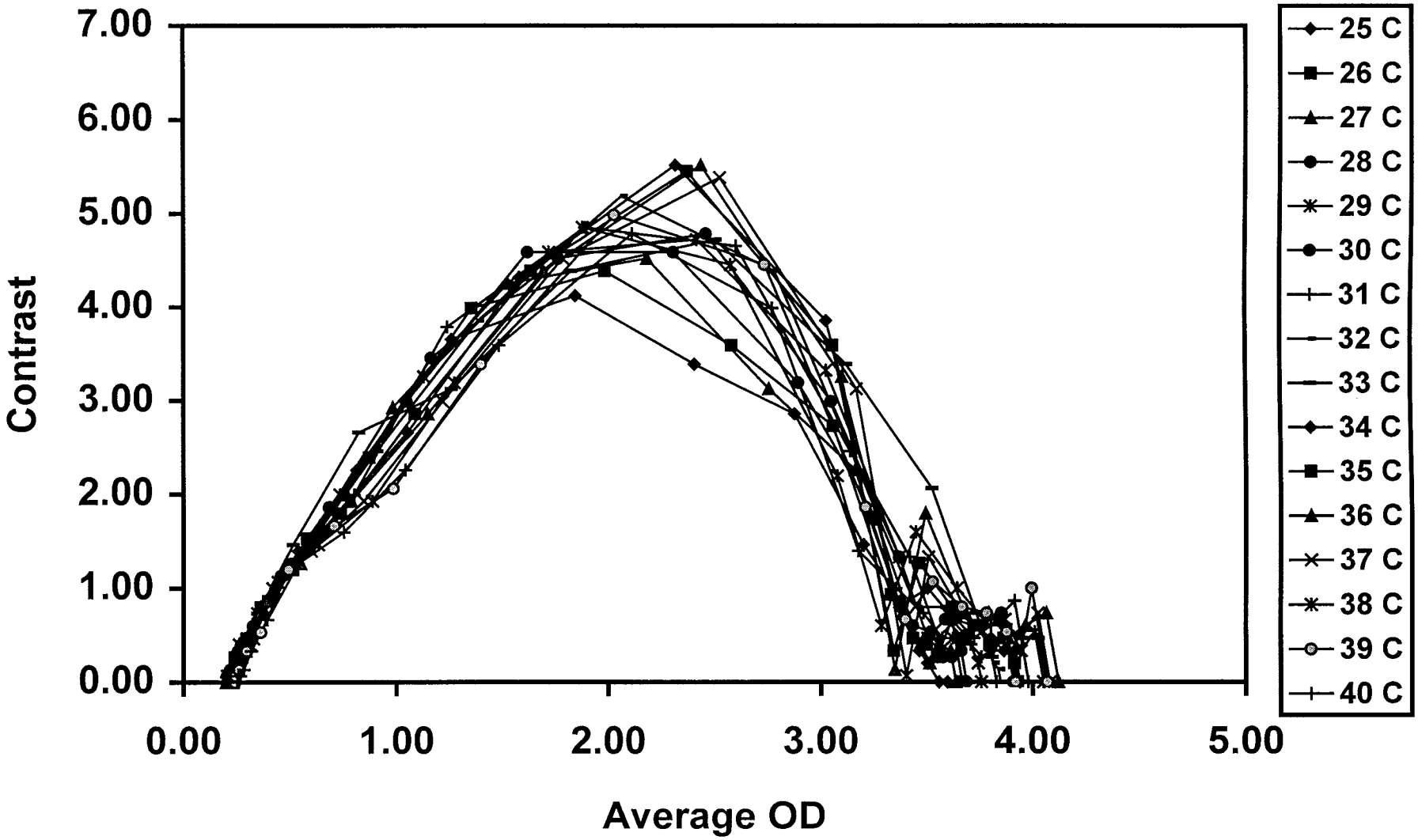
Developer Temperature Comparison
Contrast
7.00
6.00
5.00
4.00
3.00
2.00
1.00
0.00
0.00
1.00
2.00
3.00
4.00
5.00
Average OD
25 C
26 C
27 C
28 C
29 C
30 C
31 C
32 C
33 C
34 C
35 C
36 C
37 C
38 C
39 C
40 C

Figure 12

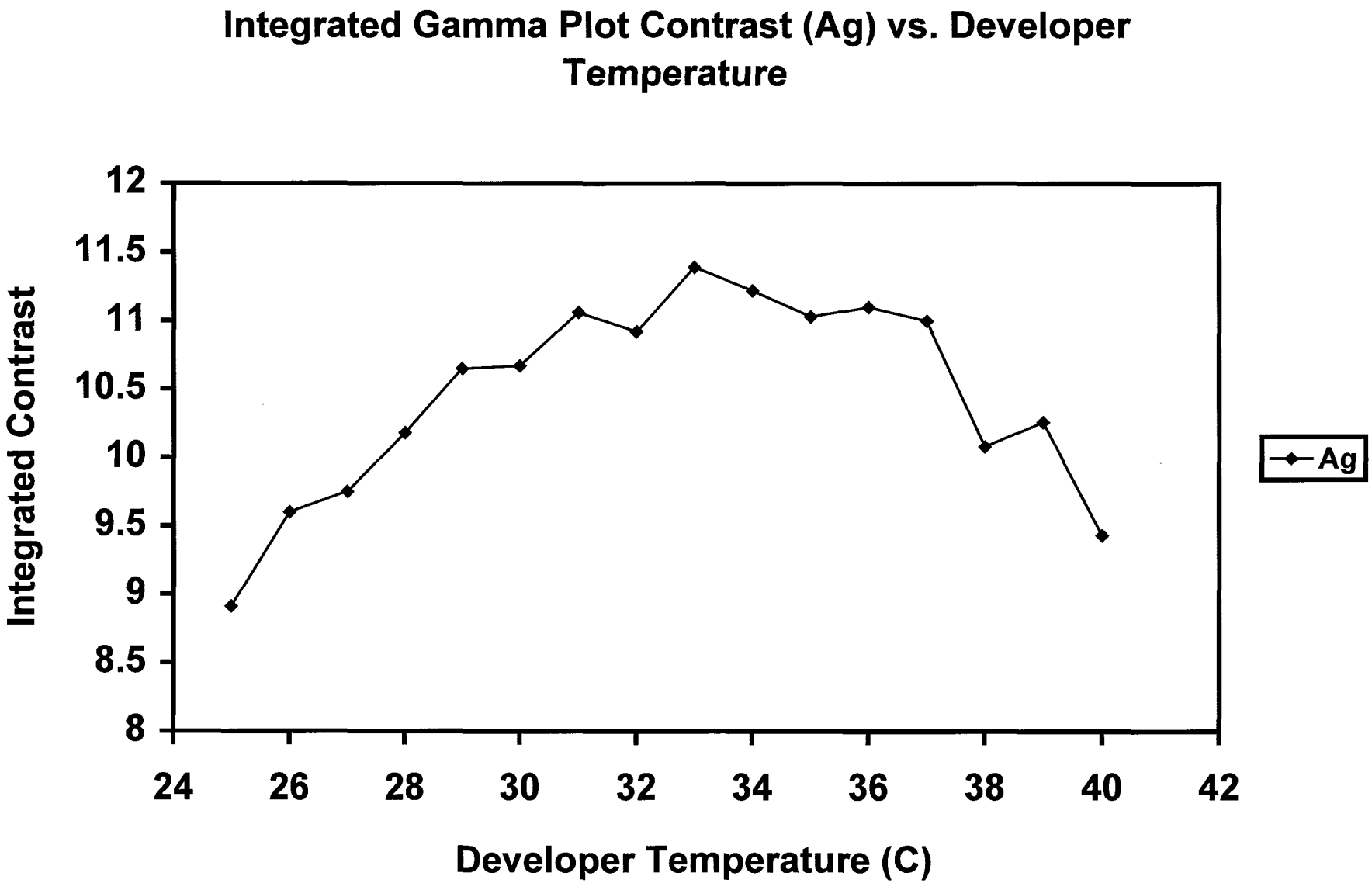
Integrated Gamma Plot Contrast (Ag) vs. Developer Temperature
Integrated Contrast
12
11.5
11
10.5
10
9.5
9
8.5
8
24
26
28
30
32
34
36
38
40
42
Developer Temperature (C)
Ag

Figure 13

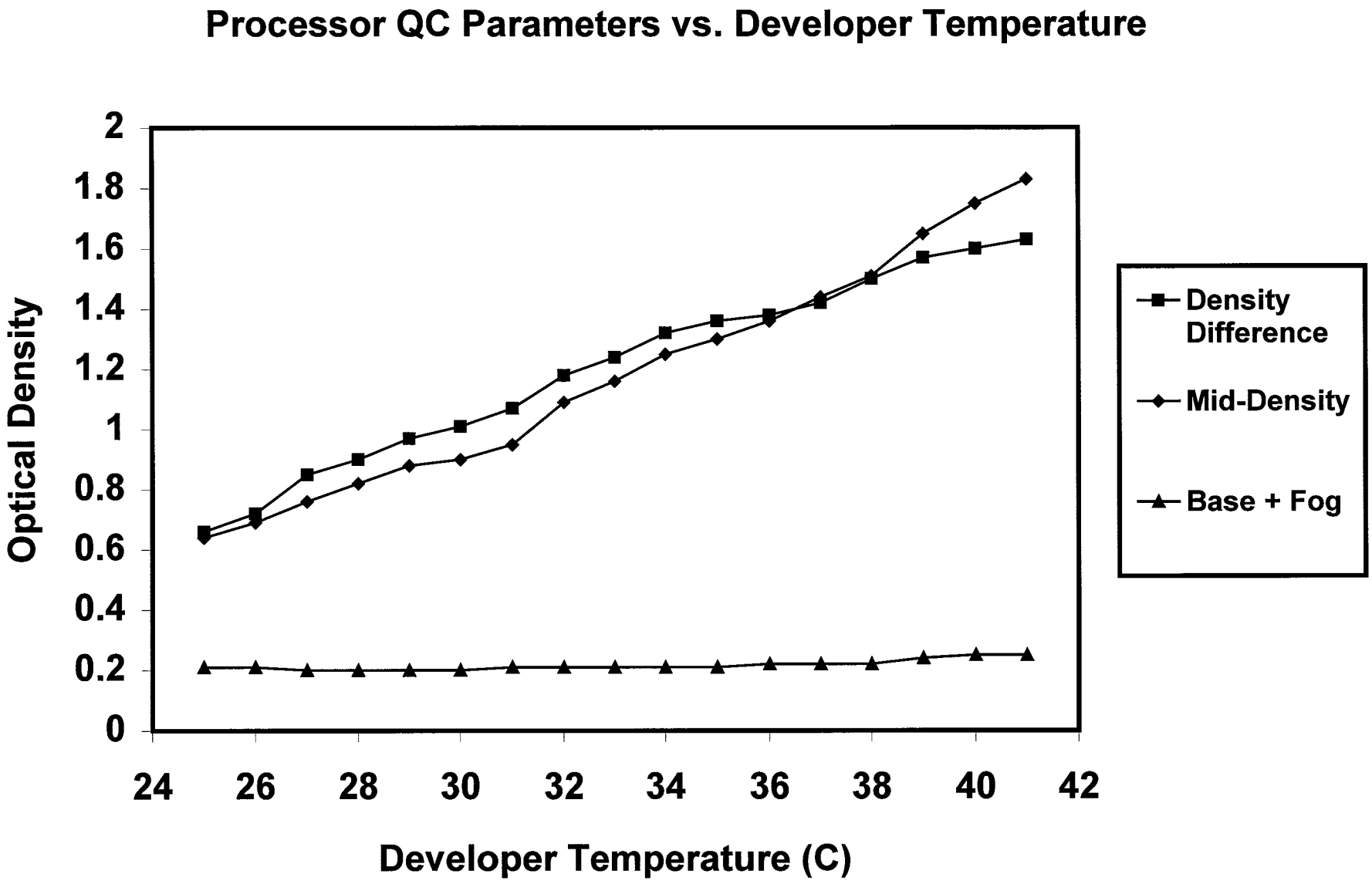
Processor QC Parameters vs. Developer Temperature
Optical Density
2
1.8
1.6
1.4
1.2
1
0.8
0.6
0.4
0.2
0
24
26
28
30
32
34
36
38
40
42
Developer Temperature (C)
Density Difference
Mid-Density
Base + Fog

Figure 14

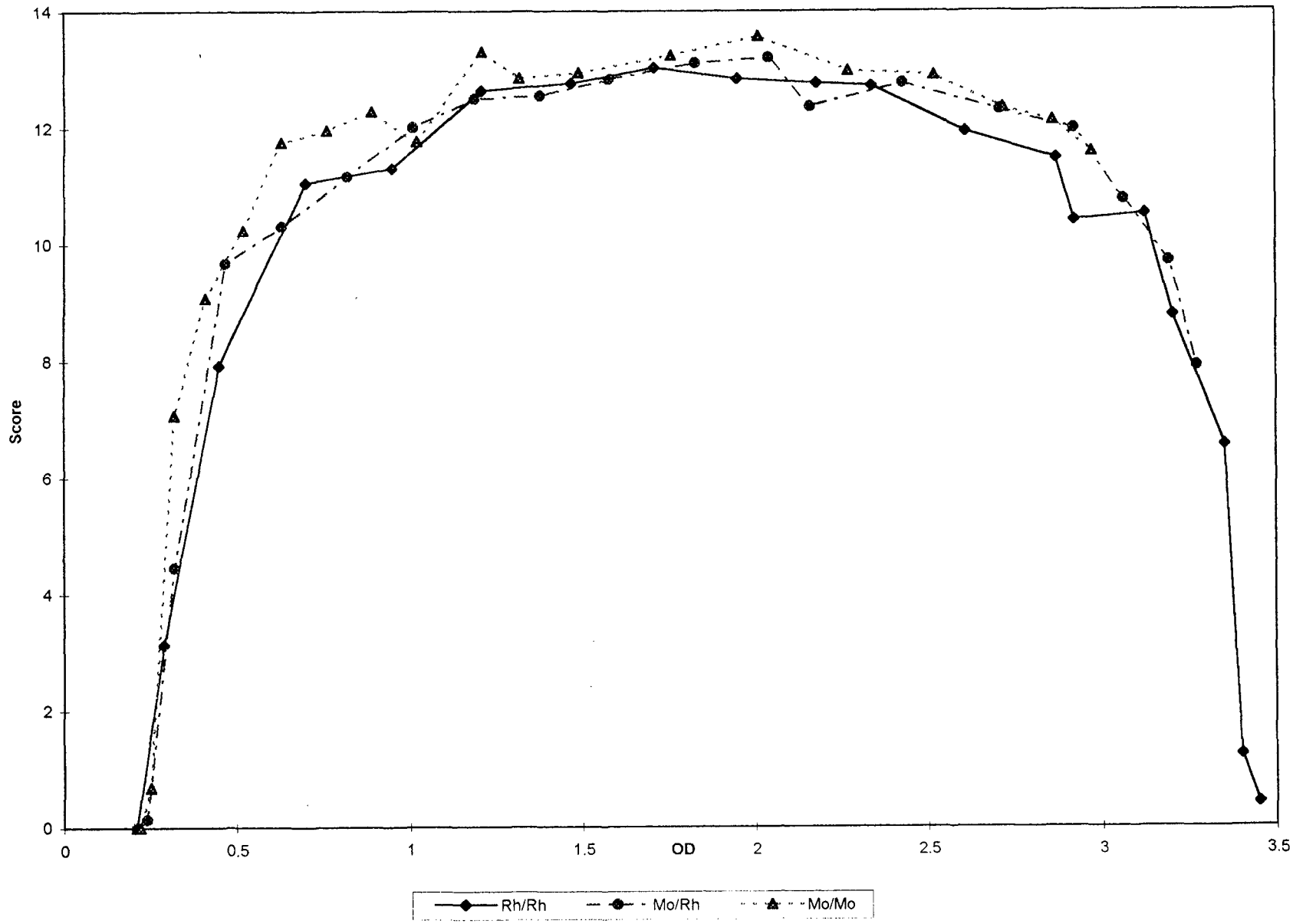

Figure 15A

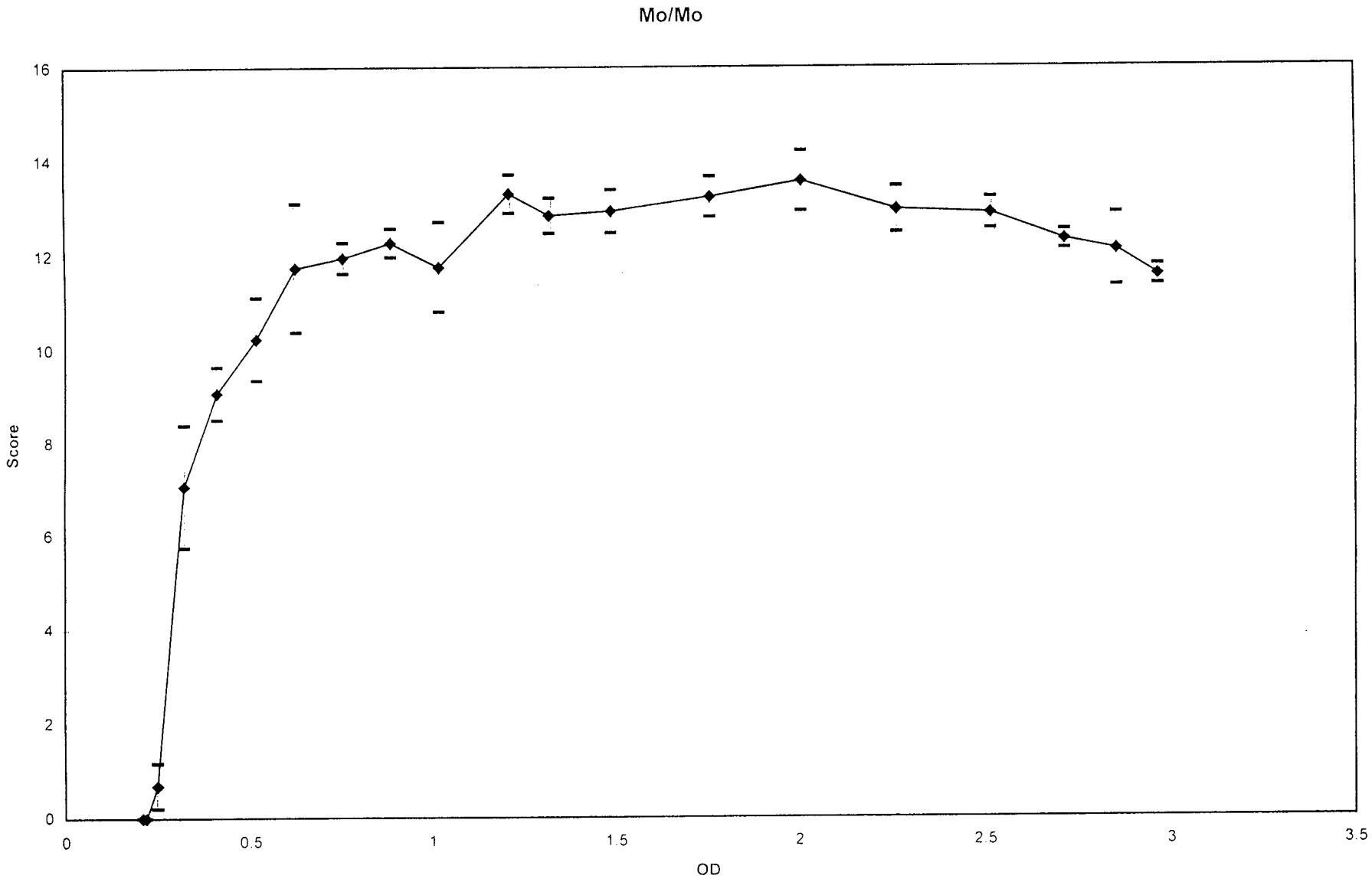

Figure 15B

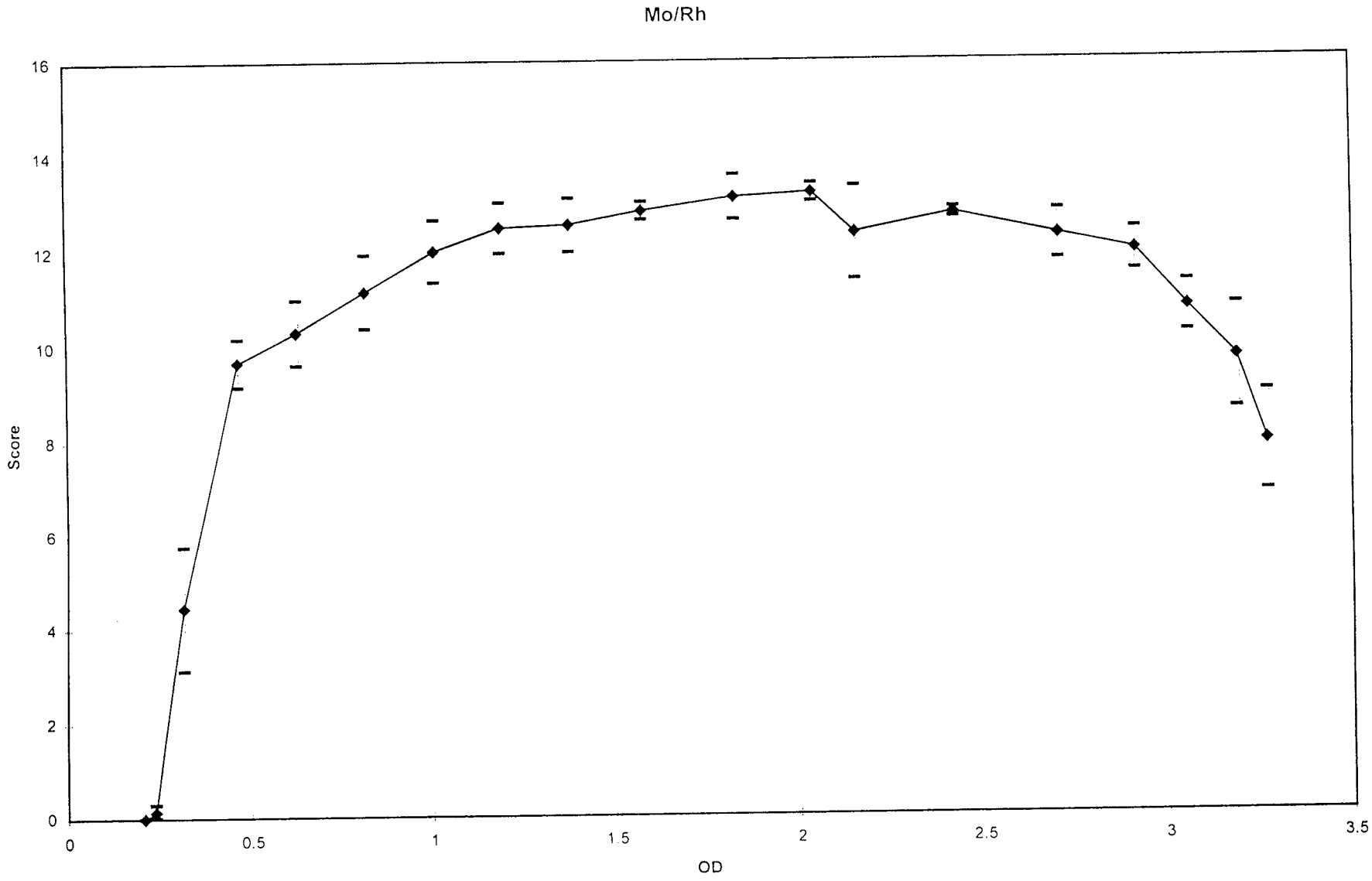

Figure 15C

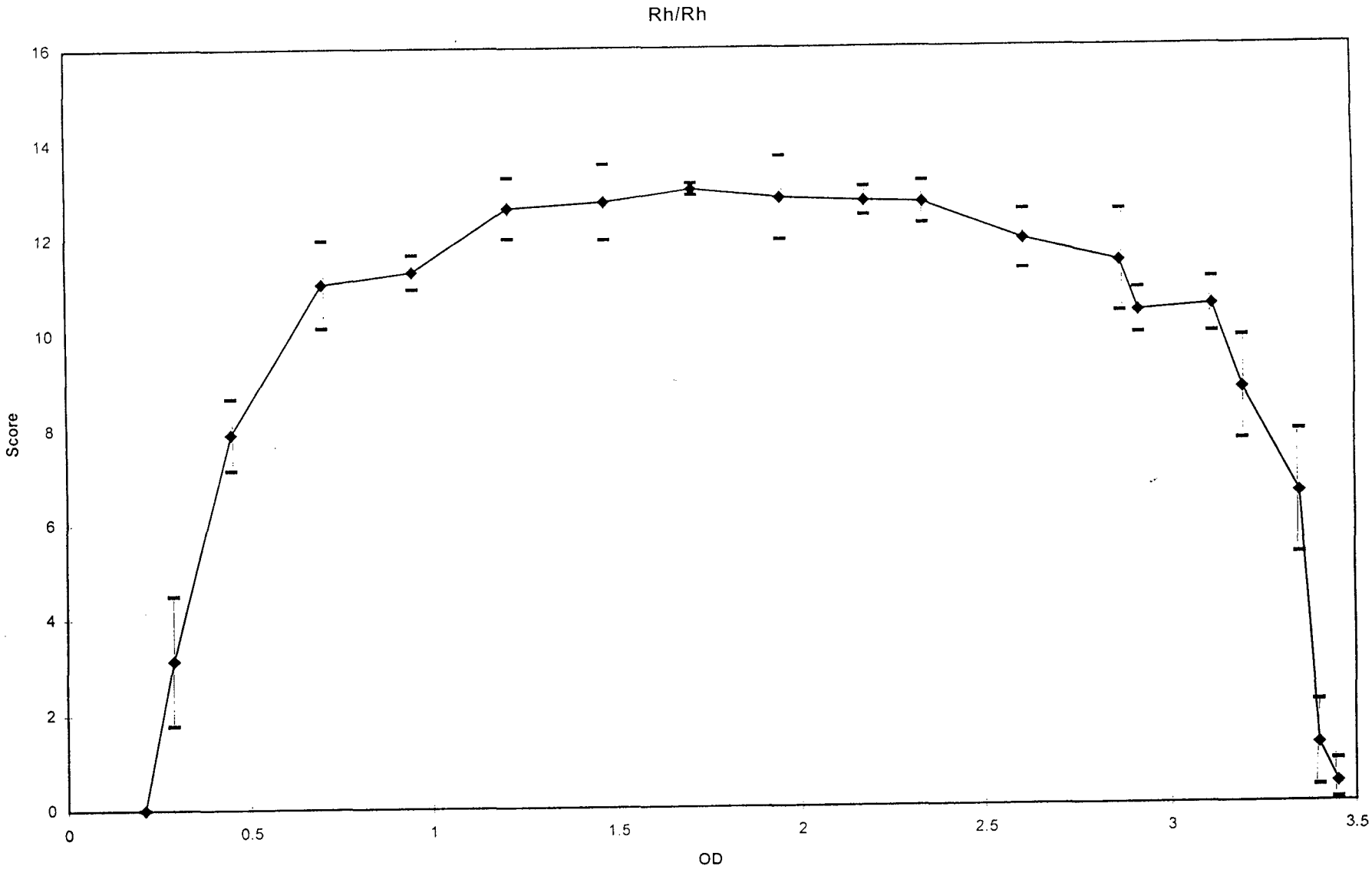

Figure 15D

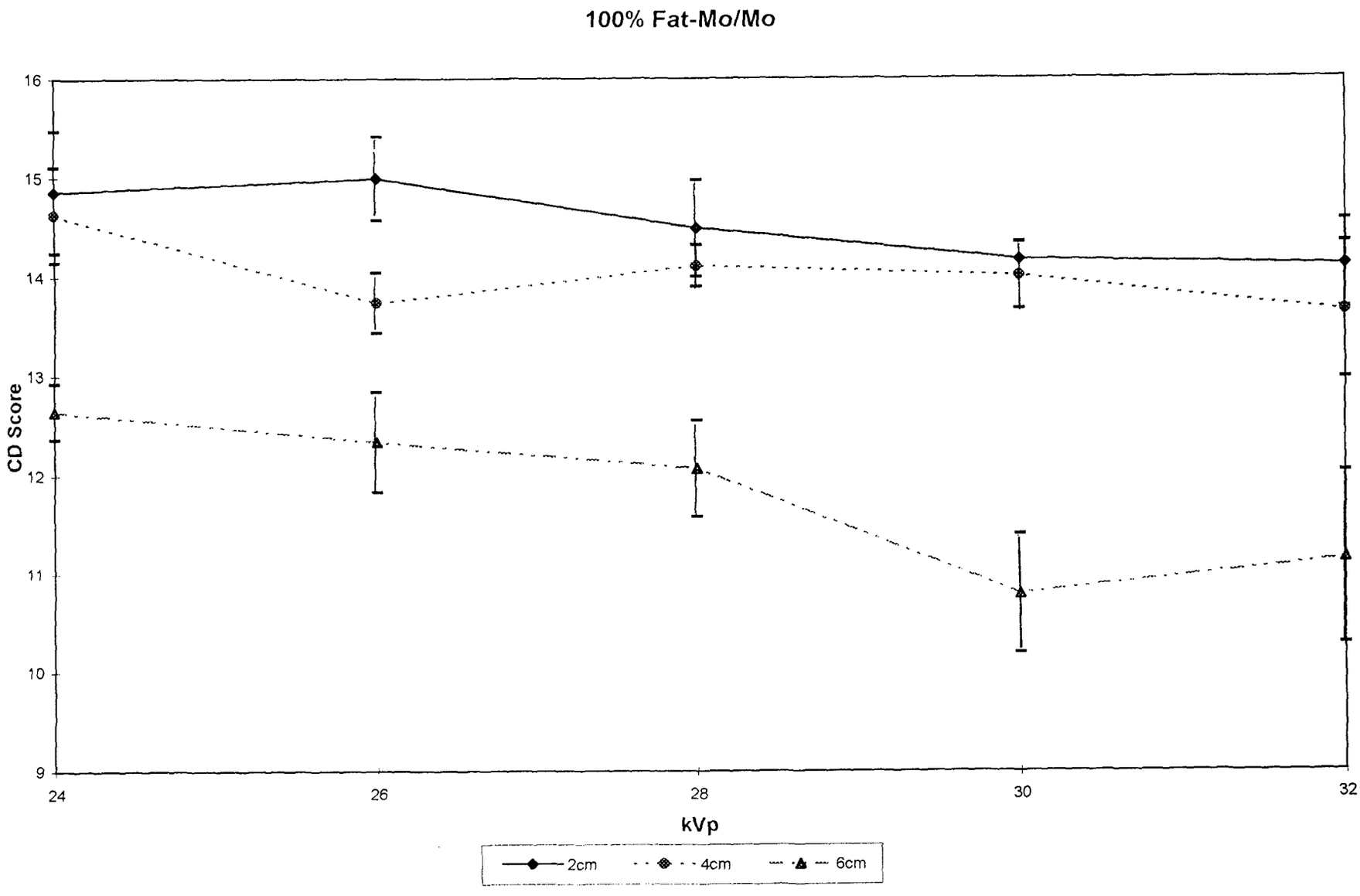
100% Fat-Mo/Mo
CD Score
16
15
14
13
12
11
10
9
24
26
28
30
32
kVp
2cm
4cm
6cm

Figure 16A

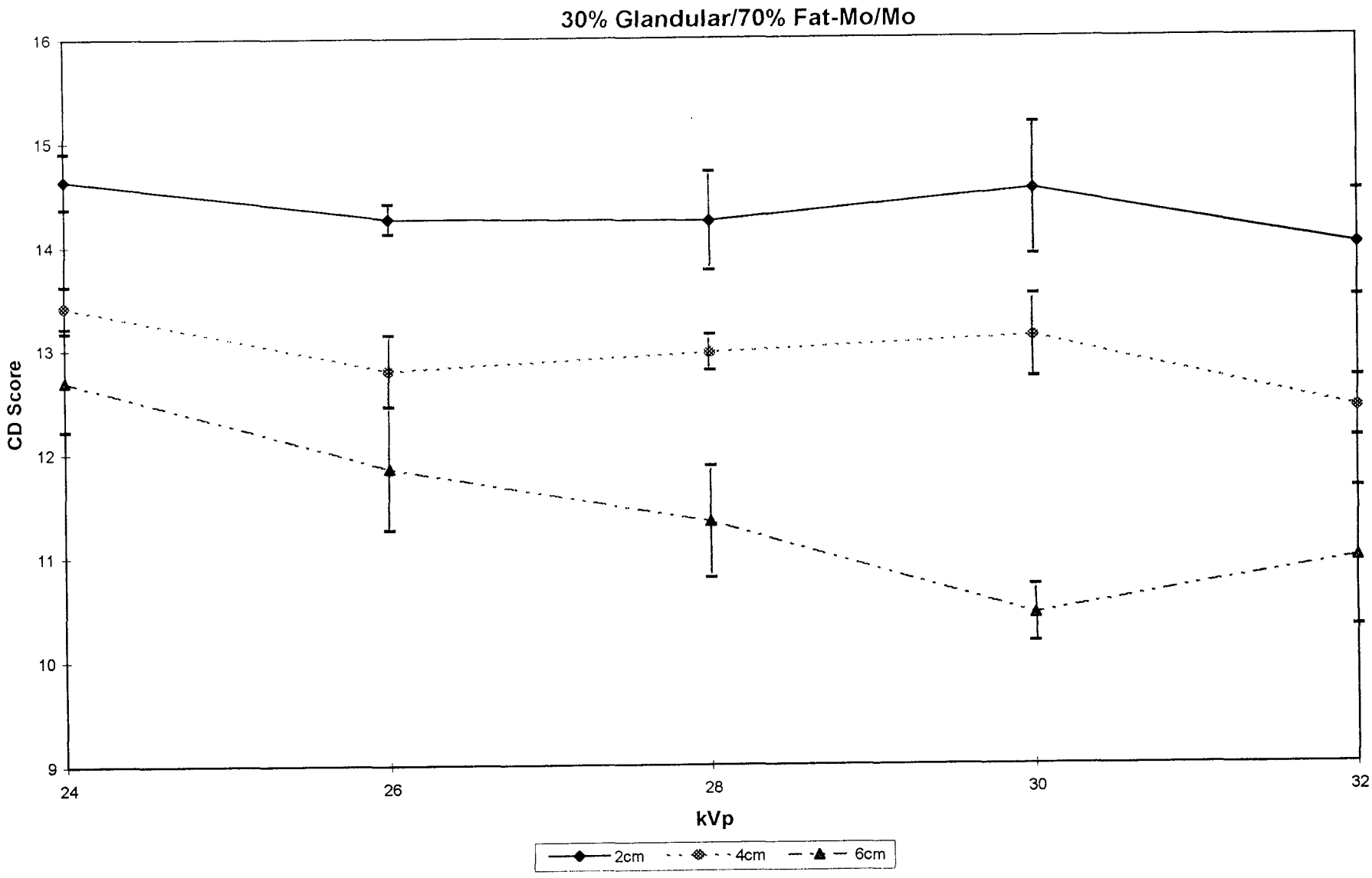
30% Glandular/70% Fat-Mo/Mo
CD Score
16
15
14
13
12
11
10
9
24
26
28
30
32
kVp
2cm
4cm
6cm

Figure 16B

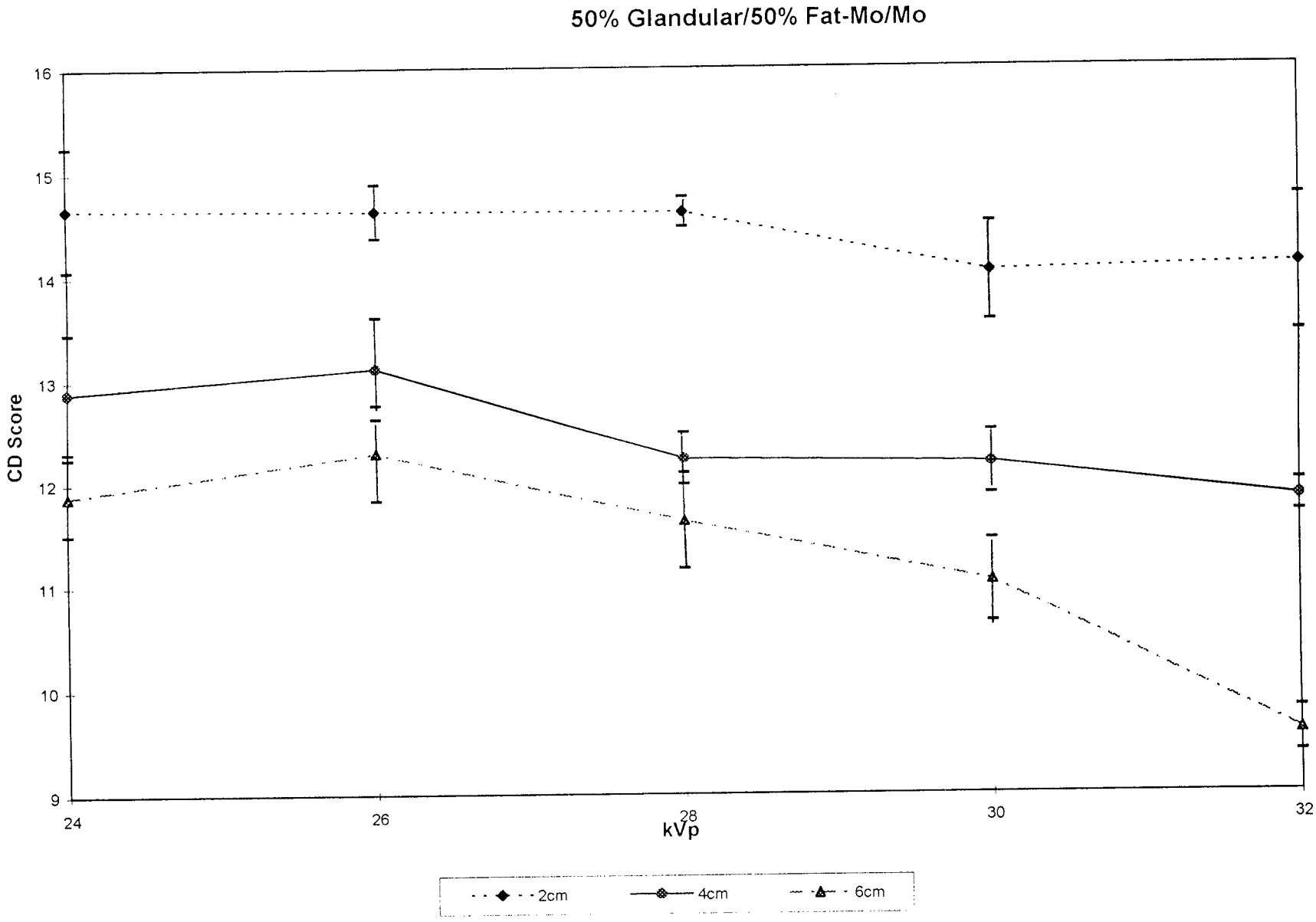
50% Glandular/50% Fat-Mo/Mo
CD Score
16
15
14
13
12
11
10
9
24
26
28
30
32
kVp
2cm
4cm
6cm

Figure 16C

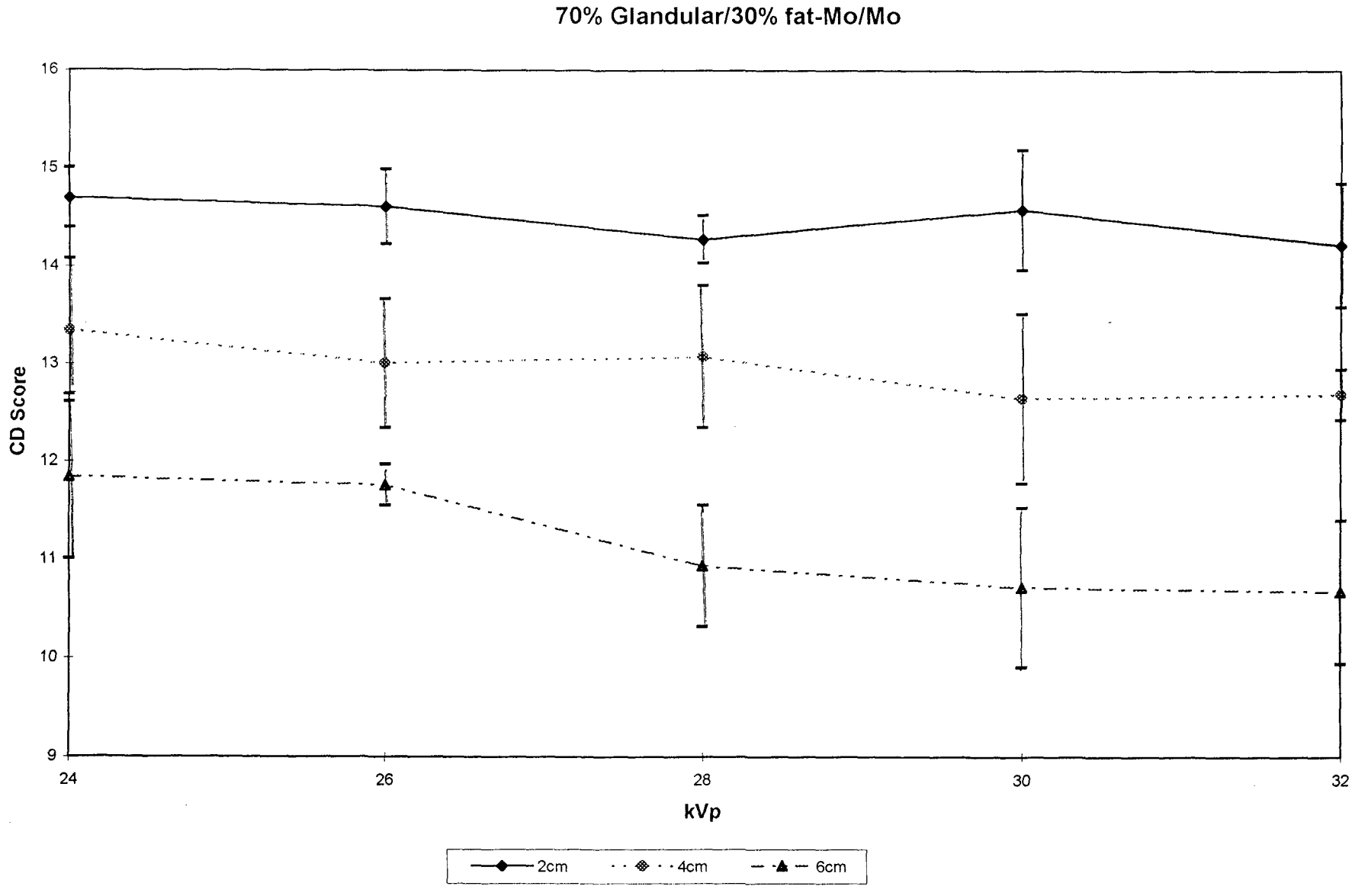
70% Glandular/30% fat-Mo/Mo
CD Score
16
15
14
13
12
11
10
9
24
26
28
30
32
kVp
2cm
4cm
6cm

Figure 16D

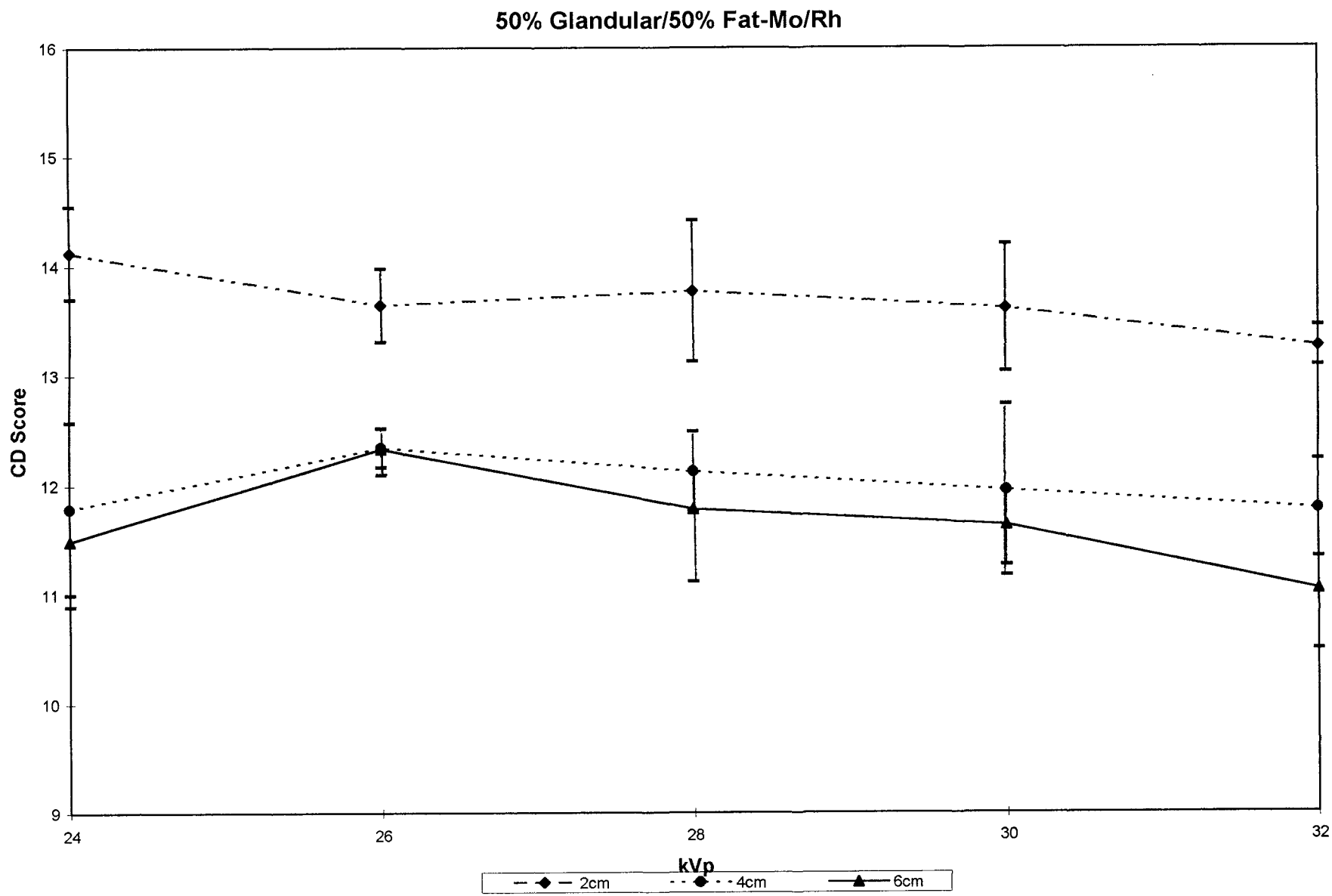
50% Glandular/50% Fat-Mo/Rh
CD Score
16
15
14
13
12
11
10
9
24
26
28
30
32
kVp
2cm
4cm
6cm

Figure 16E

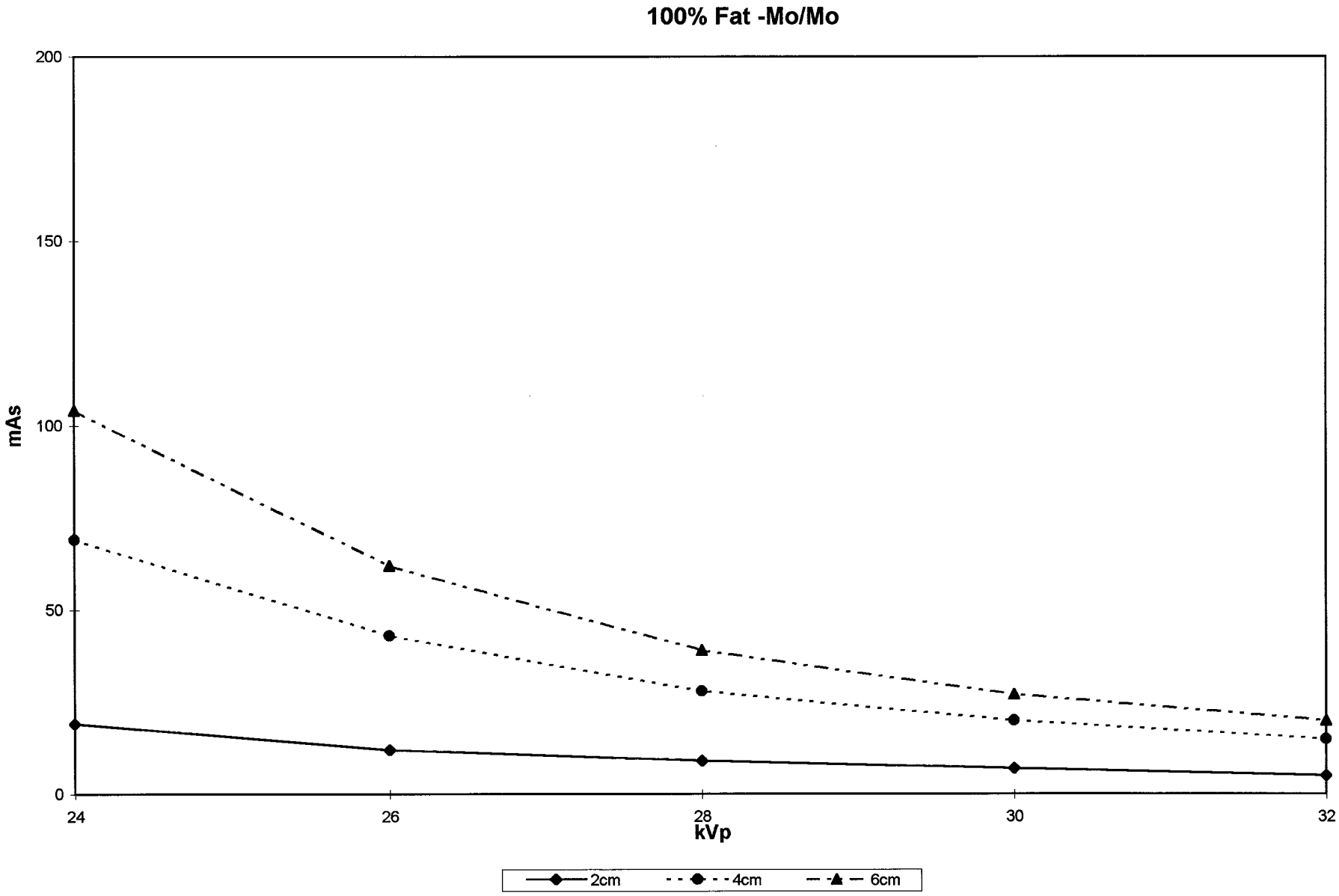

Figure 17A

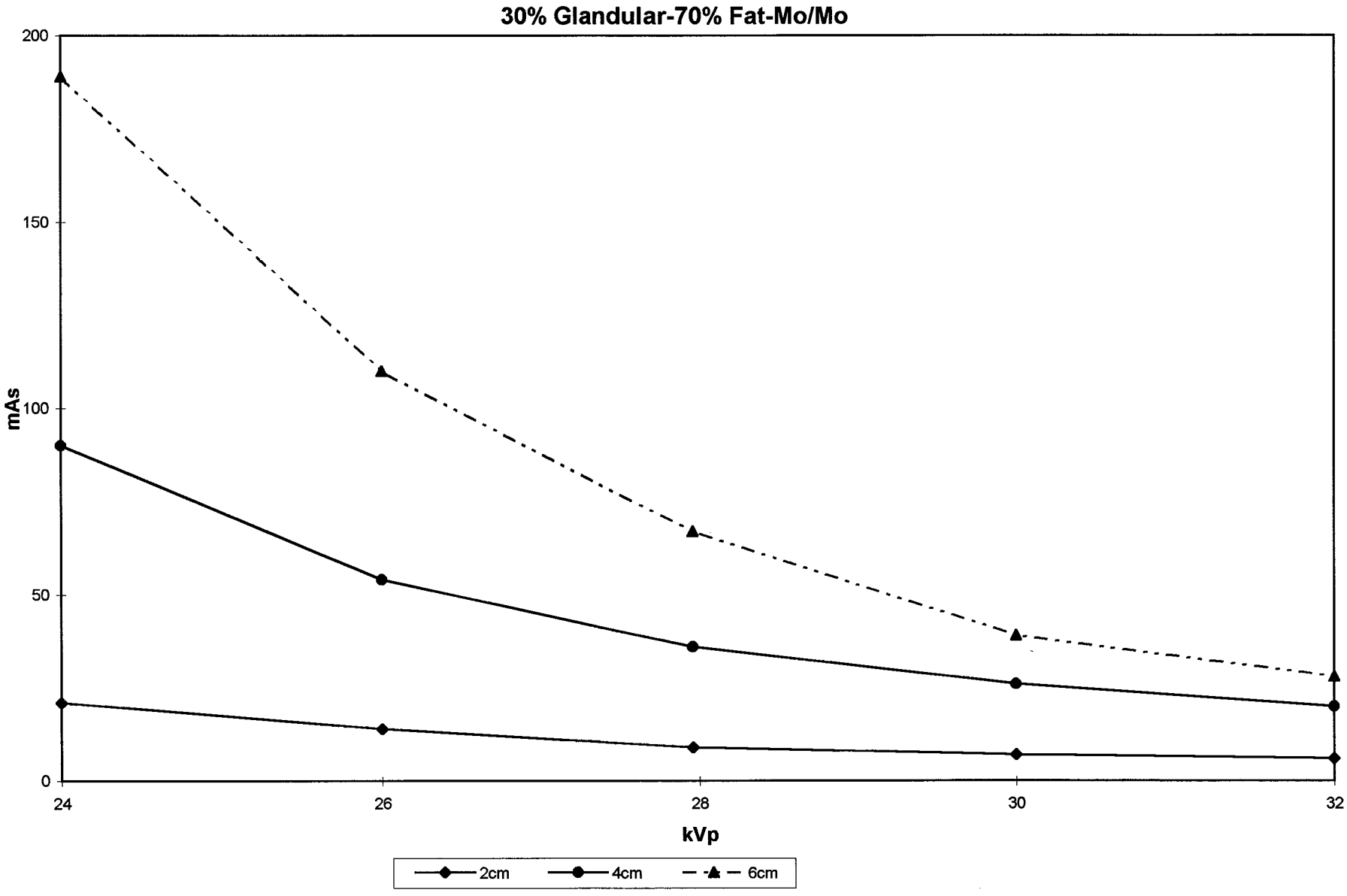
30% Glandular-70% Fat-Mo/Mo
200
150
100
50
0
mAs
24
26
28
30
32
kVp
2cm
4cm
6cm

Figure 17B

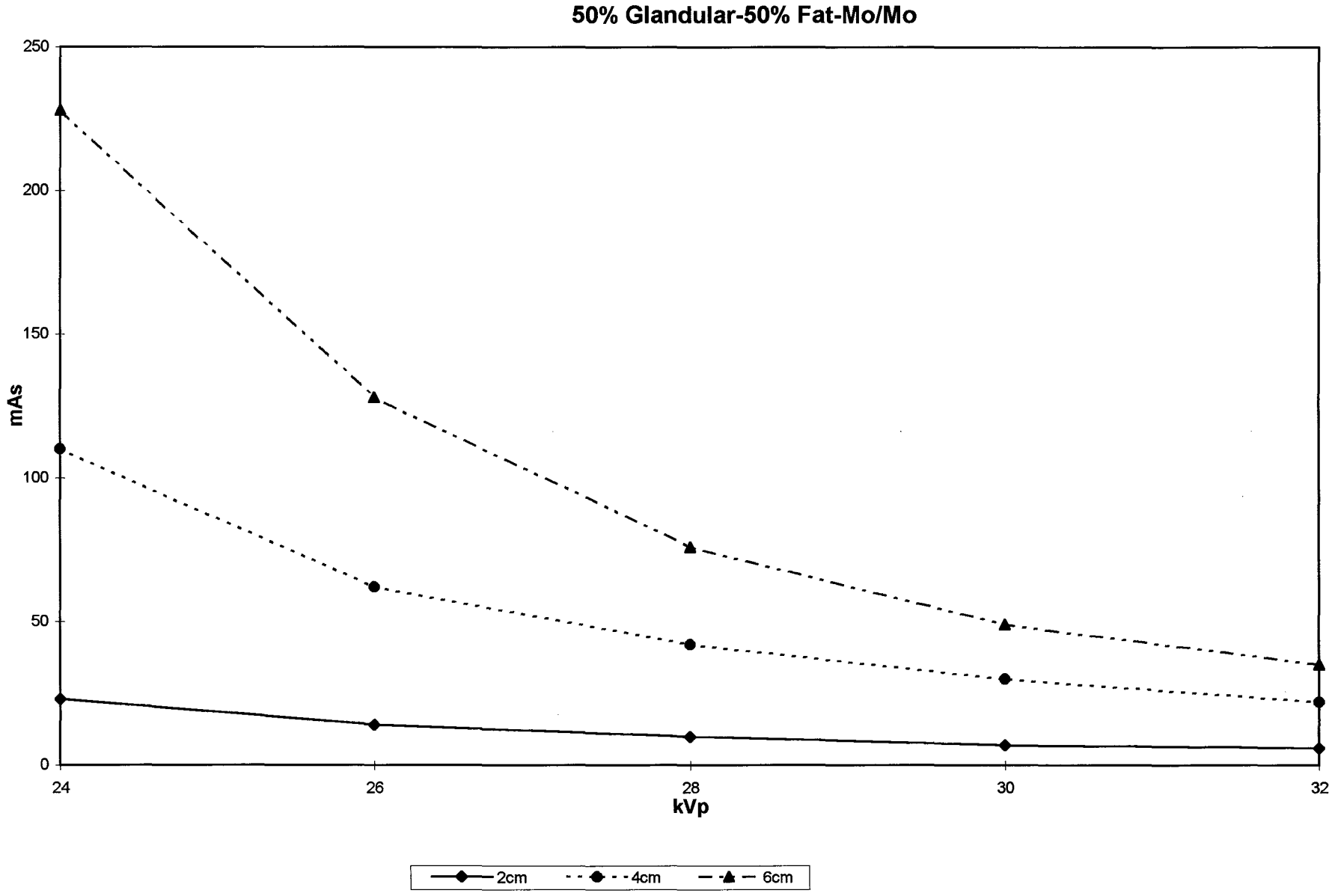
50% Glandular-50% Fat-Mo/Mo
250
200
150
100
50
0
mAs
24
26
28
30
32
kVp
2cm
4cm
6cm

Figure 17C

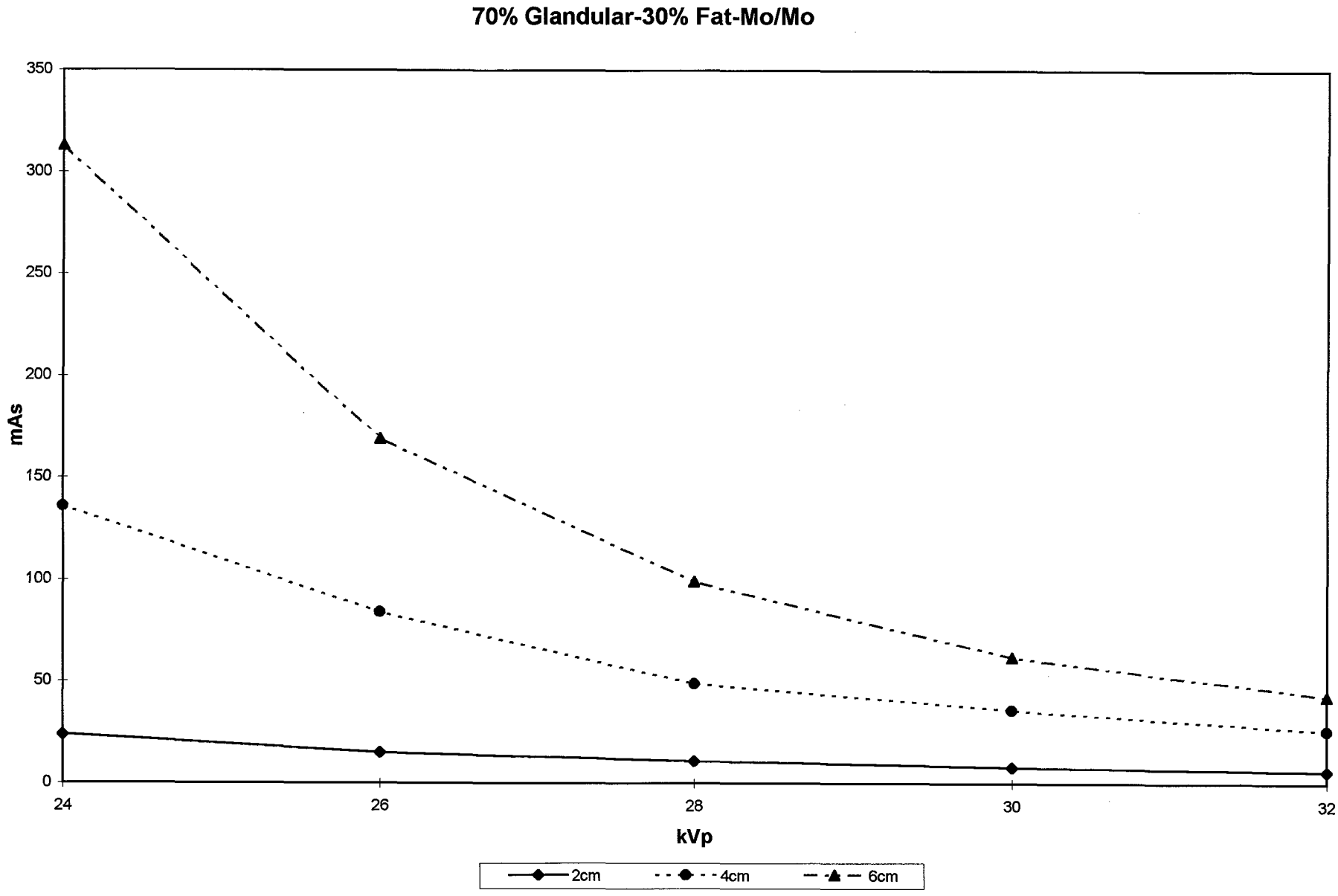
70% Glandular-30% Fat-Mo/Mo
350
300
250
200
150
100
50
0
mAs
24
26
28
30
32
kVp
2cm
4cm
6cm

Figure 17D

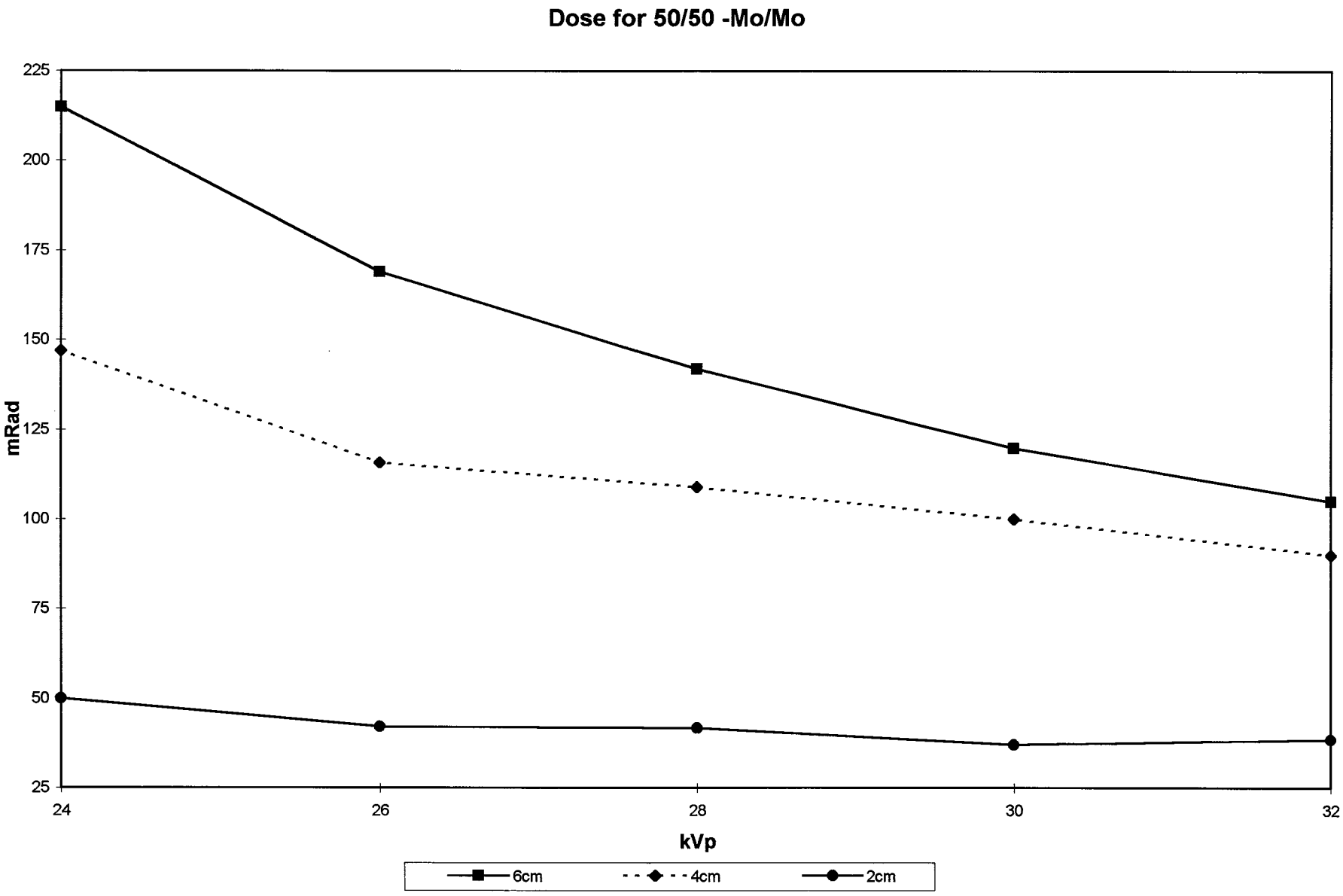
Dose for 50/50 -Mo/Mo
225
200
175
150
125
100
75
50
25
mRad
24
26
28
30
32
kVp
6cm
4cm
2cm

Figure 18A

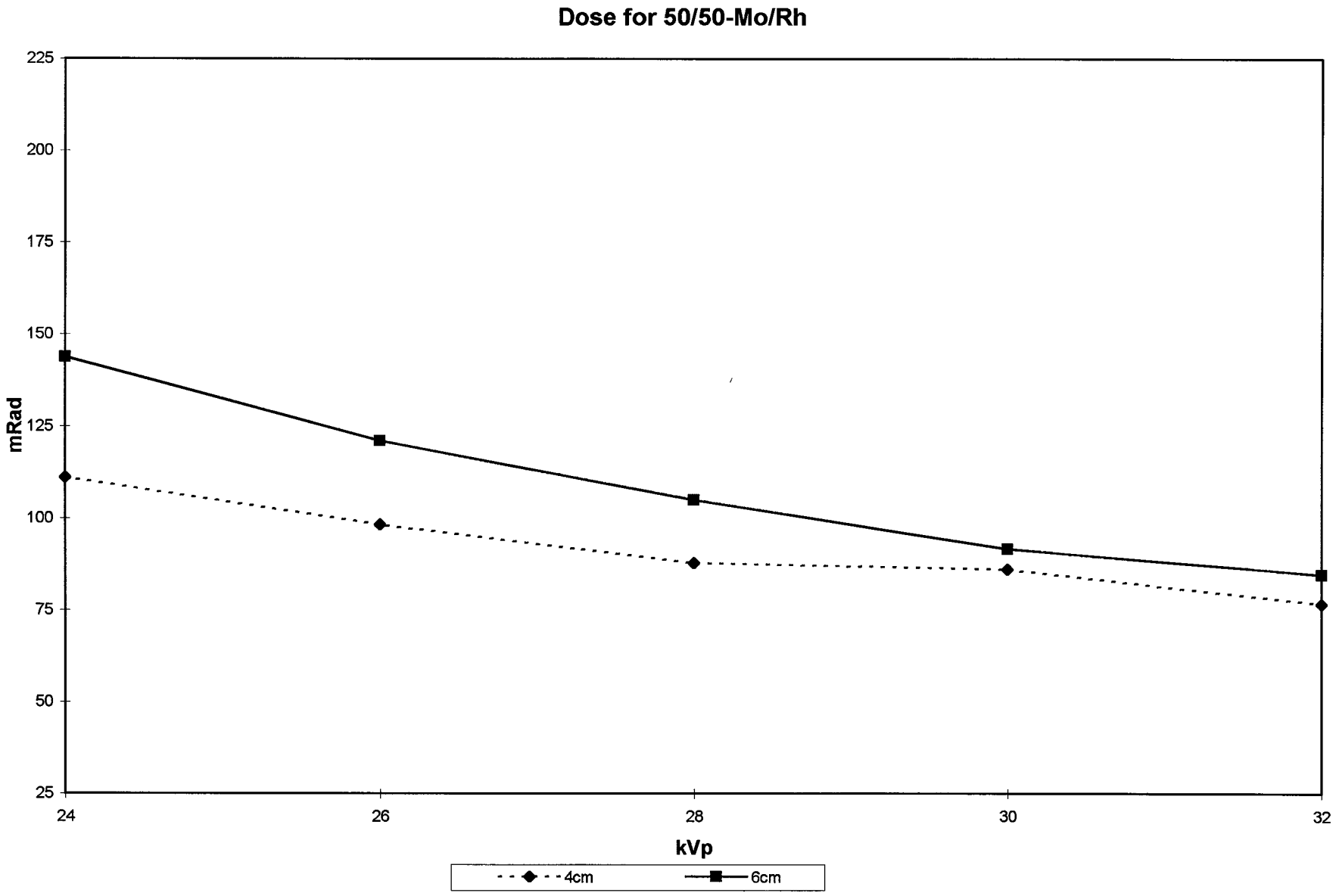
Dose for 50/50-Mo/Rh
225
200
175
150
125
100
75
50
25
mRad
24
26
28
30
32
kVp
4cm
6cm

Figure 18B

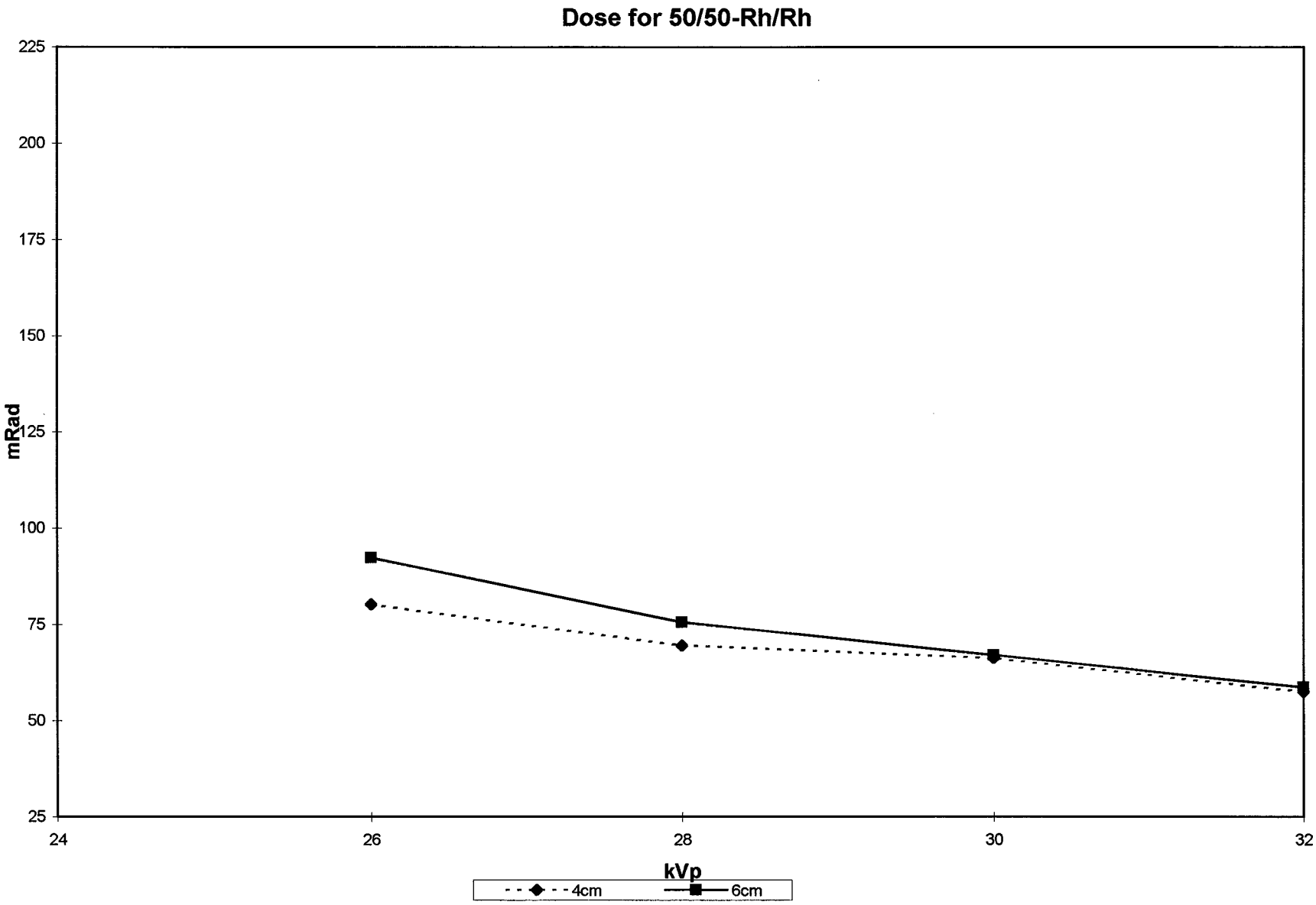
Dose for 50/50-Rh/Rh
225
200
175
150
125
100
75
50
25
mRad
24
26
28
30
32
kVp
4cm
6cm

Figure 18C

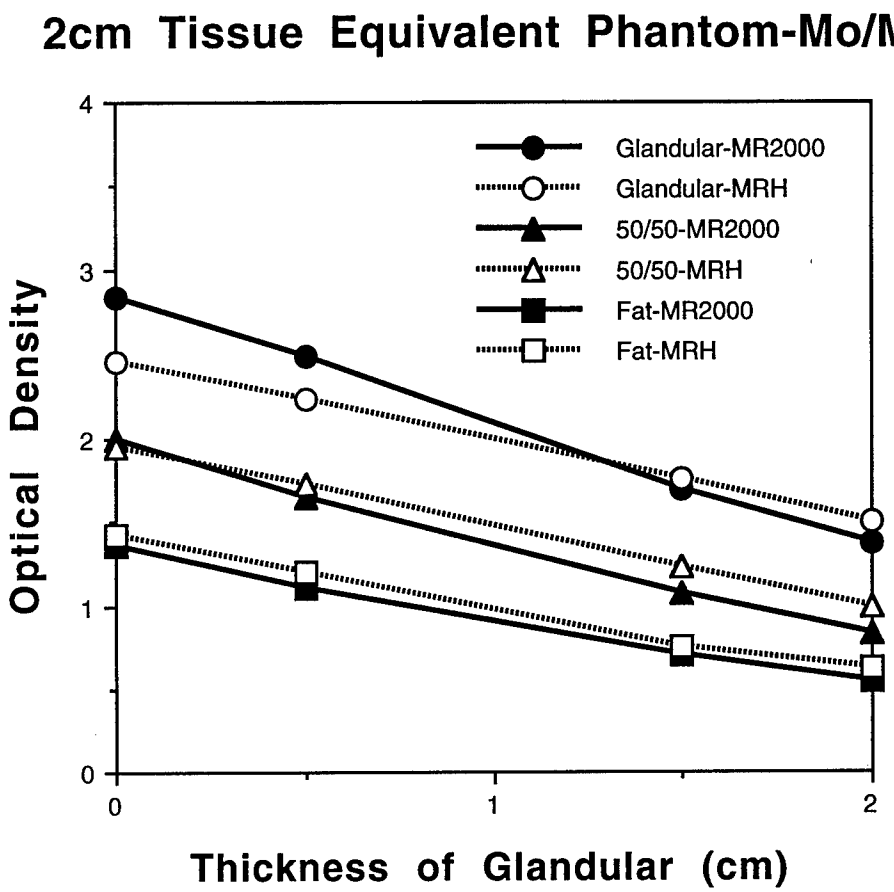
2cm Tissue Equivalent Phantom-Mo/Mo
Optical Density
Thickness of Glandular (cm)
Glandular-MR2000
Glandular-MRH
50/50-MR2000
50/50-MRH
Fat-MR2000
Fat-MRH
0
1
2
3
4
0
1
2

Figure 19A

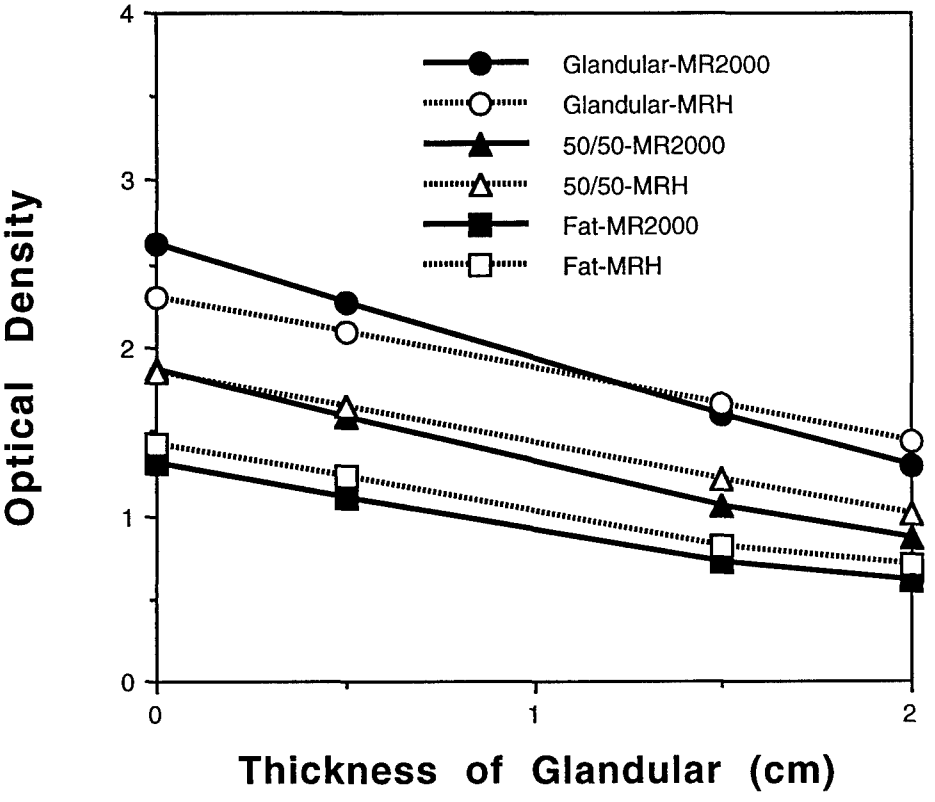
2cm Tissue Equivalent Phantom-Mo/Rh
Optical Density
Thickness of Glandular (cm)
Glandular-MR2000
Glandular-MRH
50/50-MR2000
50/50-MRH
Fat-MR2000
Fat-MRH
0
1
2
3
4
0
1
2

Figure 19B

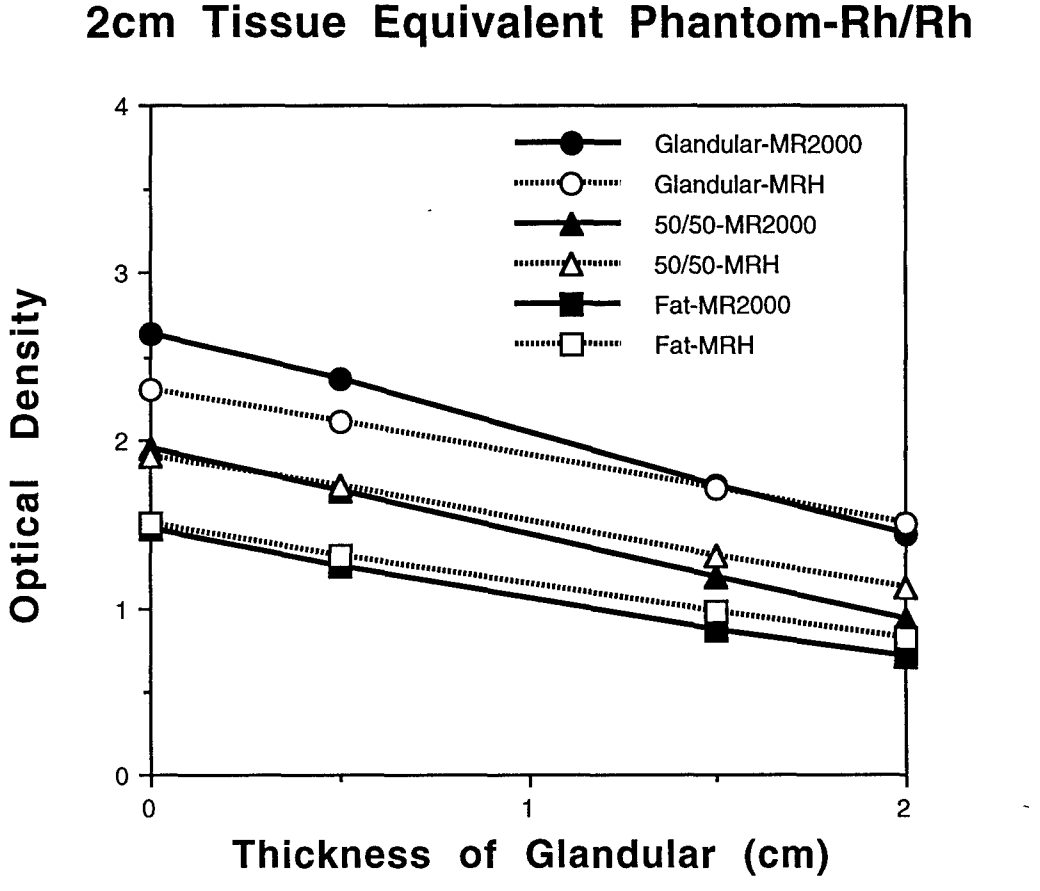
2cm Tissue Equivalent Phantom-Rh/Rh
Optical Density
Thickness of Glandular (cm)
Glandular-MR2000
Glandular-MRH
50/50-MR2000
50/50-MRH
Fat-MR2000
Fat-MRH
0
1
2
3
4
0
1
2

Figure 19C

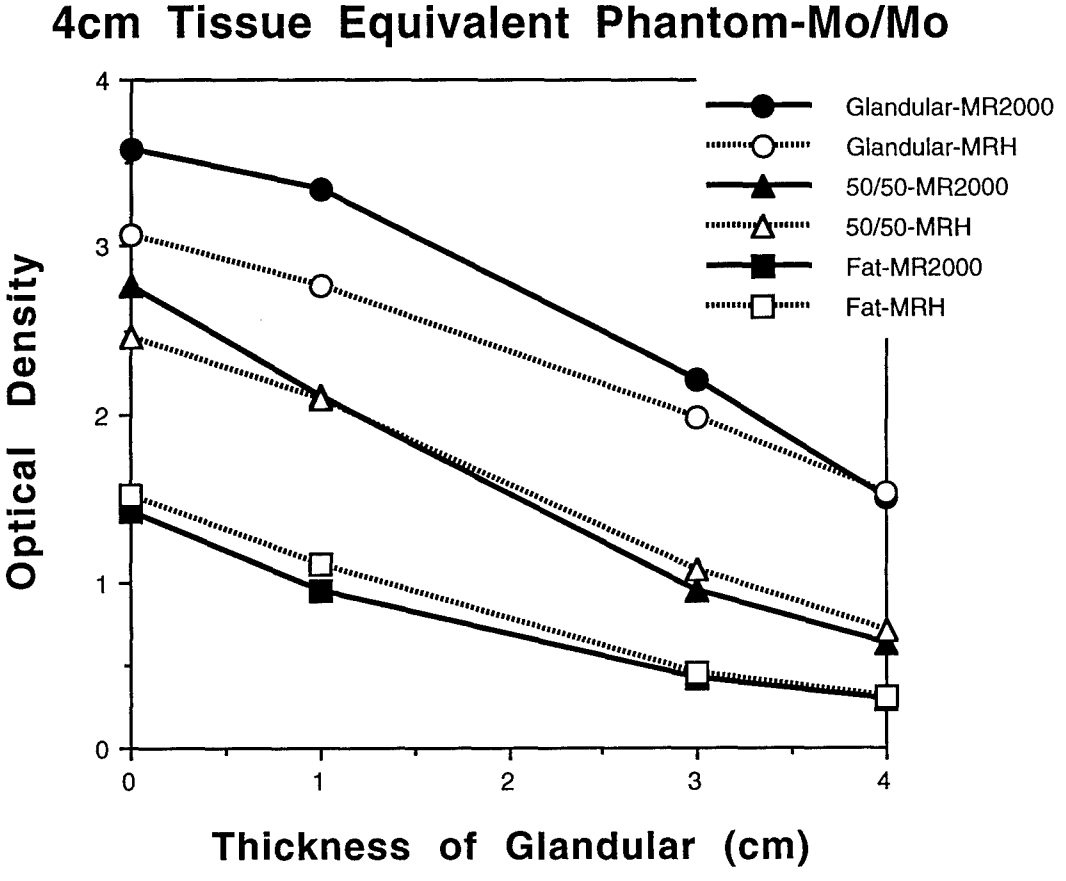
4cm Tissue Equivalent Phantom-Mo/Mo
Optical Density
Thickness of Glandular (cm)
Glandular-MR2000
Glandular-MRH
50/50-MR2000
50/50-MRH
Fat-MR2000
Fat-MRH
0
1
2
3
4

Figure 19D

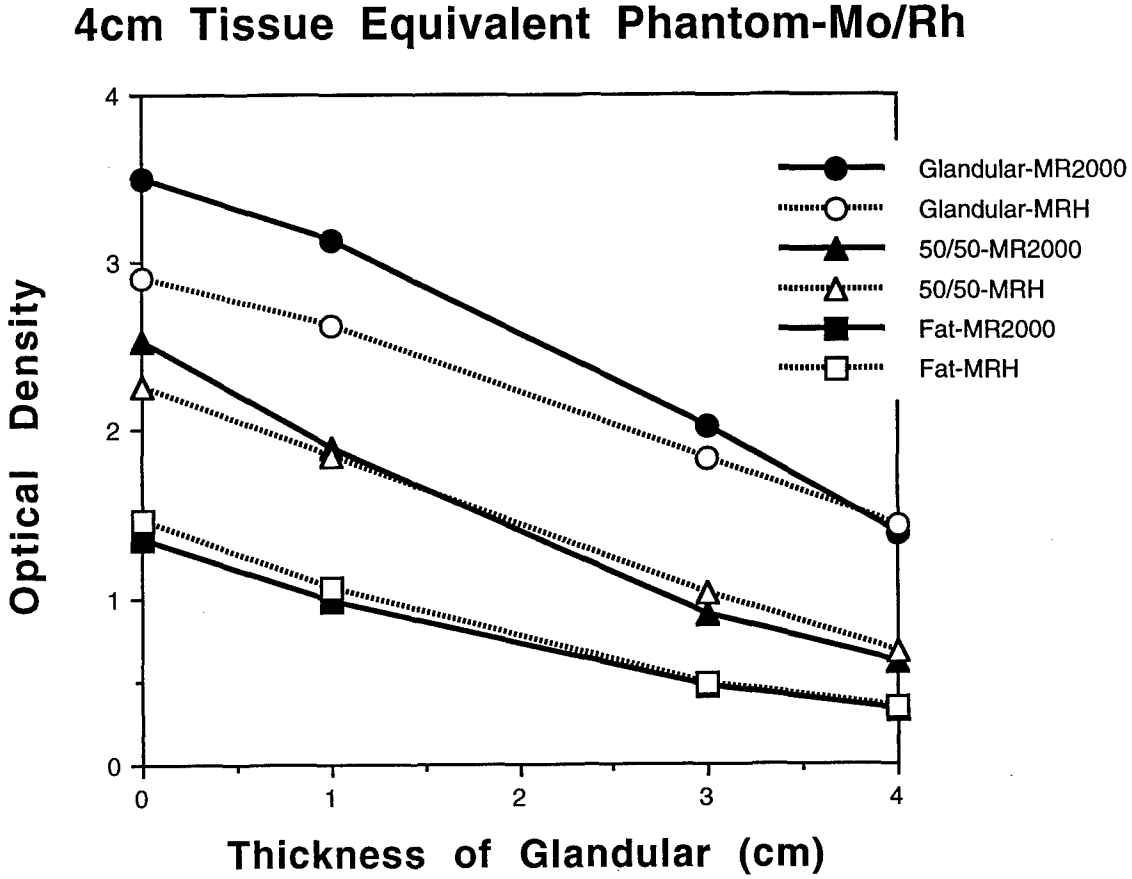
4cm Tissue Equivalent Phantom-Mo/Rh
Optical Density
Thickness of Glandular (cm)
Glandular-MR2000
Glandular-MRH
50/50-MR2000
50/50-MRH
Fat-MR2000
Fat-MRH
0
1
2
3
4

Figure 19E

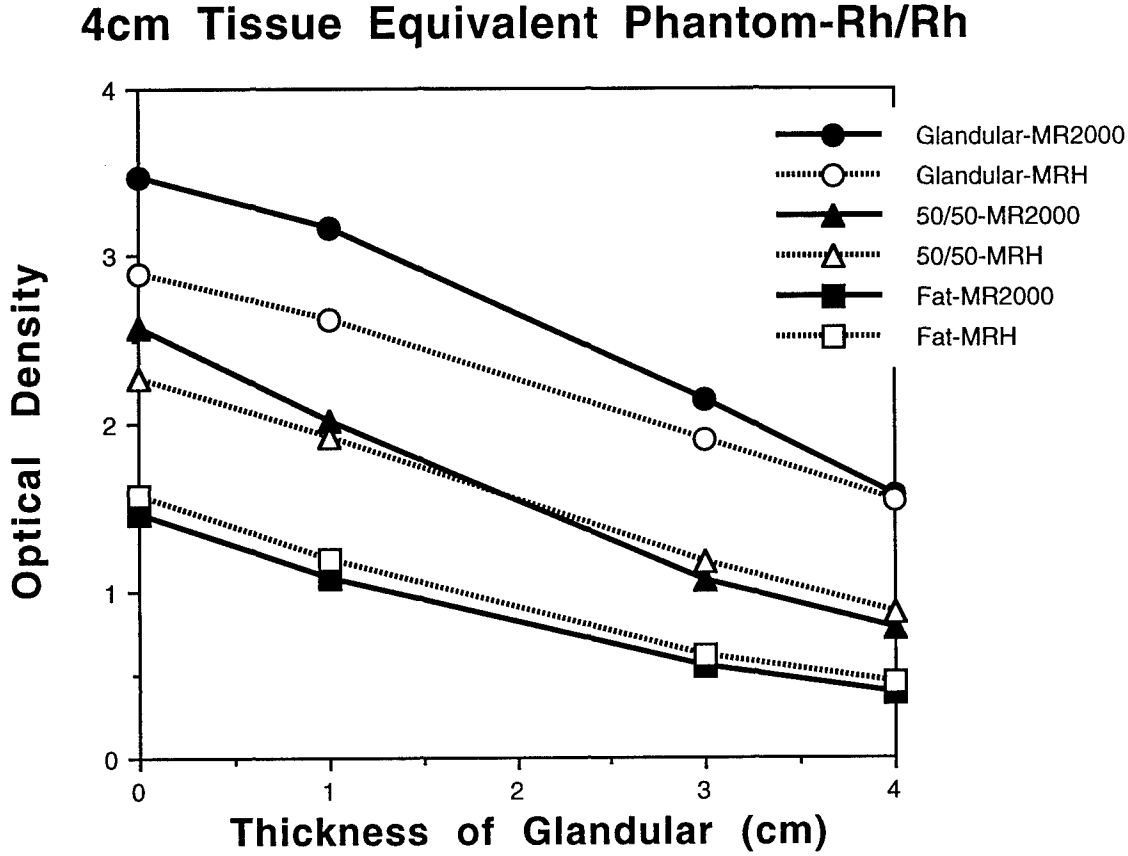
4cm Tissue Equivalent Phantom-Rh/Rh
Optical Density
Thickness of Glandular (cm)
0
1
2
3
4
Glandular-MR2000
Glandular-MRH
50/50-MR2000
50/50-MRH
Fat-MR2000
Fat-MRH

Figure 19F

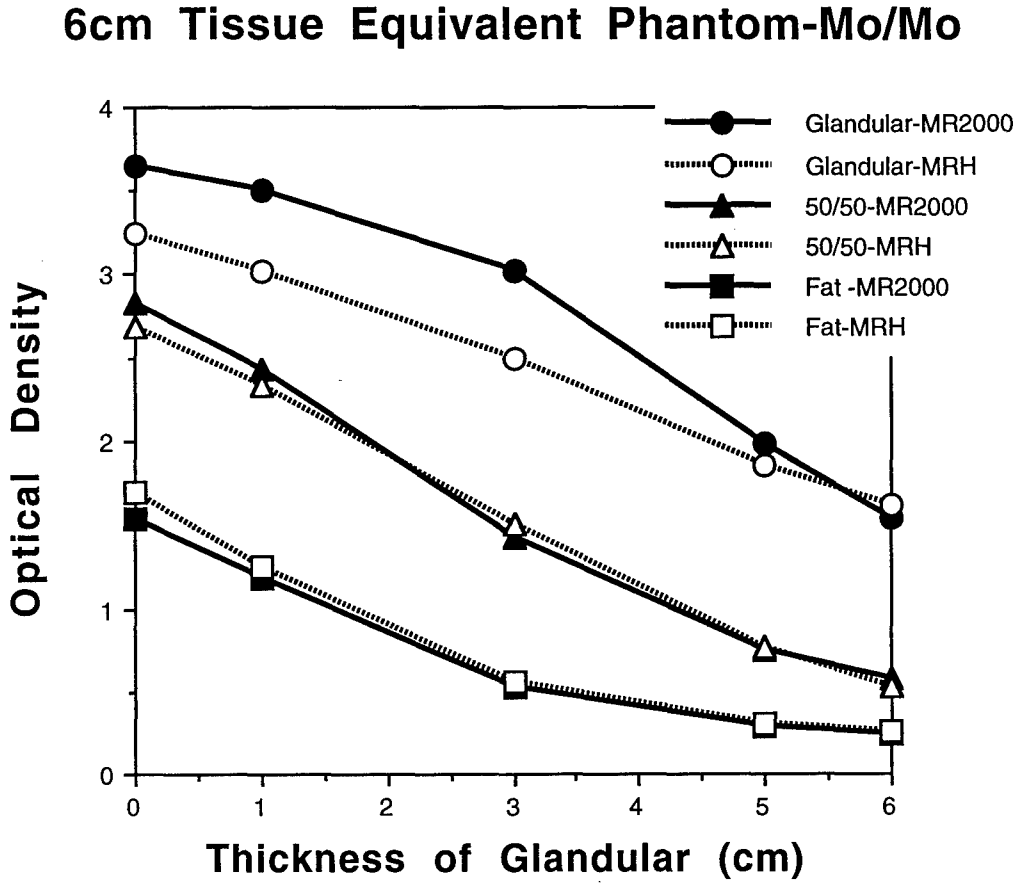
6cm Tissue Equivalent Phantom-Mo/Mo
Optical Density
Thickness of Glandular (cm)
Glandular-MR2000
Glandular-MRH
50/50-MR2000
50/50-MRH
Fat -MR2000
Fat-MRH
0
1
2
3
4
5
6

Figure 19G

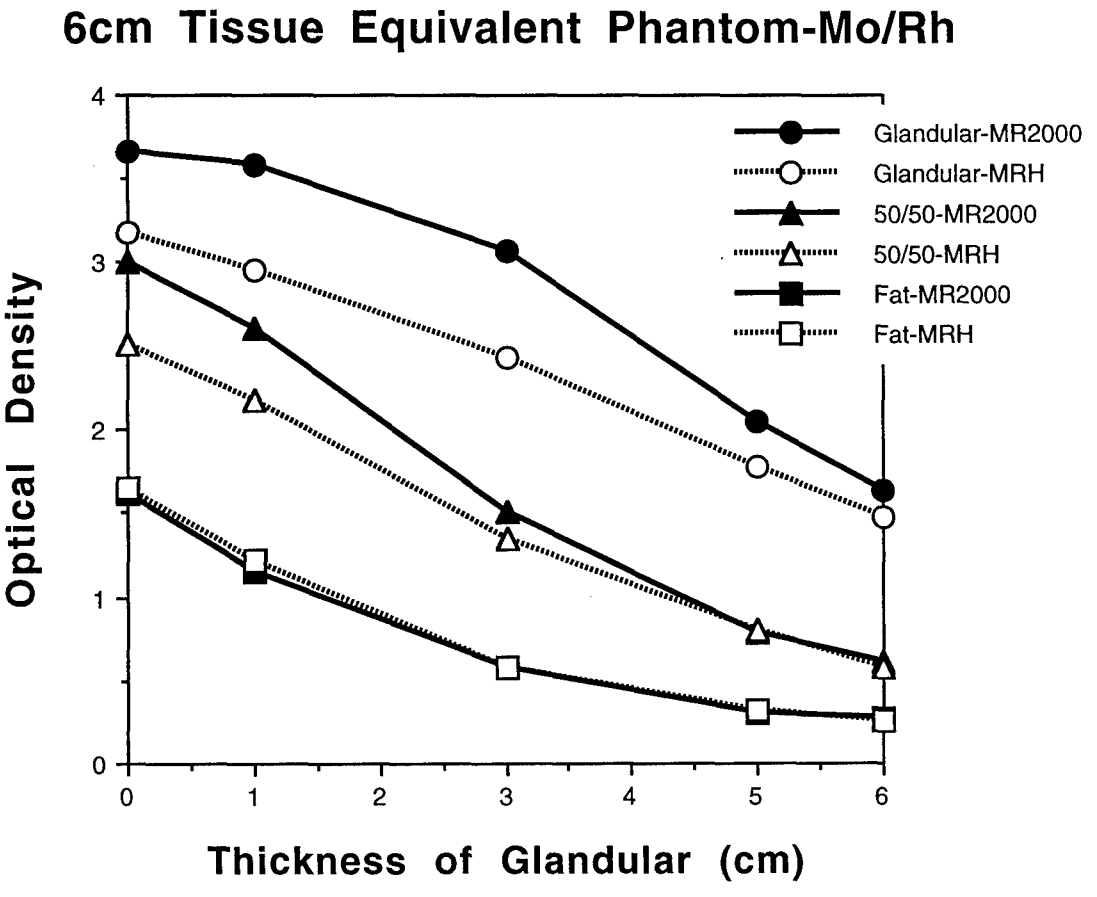
6cm Tissue Equivalent Phantom-Mo/Rh
Optical Density
Thickness of Glandular (cm)
Glandular-MR2000
Glandular-MRH
50/50-MR2000
50/50-MRH
Fat-MR2000
Fat-MRH
0
1
2
3
4
5
6

Figure 19H

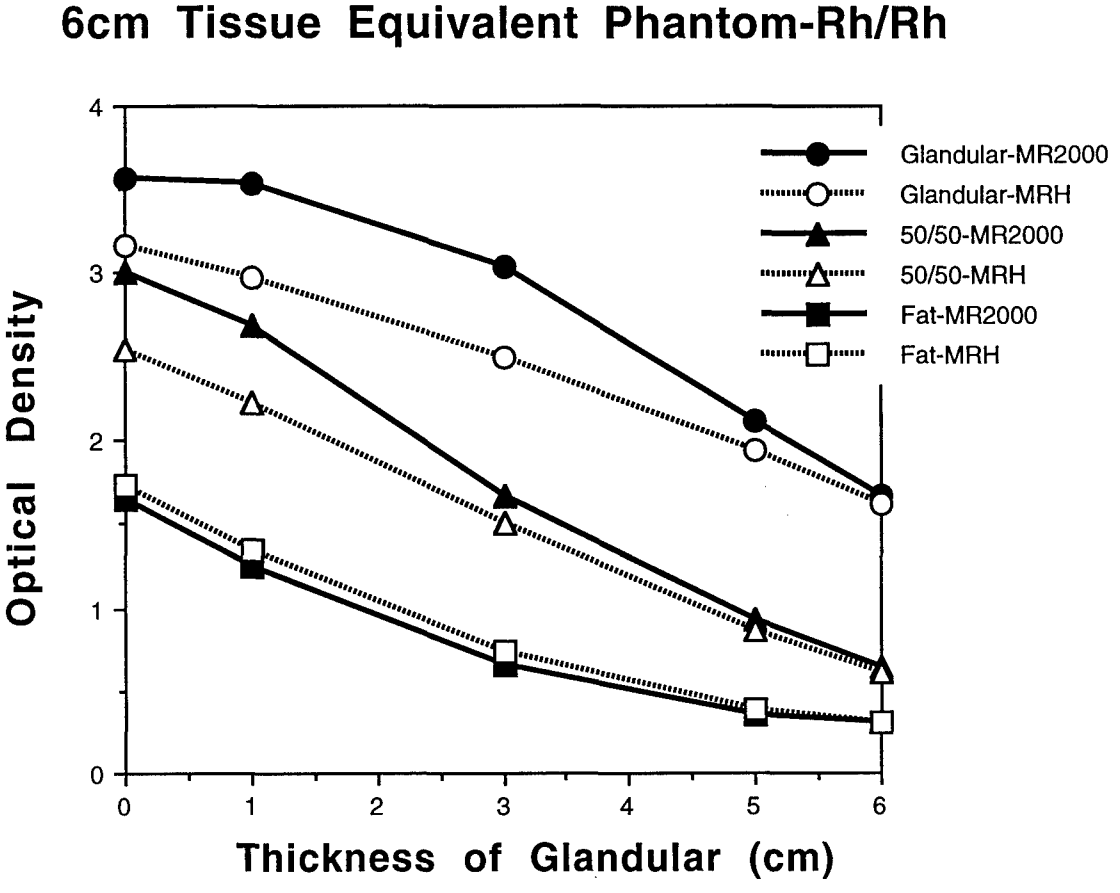
6cm Tissue Equivalent Phantom-Rh/Rh
Optical Density
Thickness of Glandular (cm)
Glandular-MR2000
Glandular-MRH
50/50-MR2000
50/50-MRH
Fat-MR2000
Fat-MRH
0
1
2
3
4
5
6

Figure 19I

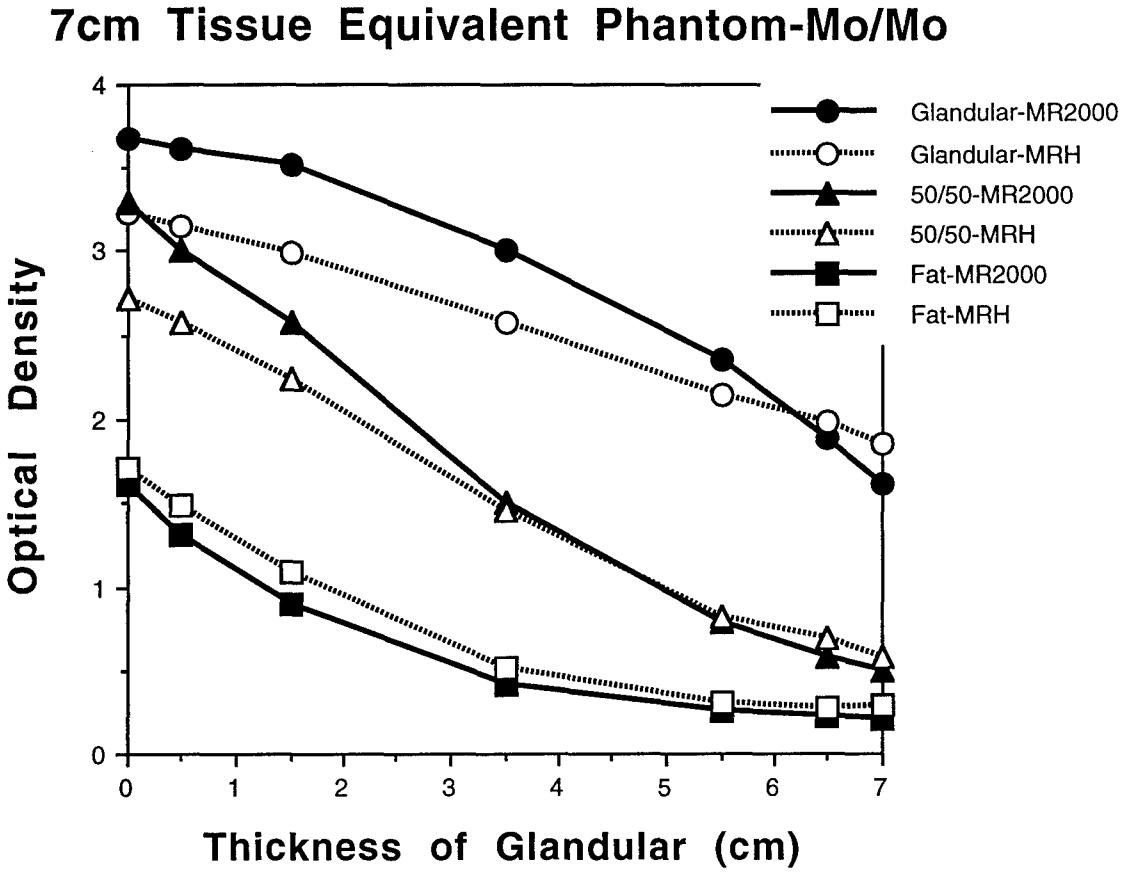
7cm Tissue Equivalent Phantom-Mo/Mo
Optical Density
Thickness of Glandular (cm)
Glandular-MR2000
Glandular-MRH
50/50-MR2000
50/50-MRH
Fat-MR2000
Fat-MRH
0
1
2
3
4
5
6
7

Figure 19J

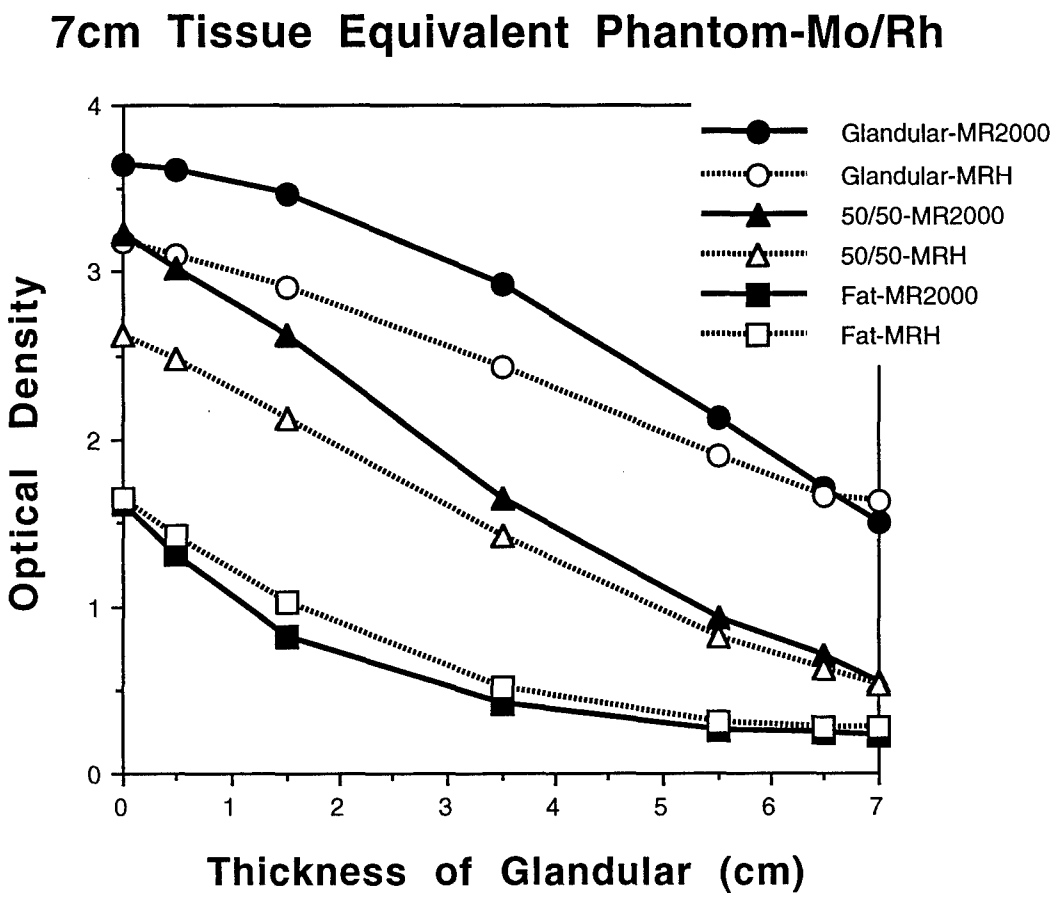
7cm Tissue Equivalent Phantom-Mo/Rh
Optical Density
Thickness of Glandular (cm)
Glandular-MR2000
Glandular-MRH
50/50-MR2000
50/50-MRH
Fat-MR2000
Fat-MRH
0
1
2
3
4
5
6
7

Figure 19K

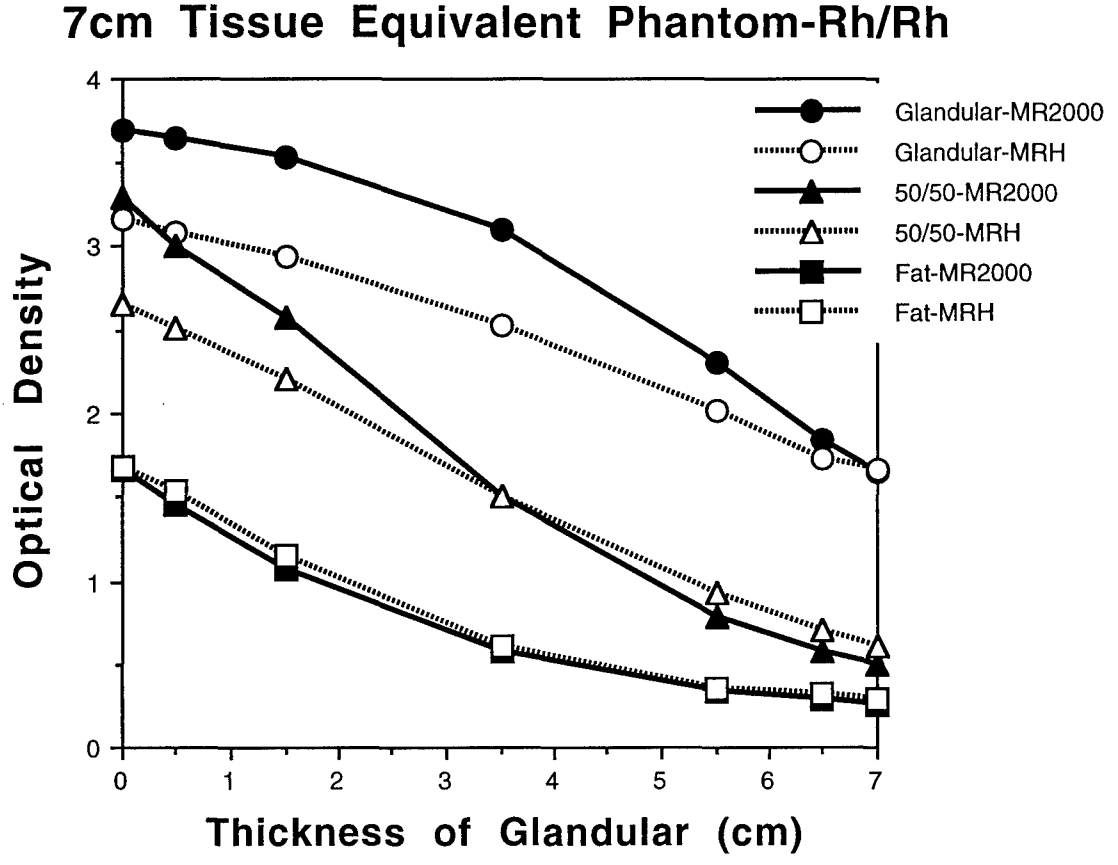
7cm Tissue Equivalent Phantom-Rh/Rh
Optical Density
Thickness of Glandular (cm)
Glandular-MR2000
Glandular-MRH
50/50-MR2000
50/50-MRH
Fat-MR2000
Fat-MRH
0
1
2
3
4
5
6
7

Figure 19L

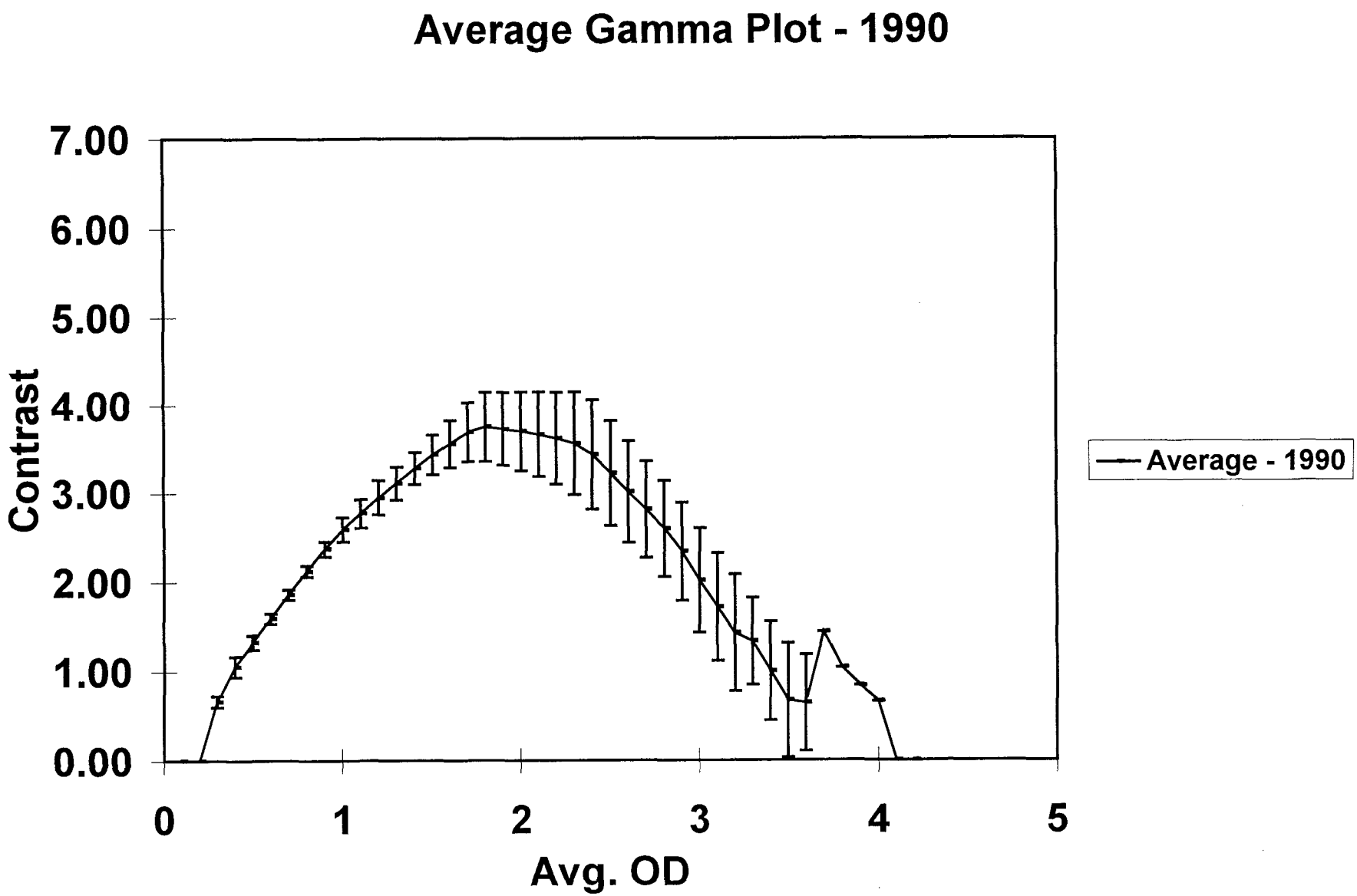
Average Gamma Plot - 1990
7.00
6.00
5.00
4.00
3.00
2.00
1.00
0.00
Contrast
0
1
2
3
4
5
Avg. OD
Average - 1990

Figure 20A

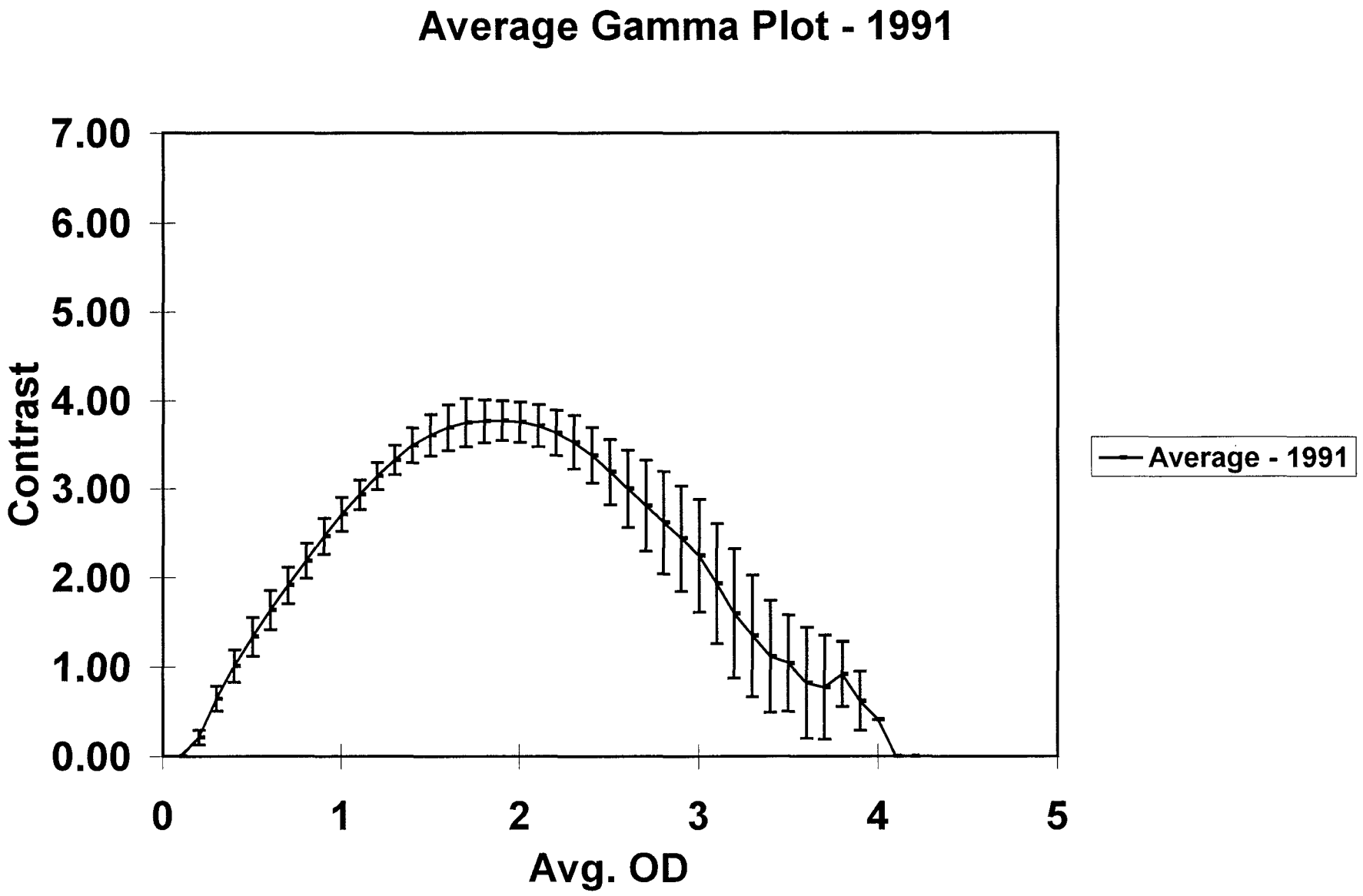
Average Gamma Plot - 1991
7.00
6.00
5.00
4.00
3.00
2.00
1.00
0.00
Contrast
0
1
2
3
4
5
Avg. OD
Average - 1991

Figure 20B

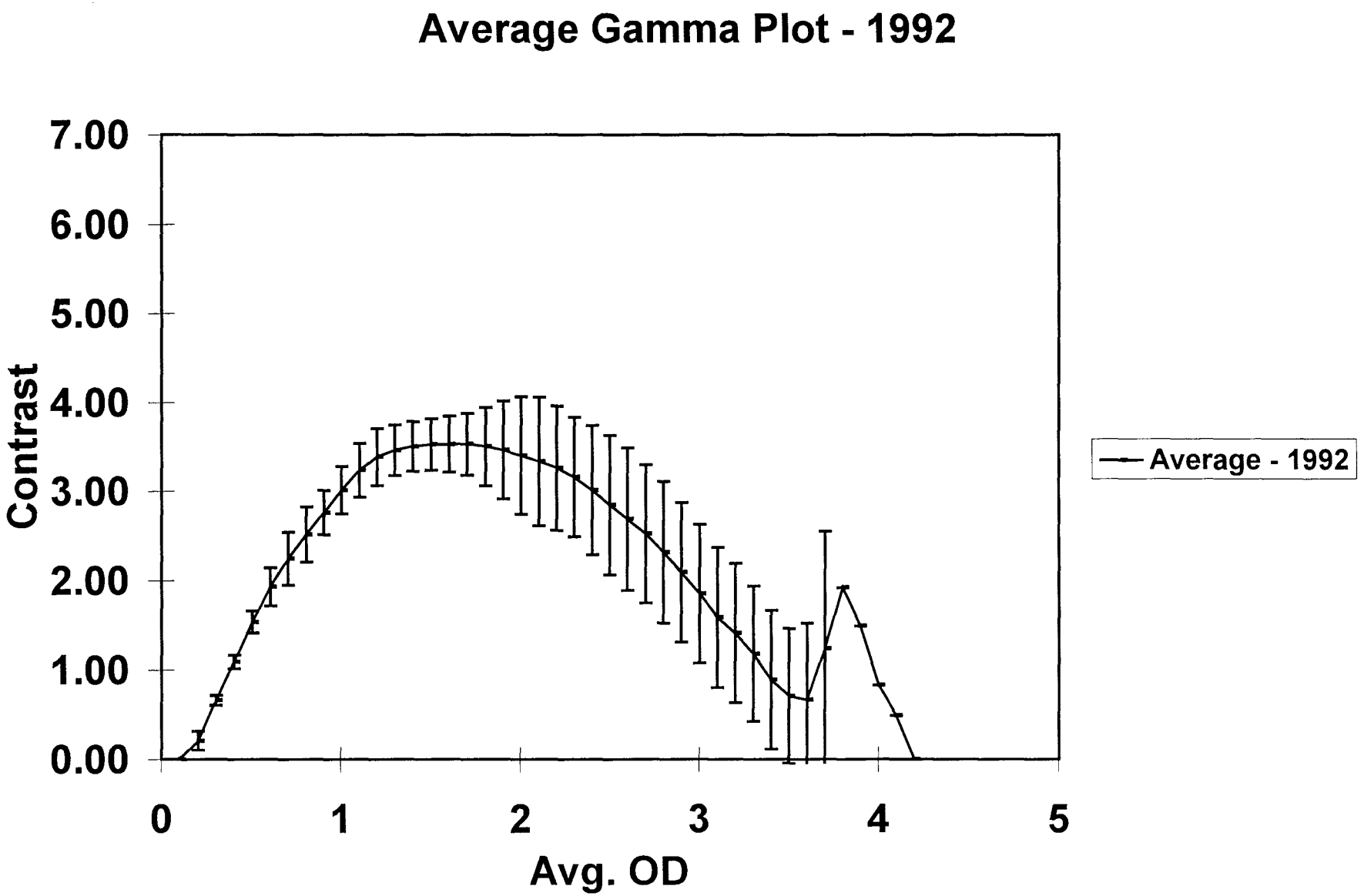
Average Gamma Plot - 1992
7.00
6.00
5.00
4.00
3.00
2.00
1.00
0.00
Contrast
0
1
2
3
4
5
Avg. OD
Average - 1992

Figure 20C

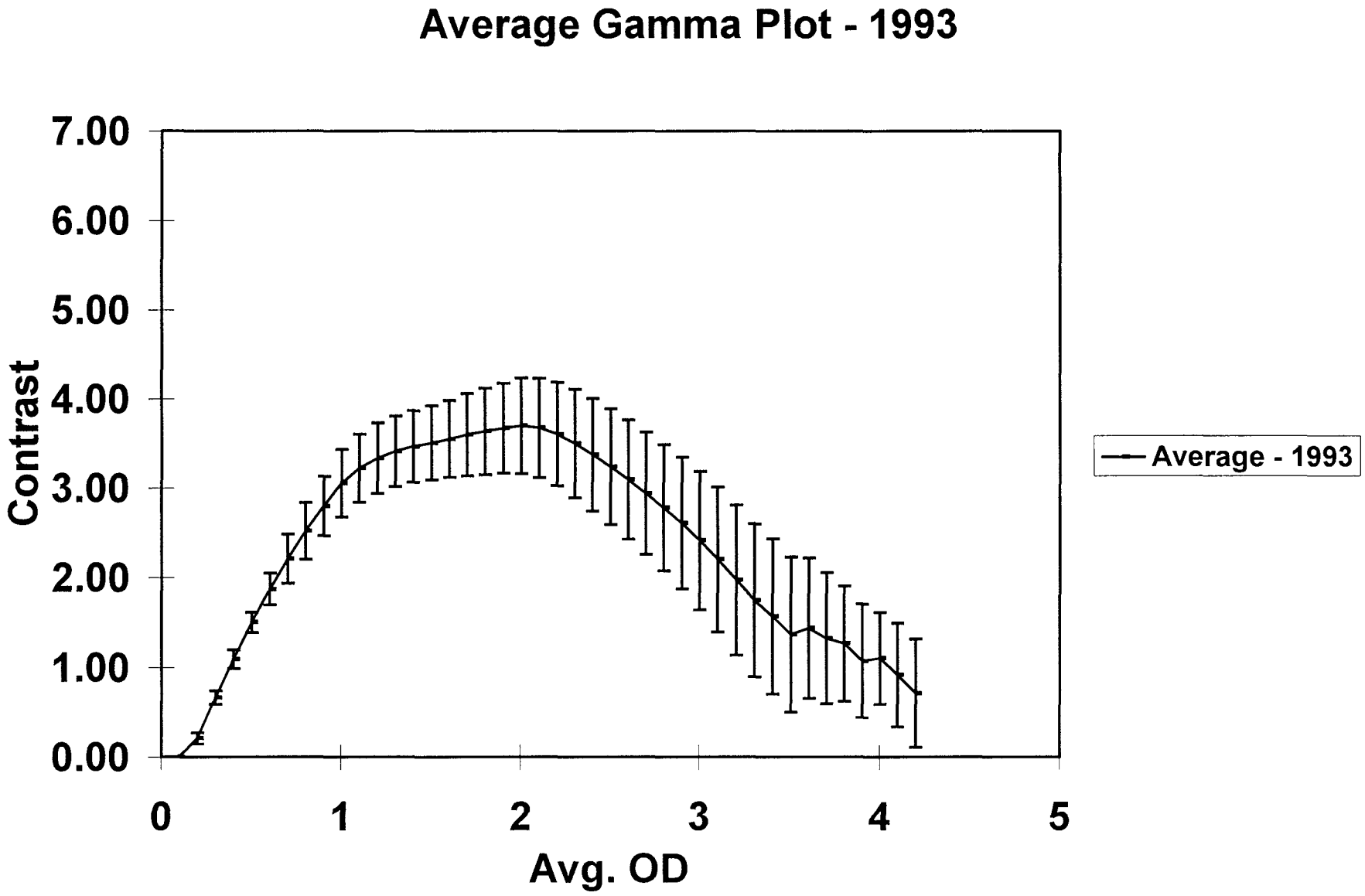
Average Gamma Plot - 1993
7.00
6.00
5.00
4.00
3.00
2.00
1.00
0.00
Contrast
0
1
2
3
4
5
Avg. OD
Average - 1993

Figure 20D

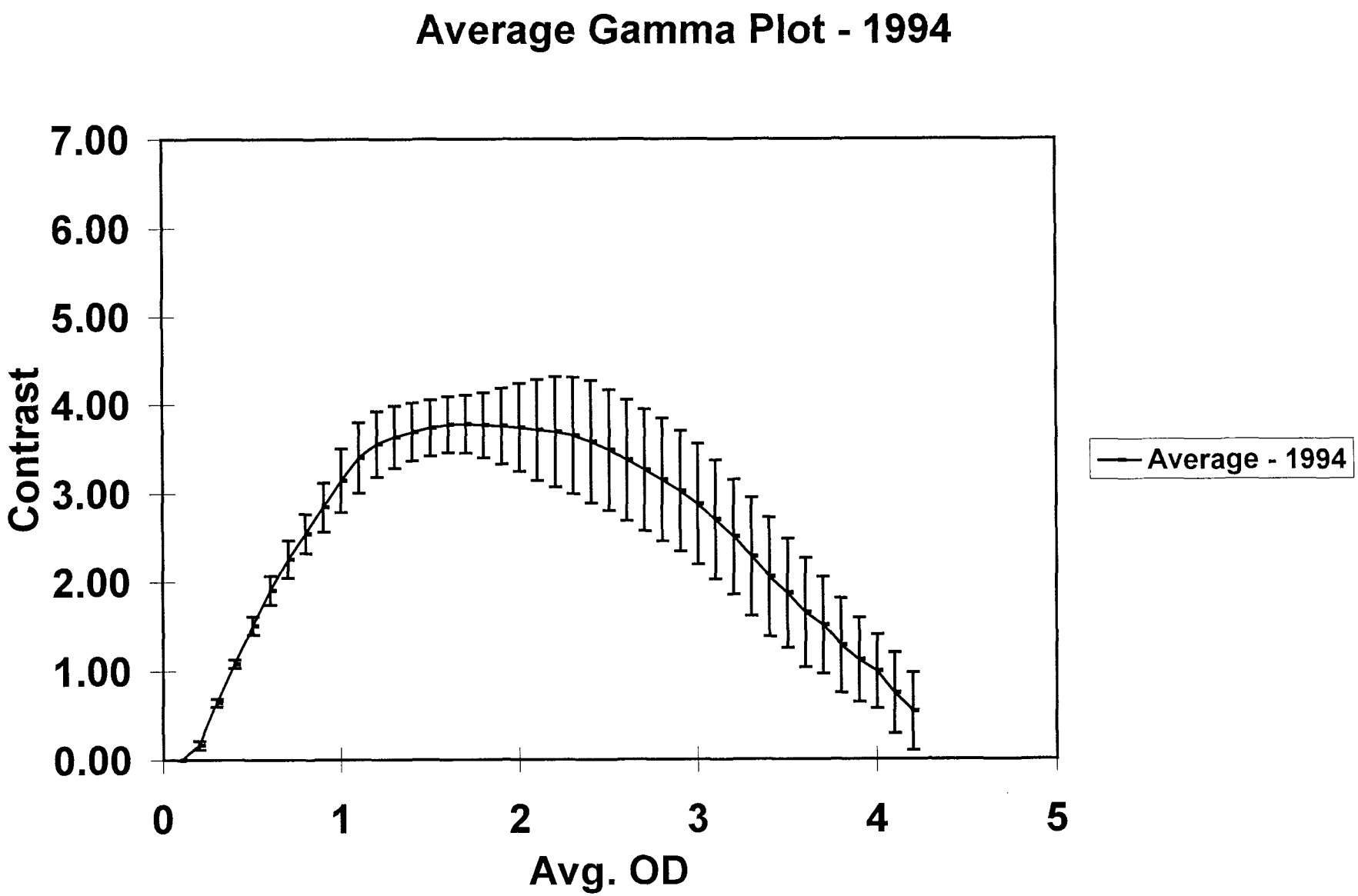
Average Gamma Plot - 1994
7.00
6.00
5.00
4.00
3.00
2.00
1.00
0.00
Contrast
0
1
2
3
4
5
Avg. OD
Average - 1994

Figure 20E

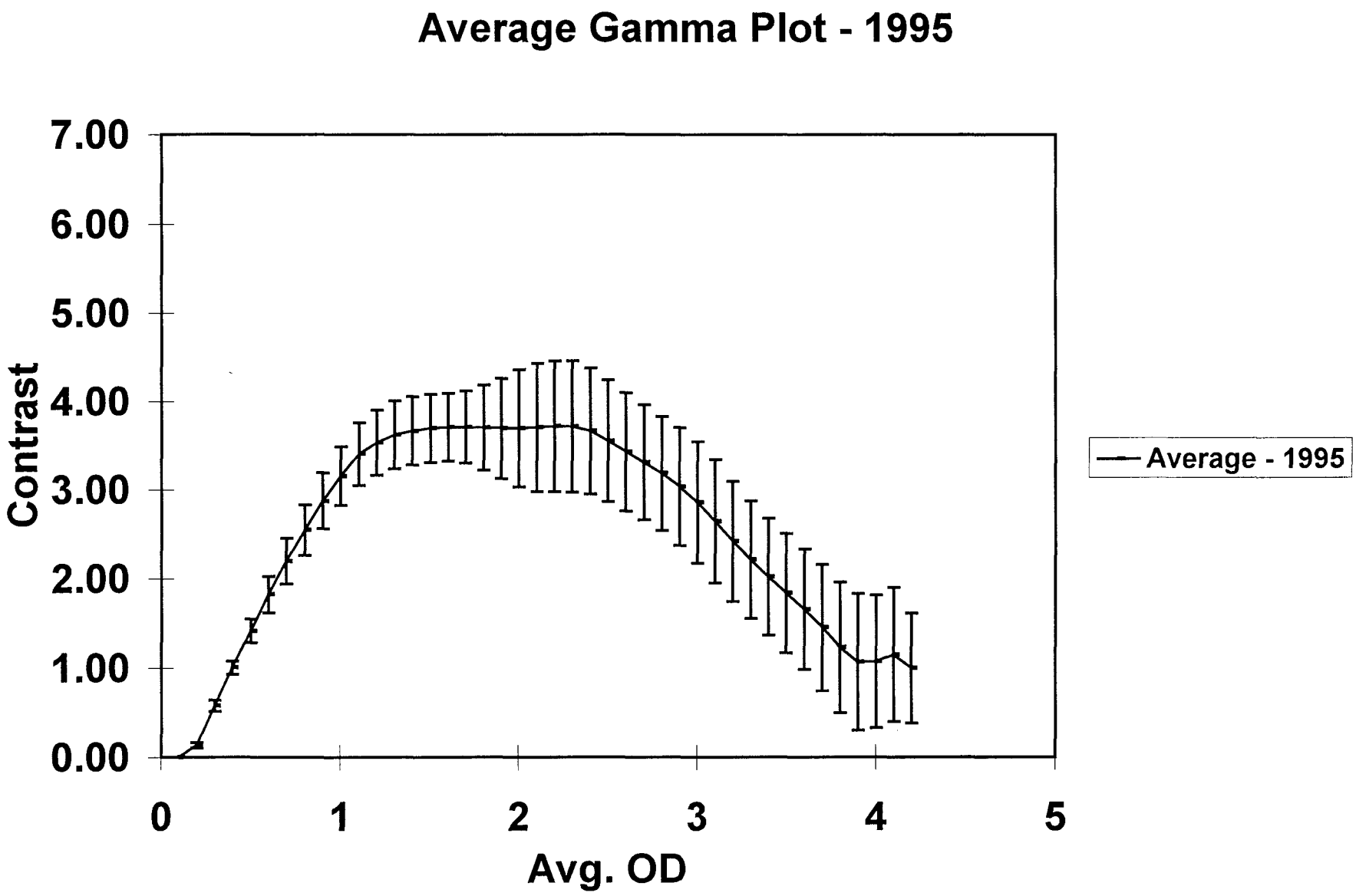
Average Gamma Plot - 1995
7.00
6.00
5.00
4.00
3.00
2.00
1.00
0.00
Contrast
0
1
2
3
4
5
Avg. OD
Average - 1995

Figure 20F

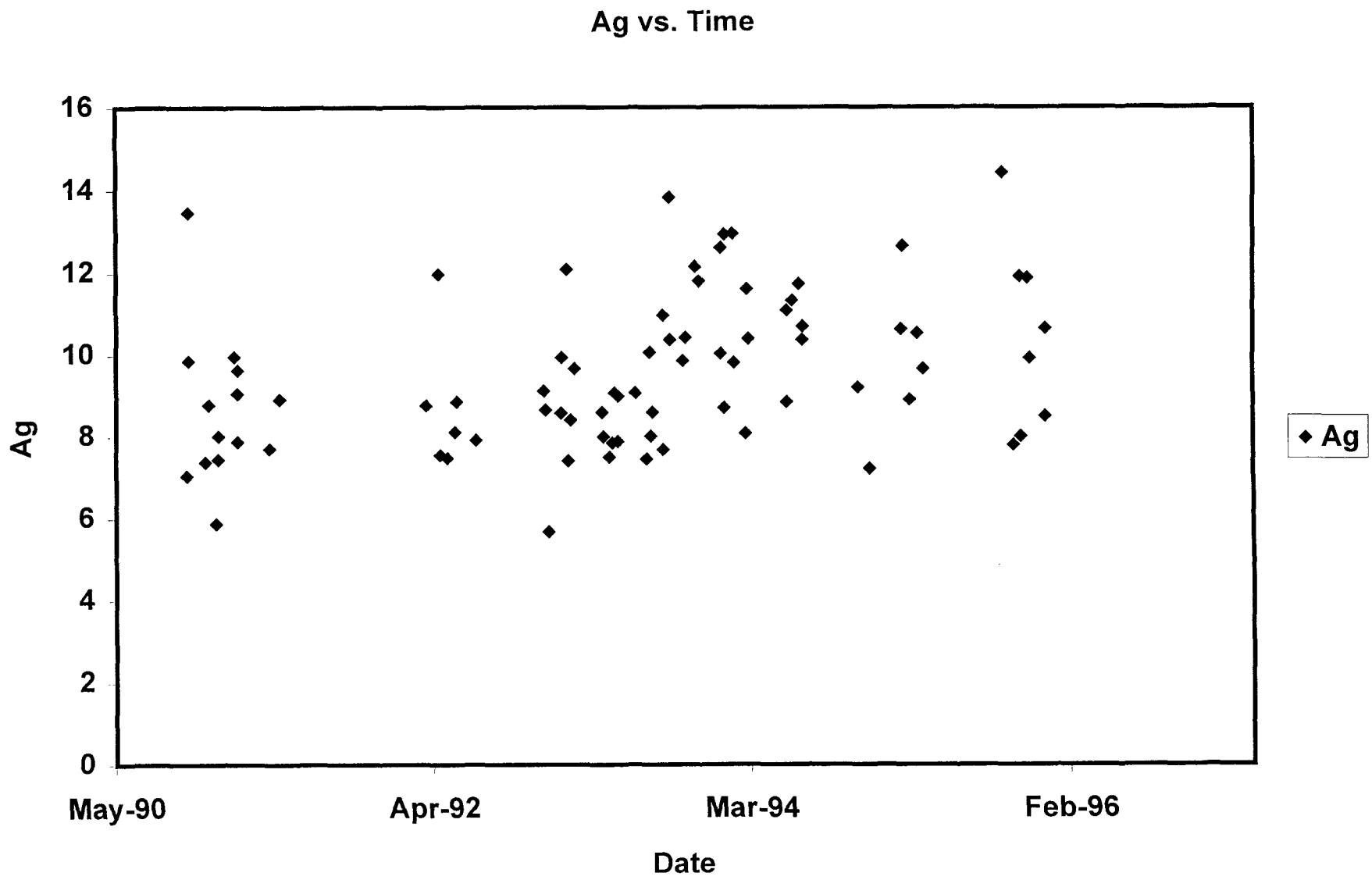

Figure 20D

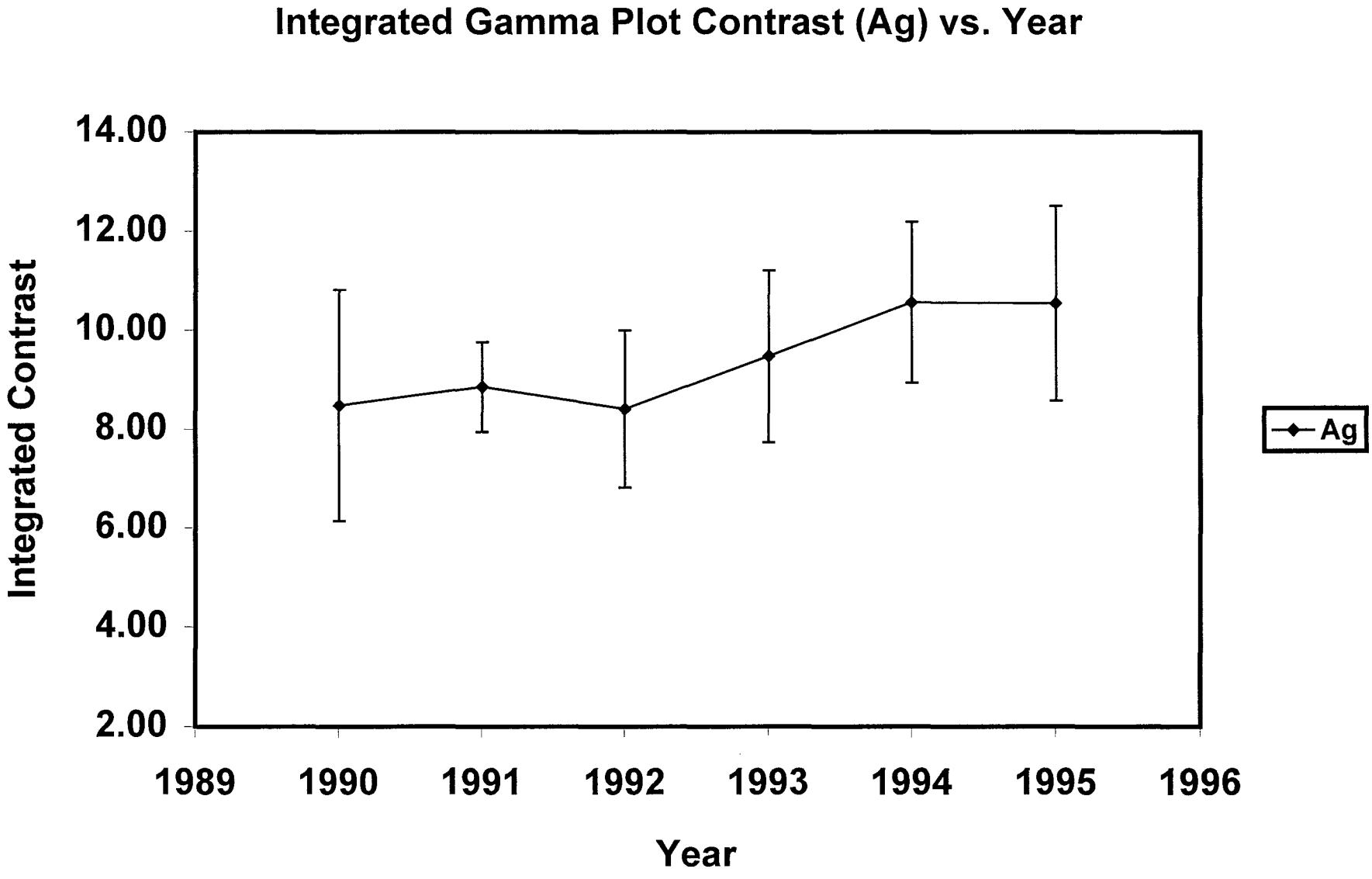
Integrated Gamma Plot Contrast (Ag) vs. Year
Integrated Contrast
14.00
12.00
10.00
8.00
6.00
4.00
2.00
1989
1990
1991
1992
1993
1994
1995
1996
Year
Ag

Figure 20H

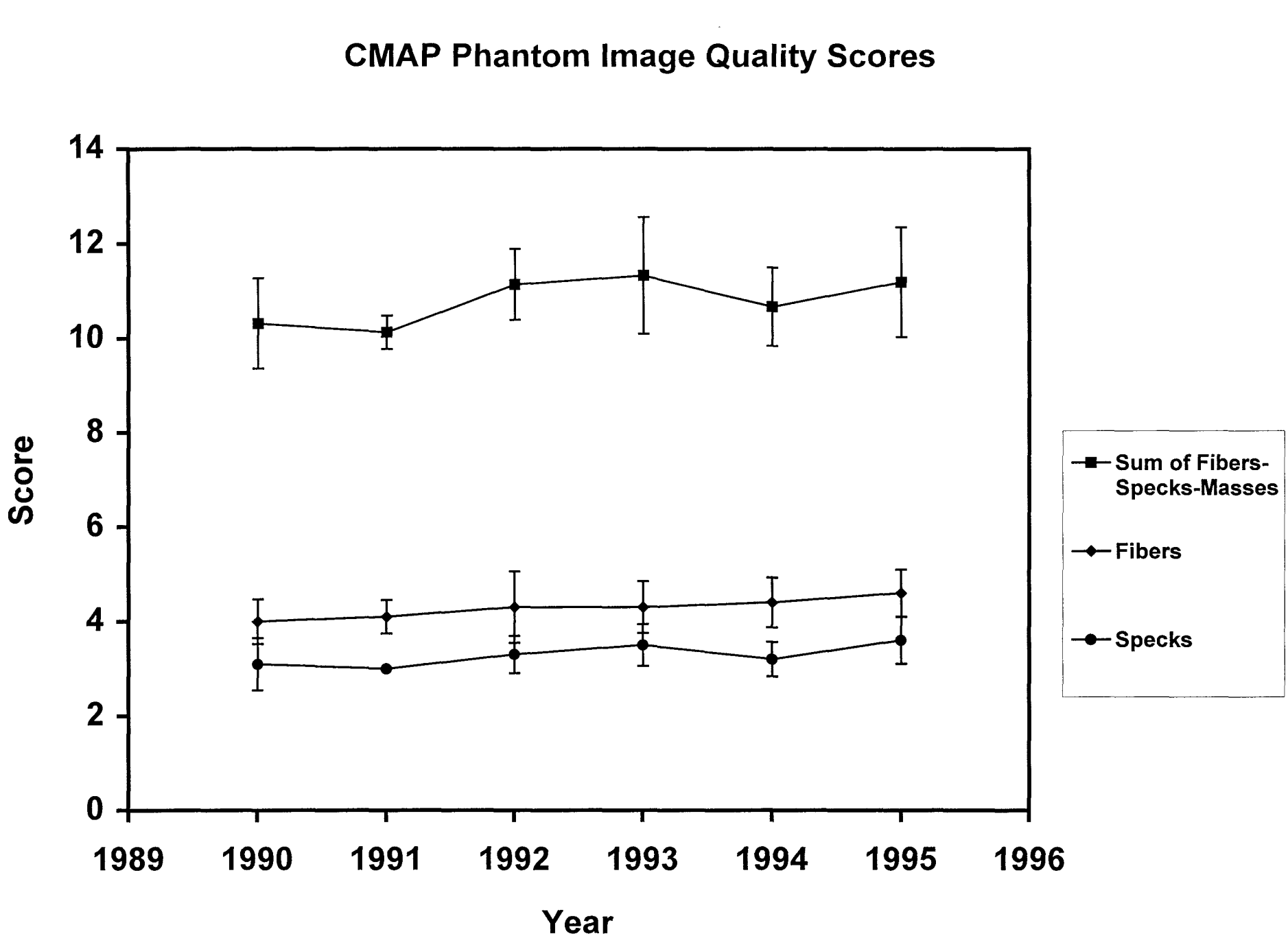
CMAP Phantom Image Quality Scores
Score
14
12
10
8
6
4
2
0
1989
1990
1991
1992
1993
1994
1995
1996
Year
Sum of Fibers-Specks-Masses
Fibers
Specks

Figure 21

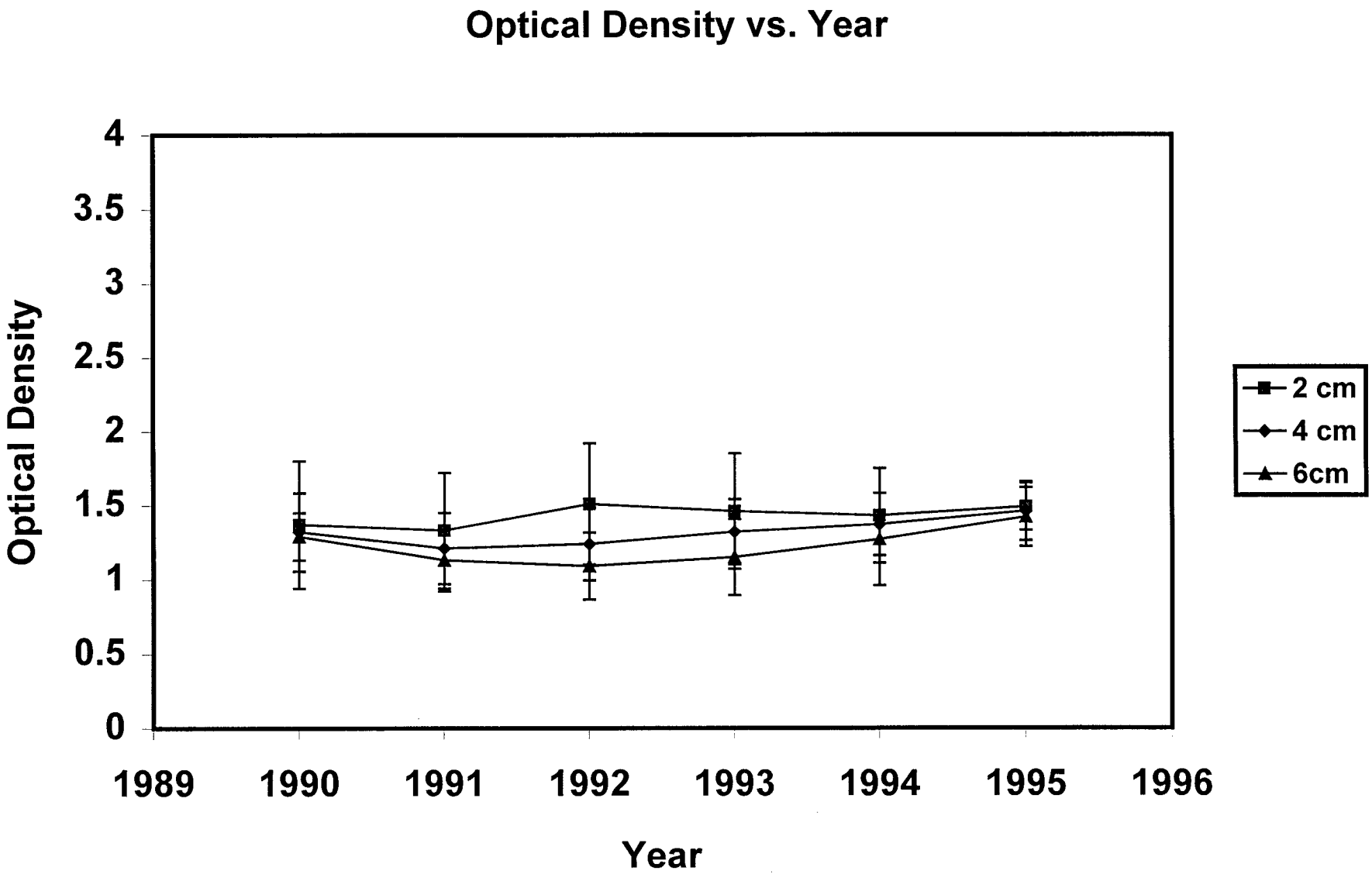
Optical Density vs. Year
Optical Density
4
3.5
3
2.5
2
1.5
1
0.5
0
1989
1990
1991
1992
1993
1994
1995
1996
Year
2 cm
4 cm
6cm

Figure 22

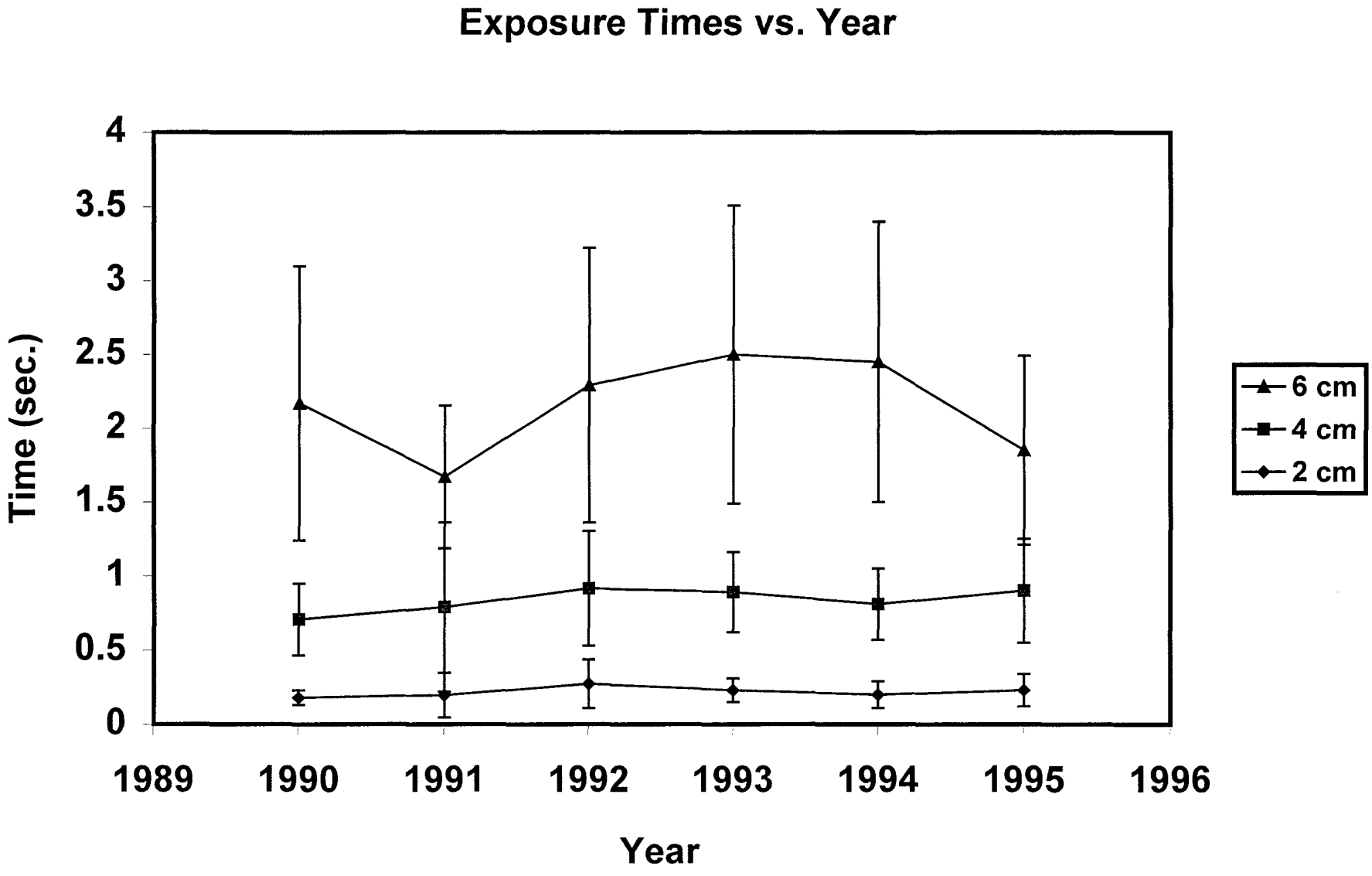
Exposure Times vs. Year
Time (sec.)
4
3.5
3
2.5
2
1.5
1
0.5
0
1989
1990
1991
1992
1993
1994
1995
1996
Year
6 cm
4 cm
2 cm

Figure 23